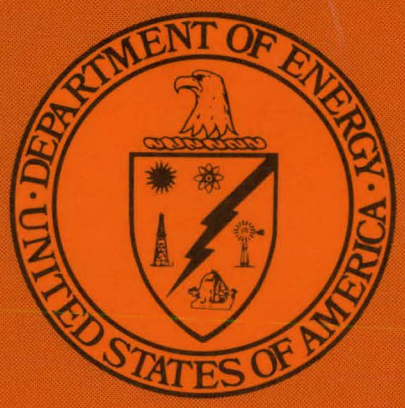

DOE/MC/14129-171
(DE82011078)

PRESSURIZED FLUIDIZED BED COMBUSTION PART LOAD BEHAVIOR

Volume 1—Summary Report

By
A. G. Roberts
K. K. Pillai
P. Raven
P. Wood

September 1981

Work Performed Under Contract No. AC21-80MC14129

NCB Coal Utilization Research Laboratory
Leatherhead, England

TECHNICAL INFORMATION CENTER
UNITED STATES DEPARTMENT OF ENERGY

DISCLAIMER

DISCLAIMER

DOE/MC/14129-171
(DE82011078)
Distribution Category UC-90e

PRESSURIZED FLUIDIZED BED COMBUSTION

PART LOAD BEHAVIOR

VOLUME I - SUMMARY REPORT

By

A.G. Roberts, K.K. Pillai, P. Raven and P. Wood

NCB COAL UTILIZATION RESEARCH LABORATORY

Leatherhead, England

September 1981

Prepared For

UNITED STATES DEPARTMENT OF ENERGY
Morgantown Energy Technology Center
Morgantown, West Virginia

Under Contract No. DE-AC21-80MC-14129

ACKNOWLEDGEMENTS

The programme was carried out under the direction of H.R. Hoy, OBE, Director of NCB-CURL.

The principal members of staff involved were: A.G. Roberts (Planning and Co-ordination); P. Raven (Project Leader): R.N. Phillips (Project Engineer); R.V. Wardell, J. Curtis and S.N. Barker (Plant Operation): D. Crawford (Design); K.K. Pillai and P. Wood (Data assessment); and K. Cox, W.A. Gearing, R. Keating, A.W. Lindsay, R. Lowman, L.E. Mummery.

CONTENTS

Contd.

SUMMARY

During 1980, a short series of tests was carried out on the Leatherhead combustor (Fig. A) with the general objective of providing data on the part-load characteristics of PFBC and its behaviour during load changing.

In a supercharged boiler combined cycle, the first step in changing load is to alter the bed temperature. A variation of 200 to 300°F is sufficient to alter the load by approximately 30%. To change the load over a wider range requires some additional method. Several solutions are possible but the one with which this report is specifically concerned involves changing the bed depth by transferring bed material at a high rate to and from a storage system. This procedure exposes some of the steam generating tubes to conditions above the bed surface and hence to a lower heat flux. The exposed tubes also cool the gases and hence reduce the gas turbine power output.

The system used to change bed level on the Leatherhead combustor is shown in Fig. B. The rate of solids transfer was controlled by a combination of conveying gas flows and pressure differential between the two vessels. In the course of the investigation bed depth was changed many times between about 9 ft and 4 ft at rates varying between 0.2 ft/min and 0.5 ft/min. On some occasions the bed temperature and pressure were also changed simultaneously in a controlled manner. Although there were consequent changes in gas composition (CO, O_2, SO_2, NO_x), these did not cause any operational problems and it is concluded that changing bed depth is a method of changing load which can be considered for full-scale plant. Load changing down to at least 25% should be possible.

Operation at part-load steady-state conditions. The performance of the combustor was determined with a number of combinations of bed temperature and bed depth, mostly at a fluidising velocity of 4 ft/s, pressure of 6 atm and excess air of 50%. Glen Brook (Ohio) coal was used.

As might be expected, performance deteriorated as load was reduced. The part-load performance of a PFBC in a commercial plant would depend on details of the design, such as gas turbine characteristics and steam conditions (the latter having an influence on bed depth), but the following comments are intended as a guide. When a specific commercial or demonstration plant is designed, with specific load following characteristics, it would be advisable to reproduce the exact conditions on the Leatherhead rig.

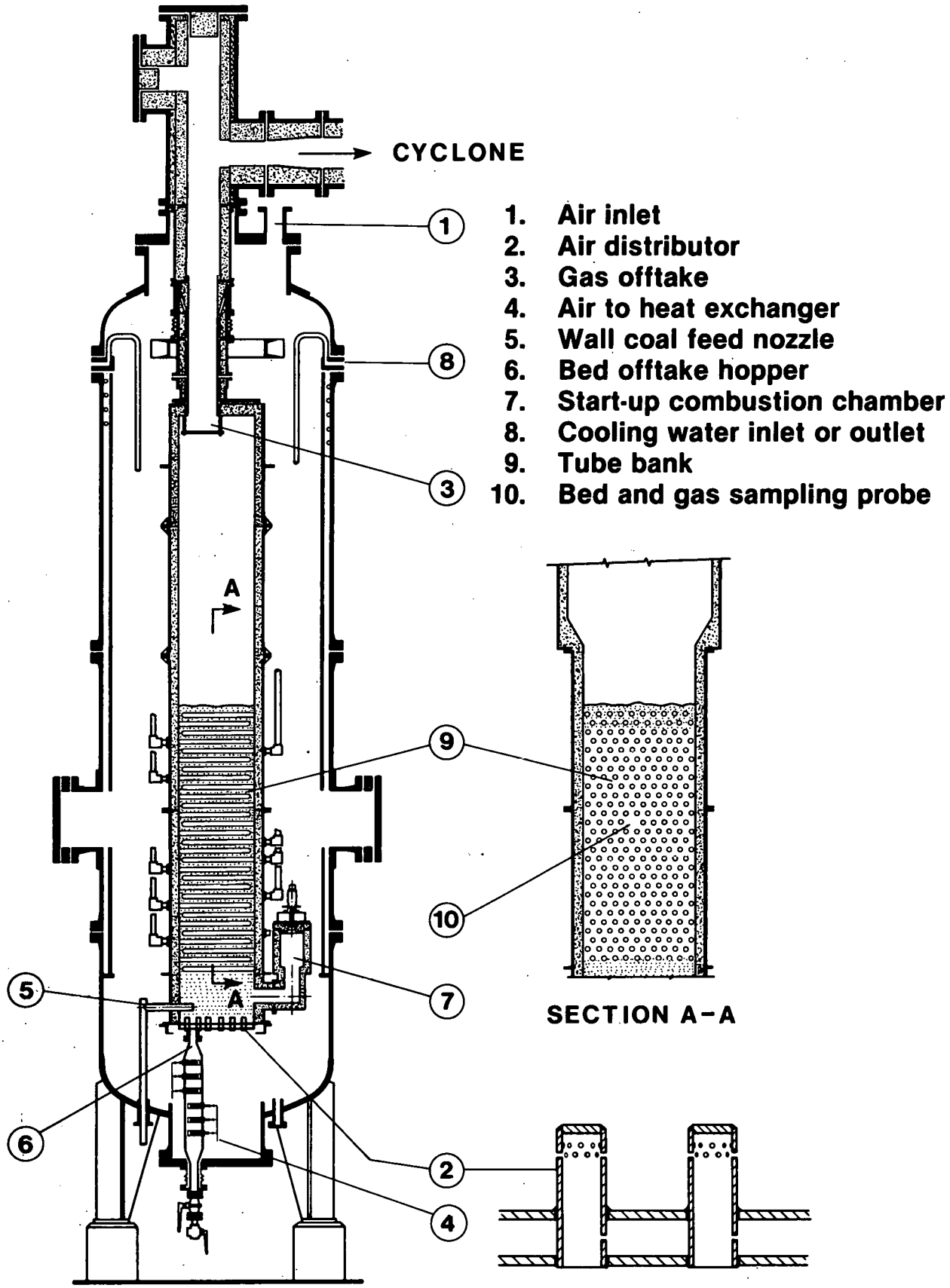

Fig. A. Arrangement of fluid bed combustor MK.VIII

1. High temperature Kamyr valve
2. Conveying air
3. Purge nitrogen
4. Fluidising distributor
5. Adjustable tube
6. Preheater
7. Gas offtake
8. Quench water
9. Venturi scrubber

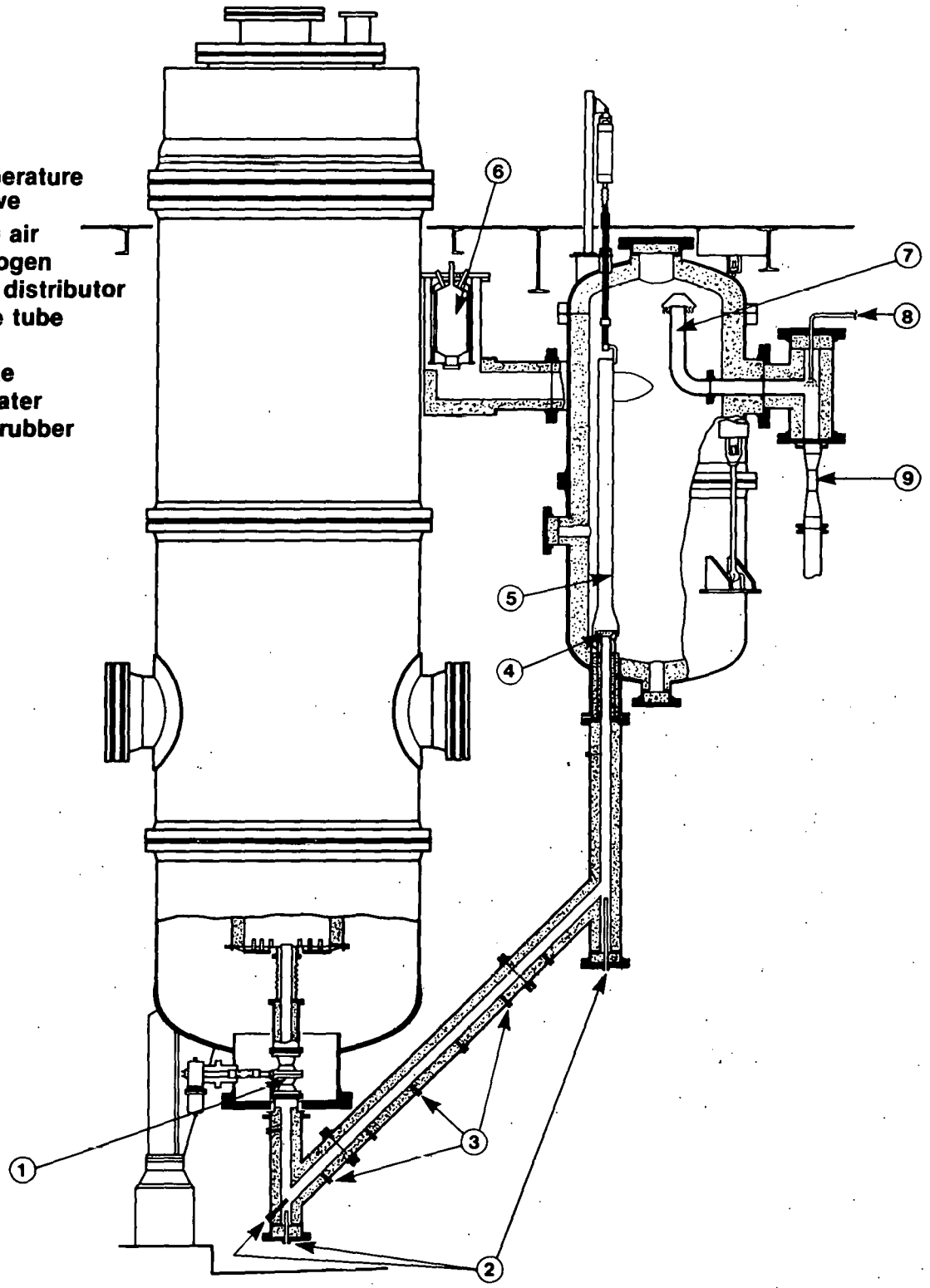

Fig. B. Arrangement of bed transfer system

D519

Combustion: Combustion efficiency was typically 99% at "full load" conditions of 9 ft bed depth and 1650°F bed temperature, falling to 95% at 4 ft bed depth and 1390°F bed temperature. Part of this loss of efficiency was due to the suppression of combustion above the bed because the gas was cooled by the exposed cooling tubes. There was no significant freeboard combustion at full load. Even though the minimum bed depth on a commercial plant might not be as low as 4 ft, it seems that some remedy such as recycle may be necessary if prolonged operation at part load is planned.

Sulphur emissions: sulphur retention fell from about 95% at full-load (Ca/S ratio of 1.7, gas residence time in the bed of 2.3 seconds) to about 80% at conditions of low bed temperature and low bed depth (i.e. low gas residence times). The adverse effect of bed temperature may have been partly due to the fact that at low temperatures the $CaCO_3$ component of the dolomite was only partially calcined and even the calcination of $MgCO_3$ (and hence the generation of porosity) may have been incomplete.

Emissions of SO_3 (measured during one test only) were generally less than 4 ppm (v/v) with occasional higher values (8 to 15 ppm). It was not possible from the data to say whether load had any effect. Although these levels of SO_3 emissions are probably not a factor having a significant effect on "back-end" corrosion, more measurements need to be made.

NO_x emissions: at full load, NO_x emission was about 0.32 lb/10^6 Btu, which agrees with data obtained elsewhere at about 50% excess air. There was a tendency for NO_x emissions to increase (up to 0.5 lb/10^6 Btu) as the temperature was reduced.

Alkali emissions: the measured vapour concentrations in the exhaust gases were about 1 ppm (w/w) of Na and 1.3 ppm of K. Measurements showed a large scatter (about ±0.5) and no effect of bed temperature could be detected.

Heat transfer: particular attention was paid to measuring the heat transfer to tubes in the "splash zone" at the surface of the bed. In general, heat transfer coefficients decreased exponentially by 65% over a distance of 2 ft above the bed surface.

Response rate characteristics: the time constants of the system were measured at different operating conditions by altering the coal feed rate sinusoidally at varying frequencies and amplitudes. Depending on the operating conditions, the time constants varied between 300 and 700 sec - on average about 30% longer than calculated values.

Other information given in the report concerns operating with a single coal nozzle, measurements of gas and solids compositions at points within the bed, and the elutriation of solids from the bed.

1. BACKGROUND

This report is concerned with the supercharged boiler combined cycle. In such a cycle, illustrated in Fig. 1, hot gases from the PFB are expanded, after cleaning, through a gas turbine. Steam generated and superheated in tubes immersed in the bed drives a steam turbine.

Although such a utility plant will be nominally base load plant, at least in the early part of its life, it will be required to operate for significant periods at part load and to be able to accommodate load changes of up to 3 or 4% per minute.

The problems of changing load in a combined cycle are best discussed by describing the stage-by-stage steps which are required. Details will vary according to the particular gas turbine, steam conditions, and PFBC conditions being used, but the following describes a philosophy for reducing load.

(1) The first step is to reduce the bed temperature to a minimum operating value (one of the objectives of the tests reported here is to determine what this minimum value might be; traditionally it has been assumed to be about 1380°F). This has the effect of reducing the gas turbine inlet temperature and hence the gas turbine power output. Steam output is also reduced because the heat transfer to the tubes immersed in the fluidised bed is reduced.

(2) To reduce the gas turbine output to its minimum it is necessary to reduce the turbine inlet temperature considerably below 1380°F and this can be done to some extent by by-passing some of the compressed air around the combustor and so diluting the combustion products. However in doing this, two limitations must be borne in mind: (i) the fluidising velocity must not decrease too much, otherwise segregation could occur in the bed; and (ii) the excess air must not fall below some minimum value. With most gas turbines the first limitation does not normally arise. Although single-shaft and multi-shaft gas turbines have vastly different part-load characteristics, both types operate with a volumetric flow from the fluidised bed which is approximately constant or actually increases with reducing load.

The second limitation may apply because of the relatively inflexible nature of the amount of heat transferred to the steam circuit. Once a minimum bed temperature of, say, 1380°F has been reached, heat flux to the steam circuit remains constant as the mass flow through the bed is further reduced. As a consequence the excess air tends to decrease as load is reduced by air bypass. This is

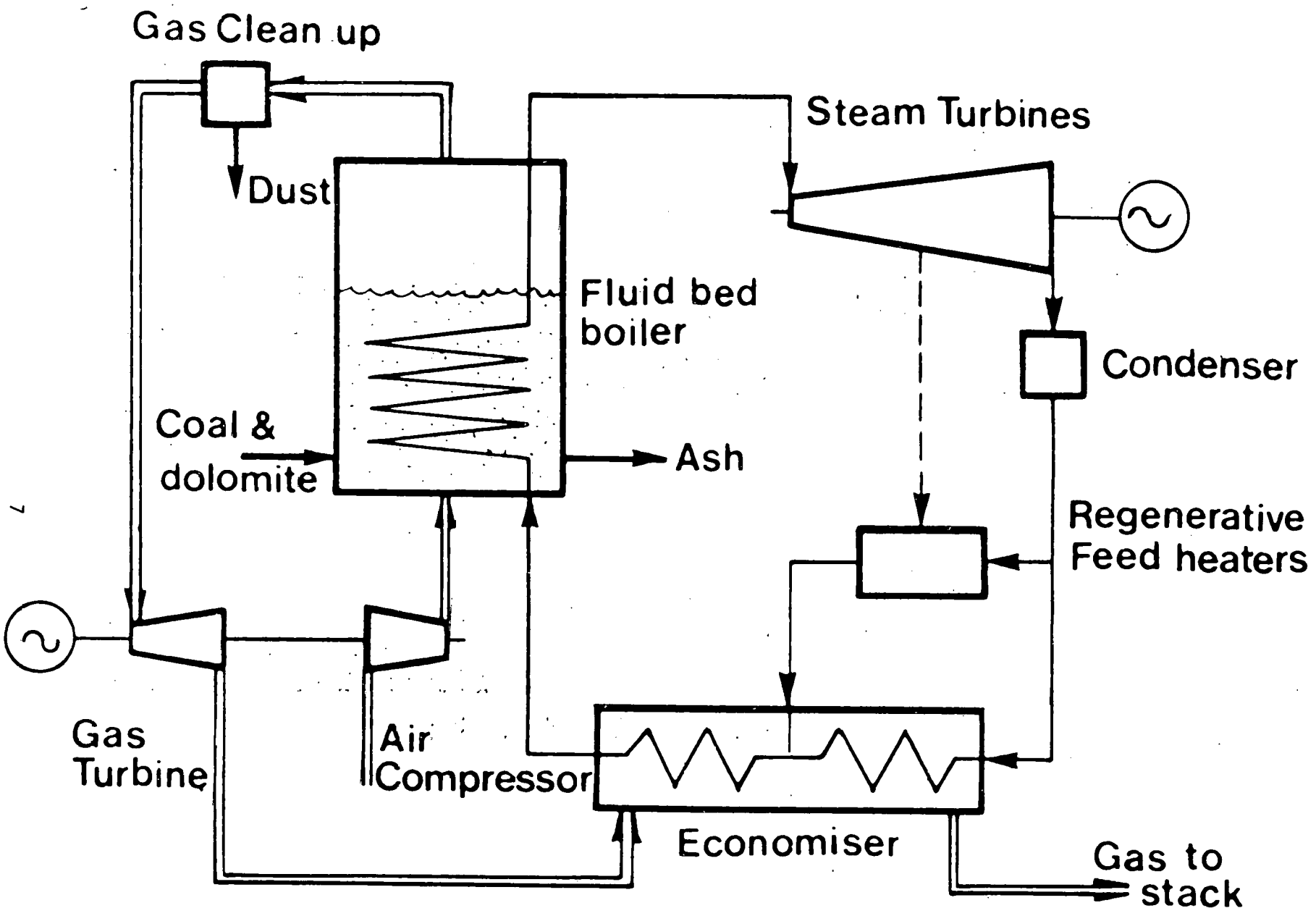

Fig.1 Supercharged boiler PFBC combined cycle

D547

particularly significant in multishaft gas turbines where there is a much greater variation in compressor flow with load.

(3) The gas turbine output at full load can be expected to be about 20-30% of the total plant output, depending on the excess air. Thus, even if the gas turbine could be operated over a load range of 100% to zero by means of (1) and (2) above (which is unlikely), the steam turbine output would need to change over a range of 100% to 30% in order to produce a total output varying over a 4:1 range. Because the heat flux is mainly dependent on the temperature differential and not on pressure or fluidising velocity, the change in heat flux between maximum (1560 to 1650^{o}F) and minimum (1380^{o}F) bed temperature is only from 100% to about 70% in the evaporator section (where the water/steam temperature is of the order of 670^{o}F) and 100% to about 65% in the superheater section.

(4) A stage is now reached where the fluidised bed is operating at its minimum temperature but neither the gas turbine nor, more importantly, the steam turbine is producing minimum power. The load at this point is probably not less than 60% of the full load and must be reduced further by one of three routes:-

(a) by slumping part of the bed and thus reducing the heat flux to those steam generating tubes in the slumped part. Although this method is used in atmospheric fluidised beds, there is no experience of slumping the deep beds which exist in PFBC.

(b) by modularising the system and arranging a number of gas turbines in conjunction with each steam turbine, and having perhaps two fluidised beds per gas turbine. Load is then reduced by shutting down modules. Both (a) and particularly (b), require complex valving arrangements and result in step changes in load. To produce a continuous reduction in load requires a reduction (step change) in one part of the system and a slight increase in the remainder.

(c) by altering the depth of the bed in the combustor and transferring bed material at a high rate to a storage system. This exposes some of the steam generating tubes to conditions above the bed surface and hence to a lower heat flux. The exposed tubes also cool the gases leaving the freeboard and hence reduce the gas turbine power output. The method is capable, in principle, of producing a continuous reduction in load. Until the present investigations, no experimental work has been undertaken, although the method was first proposed ten years ago.

An increase in load is produced by reversing the steps above.

To summarise, a PFBC will be required to operate over a wide range of bed temperature and bed depth (if the latter is used as a means of load variation). If the gas turbine is a multi-shaft machine there will also be a large variation in pressure.

2. OBJECTIVES OF TEST PROGRAMME

It will be apparent from the previous section that operation at steady-state (but at part load) is essentially operation at low bed temperature, low pressure, possibly low fluidising velocity, and (if varying bed depth is used as a means of varying load) low bed depths. Changing load at, say 3 to 4% per minute (a normal utility requirement) involves high rates of change of these parameters.

The main objectives of the test programme were:-

(1) To operate the combustor at a number of steady-state combinations of bed temperature, bed level and fluidising velocity and obtain performance data (combustion efficiency, sulphur retention, NO_x emissions, elutriation data, heat transfer data - particularly heat transfer in the splash zone).

(2) To install a system for rapidly changing bed depth and to demonstrate that this system is technically suitable as a means for changing load. Particular attention to be paid to changes in gas composition (CO, SO_2, NO_x) whilst carrying out these changes.

(3) To carry out frequency response investigations at some of the steady-state conditions in order to evaluate time constants.

Subsidiary objectives of the test programme were:-

(1) To study the in-bed variations in gas composition and solids composition across a traverse line.

(2) To obtain performance data when operating at simulated full load with one coal nozzle in use. As well as providing information in its own right (i.e. to minimise the number of coal feed points in a large plant), this was to serve as a datum for tests in a future programme when attempts are to be made to burn 'run-of-mine' coal injected at a single point.

Operating conditions which remained nominally constant for most of the programme were:-

3. SCOPE OF REPORT

The programme of three tests was carried out over the period June to November 1980. Details of these tests, together with the results obtained were given in Reports No. DE-14129-2, 4 and 5 - with minimal comment. It is the purpose of this report to assess the results from the programme and to present a general view of their impact on load changing in PFBC.

The results are discussed under four main headings:-

(i) the behavior of the system for changing bed depth.

(ii) the performance of the combustor at a number of steady-state combinations of bed temperature, bed depth and fluidising velocity (simulating part-load).

(iii) heat transfer measurement to tubes immersed in the bed and in the splash zone.

(iv) frequency response measurements consequent upon changes in fuel feed rate, at a number of operating conditions.

The opportunity has also been taken of presenting some general correlations for predicting combustion efficiency and elutriation, based on results obtained at Leatherhead over the last few years. The conditions examined in the 1980 programme were sufficiently varied to support the validity of these correlations.

Fluidising velocity	-	4 ft/s
Excess air	-	50%
Pressure	-	6 atmospheres absolute

Fluidising velocity and excess air were chosen as being typical of projected commercial designs. The pressure is the maximum at which the Leatherhead plant operates, but it also happens to approximate to the pressure by many gas turbines at low load.

The coal used was Glen Brook, a medium swelling Ohio coal. Two dolomites were used:- Plum Run from Ohio and a U.K. dolomite.

4. DESCRIPTION OF THE FACILITY

4.1 THE COMBUSTOR

The combustor was generally as shown in Fig. 2. It consisted of a refractory-lined steel vessel of rectangular cross section hanging within a 6 ft diameter pressure shell. The refractory-lined vessel - the combustor - had internal dimensions of 3 ft x 2 ft and was closed at its lower end by the distributor plate. The walls were faced with a layer of hard refractory backed by a layer of insulating material. Total refractory thickness was 3 inches in the bed space and 2.5 inches in the freeboard space. Air for fluidisation and combustion entered through the dome of the pressure shell, flowed down between the combustion chamber and the pressure shell and then upward through the distributor plate. The hot products of combustion left via a refractory-lined pipe which passed through the top closure plate of the dome. Cooling was provided by a number of tubes in the lower 8 ft section of the combustor. Attached near to the base of the combustor were two small gas-fired burners which provided hot gas for initial heating of the bed and ignition of the propane during start-up. The total height of the combustor was 16 ft.

The distributor plate is shown in Fig. 3. Air was discharged into the bed through 59 nozzles arranged on a 3.5 inch square pitch and passing vertically upwards through two mild steel plates. Each nozzle was made from 1 inch ISO pipe in Type 321 heat resisting steel, extending 2¼ inches into the bed space and closed at the top. Air passed into the bed through ten holes of 0.122 inch diameter in each nozzle, arranged 1.73 inches above the top plate. Since the bed material below the holes was unfluidised, it acted as an insulating layer protecting the mild steel plate. Also, since fluidisation started 1.73 inches above the top plate, this level is defined as the base of the fluidised bed. Vertical dimensions within the combustion chamber, such as thermocouple or pressure tapping positions are referred to this level.

The space between the two plates of the distributor served as a propane gas plenum and was divided into sections linked by external piping to form four areas for selective distribution of propane during start-up. Propane entered each air nozzle through a single hole.

Coal entered the bed through two nozzles penetrating the side walls. The nozzles were constructed from ¾ inch NB Schedule 80 pipe in Type 310 heat resisting steel. The orientation of the nozzles is shown

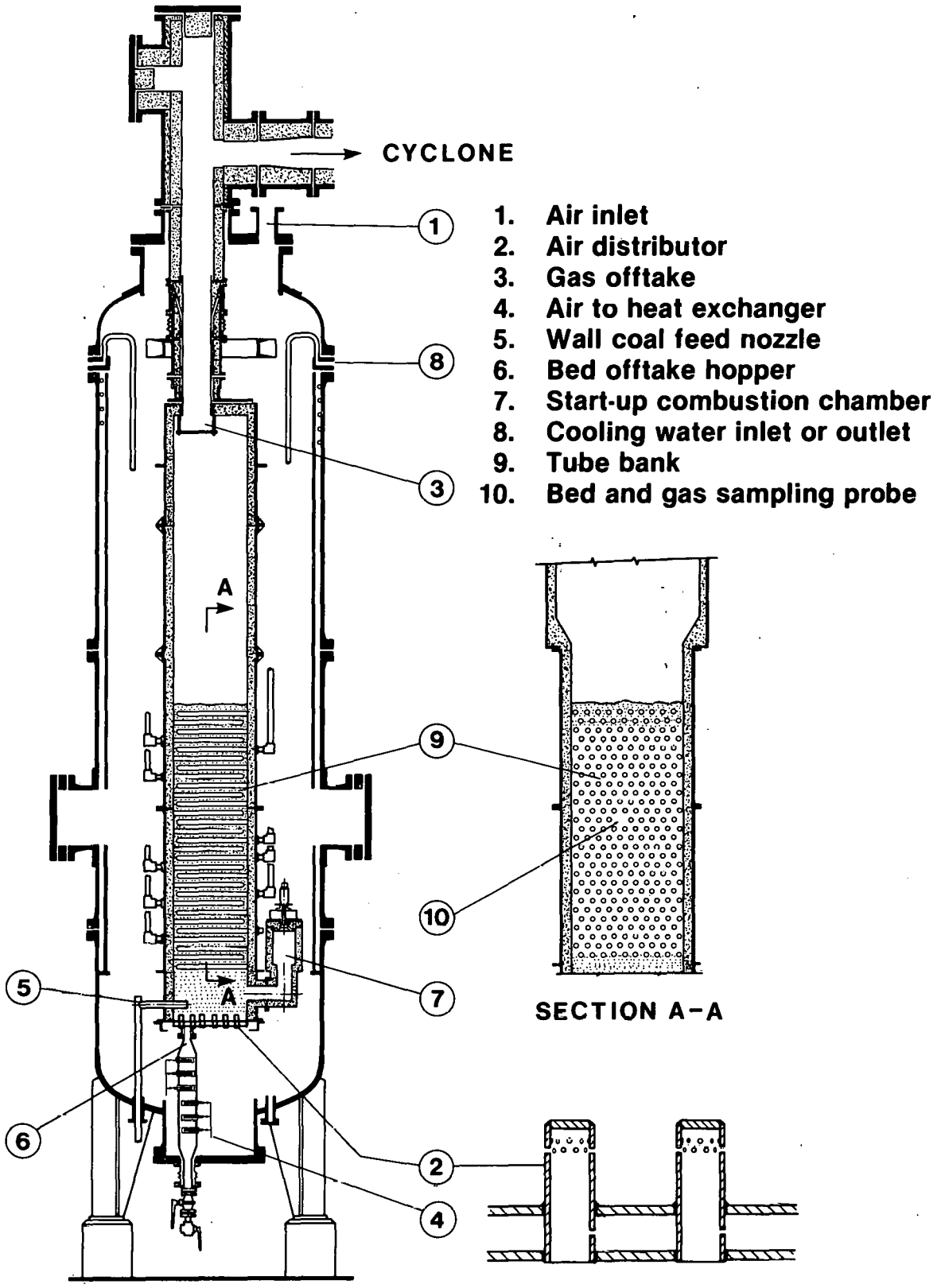

FIG.2. ARRANGEMENT OF FLUID BED COMBUSTOR Mk VIII

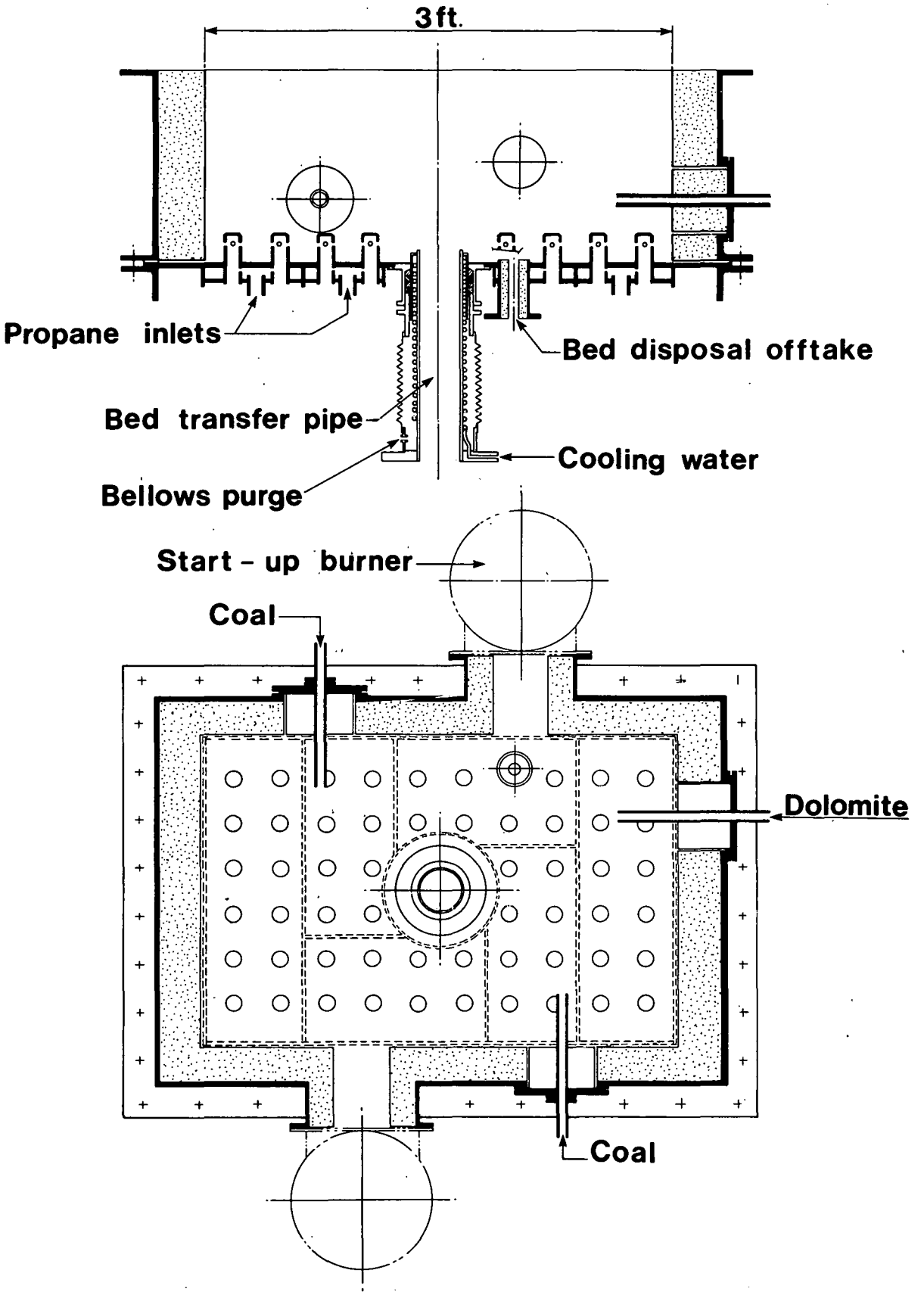

Fig. 3 Distributor zone Mk.VIII combustor D540

shown in Fig. 3. For one of the steady-state conditions, a single coal nozzle was used. By using the dolomite nozzle as the new coal nozzle and feeding the dolomite through the nearest coal nozzle, the change-over from two coal nozzles to one was made without shutting down the plant (a single nozzle coal feed required a larger pipe from the coal feeder).

A 1.5 inch diameter hole in the distributor plate, leading via a heat resisting steel hopper through the pressure casing to external high temperature valves, allowed the removal of bed material during operation. The removal system is shown in Fig. 4. Material was moved in dense phase transport from the combustor to a seal vessel with a pressure differential of about 50 psig. The level in the seal vessel was maintained by emptying the latter into the batch conveyor vessel, using a pulsed air conveying supply. Under these conditions material could be removed from the combustor continuously at a rate of up to 200 lb/h. A sensitive control on the rate of flow, and therefore on the bed level in the combustor, was obtained by varying the frequency of the pulses in the conveying air supply. Periodically the isolating valves below the combustor were shut and material in the batch conveyor emptied into a bag filter unit for weighing. A small air-cooled recuperative heat exchanger was installed in the dense phase stream below the combustor. This cooled the bed material to an extent that the pipe metal temperature at the cooler outlet was about 500°F.

The combustor was equipped with two natural gas-fired burners for initial bed heating. These burners also acted as a source of ignition for propane vapour, supplied via the air tubes, which augmented the heat output from the burners once a bed temperature of 390-480°F had been reached. The burners consisted of a proprietory air/natural gas burner, complete with flame failure control, which fired into a small refractory-lined combustion chamber into which dilution air was added to reduce the gas temperature to about 1650°F. Each burner had a nominal maximum heat input of 0.2×10^6 Btu/h and the combustion gases were emitted into the bed through a 4 inch diameter hole in the walls of the main combustor. These holes were sited approximately 7 inches above the base of the fluidised bed.

Contained within the bed space was a total of 178 ft^2 of water-cooled heat transfer surface arranged as horizontal tubes on a triangular pitch space 3.5 inch horizontally and 3.0 inch vertically. The tubes were 1.25 inch outside diameter and were constructed from type 310 heat-resisting steel. Within the tube bank, the tubes occupied about 12% of the bed volume. They were arranged in 28 rows each (except row 16) containing a hairpin arrangement as shown

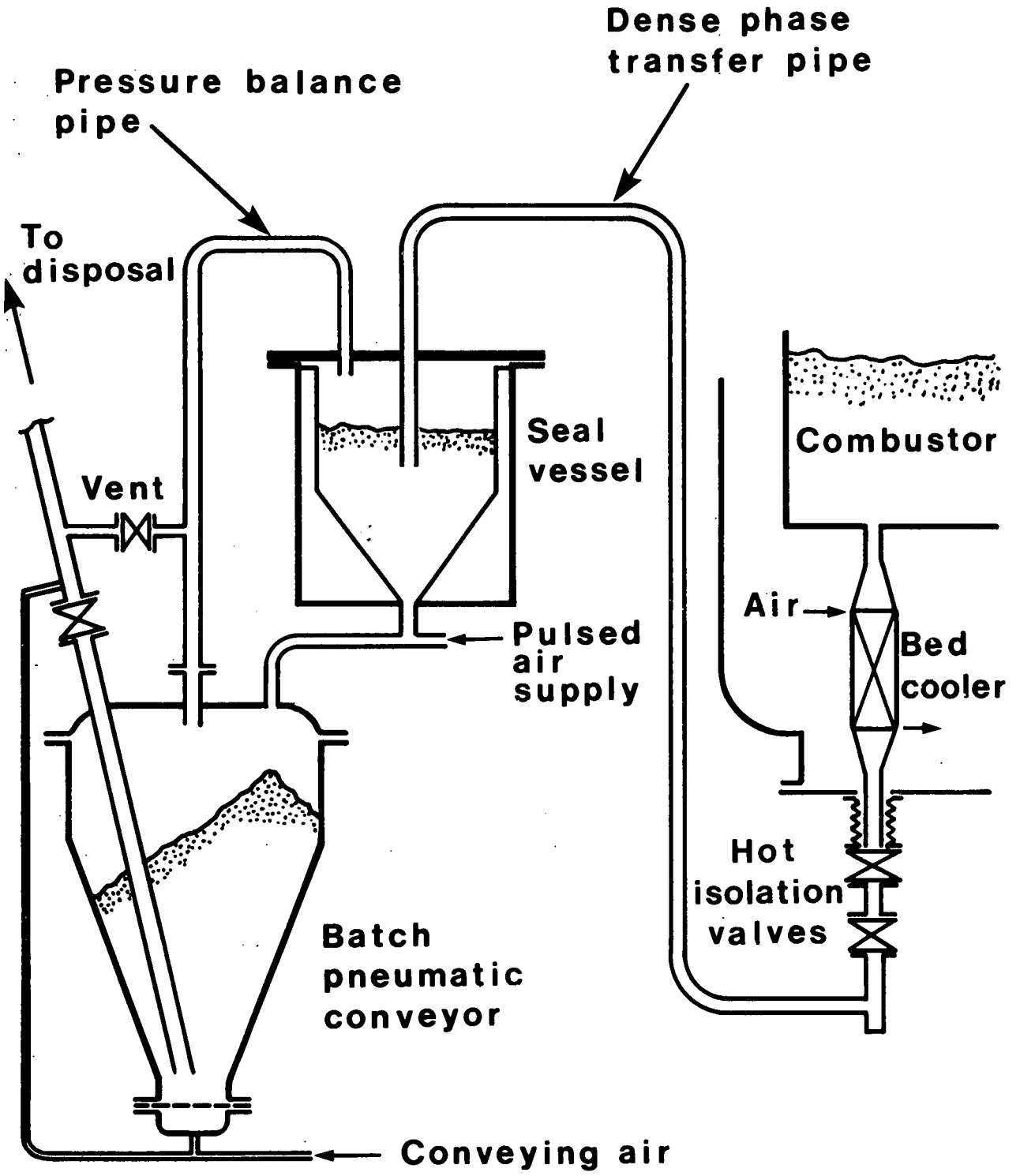

Fig.4 Schematic of bed removal system.

D542

in Fig. 5 with alternate rows penetrating opposite walls. Row 16 had only 8 passes. The bottom 6 rows were piped up as individual four and six-pass circuits and rows 7 - 28 were joined external to the combustion chamber to form single 10 pass units. Each circuit was provided with an inlet isolation valve, outlet manual flow control valve, variable area flow meter, and a thermocouple so that individual heat transfer measurements could be made.

4.2 EQUIPMENT FOR CHANGING BED LEVEL

For changing bed level, a storage vessel was assembled alongside the combustor pressure shell as shown in Fig. 6. A 3 inch diameter heat resisting metal tube was connected to the centre of the distributor plate using a gland and bellows assembly as shown in Fig. 3. The tube was surrounded by a water-cooled coil and the bellows and gland were purged with a small flow of nitrogen. Below this was a high temperature Kamyr ball valve leading through the bottom closure flange of the pressure vessel to an 8 inch diameter transfer leg, refractory-lined down to 3 inch internal diameter. This transfer line was fitted with conveying gas nozzles (items 2 of Fig. 6) at each change of direction and with "aeration" (N_2) taps (items 3) to maintain solids movement.

The transfer line terminated at the 4 ft diameter storage vessel which was lined with 5½ inches of a medium duty refractory. The vessel was fitted with a movable riser tube (item 5) and an additional transport gas supply (item 4) to assist entry of solids into the storage vessel. When transferring solids from the bed to the storage vessel, the riser tube was in its lowest position so that solids flowed out of the top of the riser into the vessel. When transferring solids from storage into the bed the riser was lifted by a pneumatic cylinder so that solids could flow directly into the transfer leg. The disposition of the storage vessel in relation to the combustor bed was dictated by lack of headroom below the combustor. More normal practice would be to place the storage vessel below the combustor or as a pannier alongside it in the same pressure vessel. The storage vessel was suspended from variable spring supports to allow for expansion. It was also fitted with an oil-fired burner (item 6) for preheating the refractory and also with a gas washing and pressure control system, (items 8 and 9), similar to that on the main plant, to dispoe of the spent conveying gas.

The system was operated using a combination of pressure differential and conveying gas flows to control the rate of solids transfer. When transferring bed to storage, the system was usually operated by setting a differential pressure between the combustor and storage vessel at the start of a transfer, and (because the transfer leg was full of relatively cold material) a high flow of conveying gas was

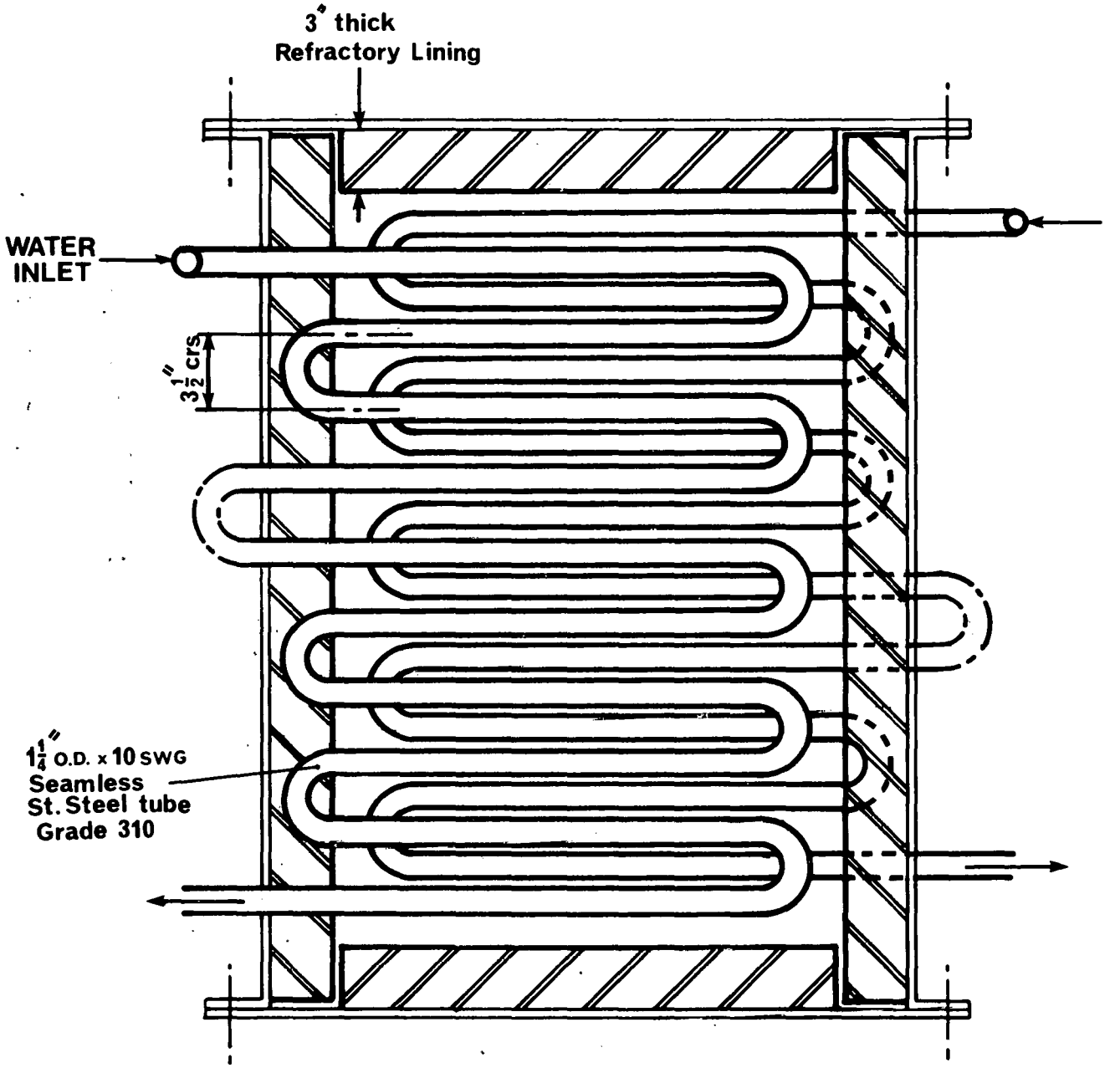

Fig. 5 Plan View of Bed Cooling Coils

1. High temperature Kamyr valve
2. Conveying air
3. Purge nitrogen
4. Fluidising distributor
5. Adjustable tube
6. Preheater
7. Gas offtake
8. Quench water
9. Venturi scrubber

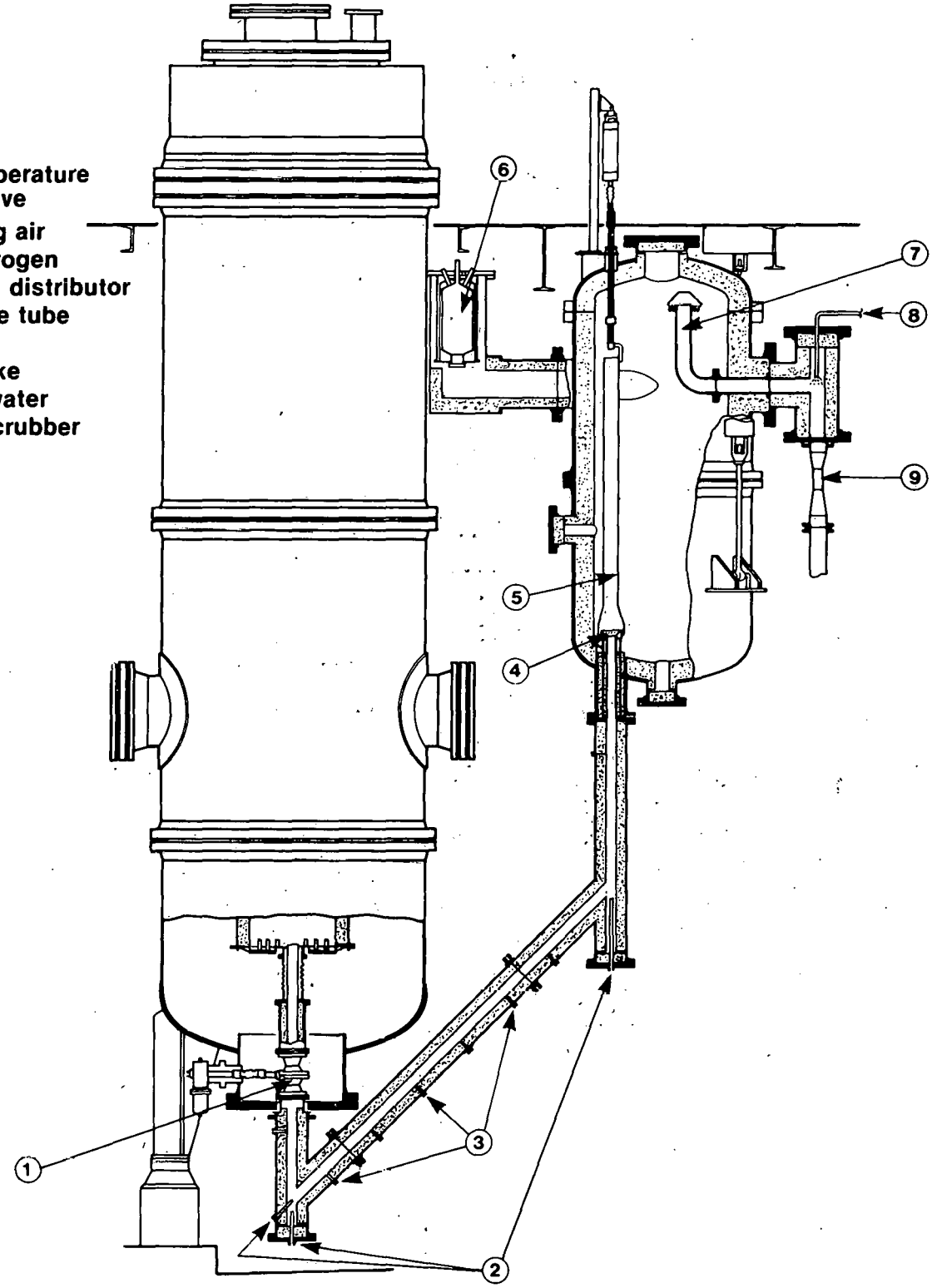

Fig.6 Arrangement of bed transfer system

required to initiate solids movement. The flow rate of solids generally increased as the material in the transfer leg heated up and began to entrain combustion gases from the combustor. Once a high transfer rate had been established, the conveying gas flows could be considerably reduced without affecting the flow rate providing the differential pressure was above about 3 psi. The differential pressure was then the main controlling factor although the additional gas (N_2) added at the bottom of the riser tube was essential to maintain transfer. At differential pressures below about 3 psi, the solids did not entrain combustion gases, and conveying gas was necessary for transport and could be used to control the rate.

The transfer rates achieved varied between 1500 lb/h at a differential of 3¼ psi and 13000 lb/h at a differential of 4¼ psi. There was always a minimum flow on the conveying air nozzles and aeration taps to prevent their becoming blocked by solids. The total flows of these gases gave a superficial gas velocity at the end of the transfer leg of about 3 ft/s (i.e. excluding any gases entrained from the combustor).

Transfer from storage to the combustor was a very steady operation with rates varying between 2500 lb/h at a differential pressure of 2½ psi and 15000 lb/h at a differential of 5 psi. The only conveying gas flow was the vertical jet at the bottom of the final vertical pipe to the combustor. The quantity of this gas had a more marked effect on the solids flow in this direction. At the higher values of differential pressure a wide range of control was obtainable. At low differential pressures the rate at which solids could fall down the inclined pipe was controlling.

4.3 SOLIDS FEED SYSTEMS

A flow diagram of the coal feed system is shown in Fig. 7. Coal prepared by an external contractor was loaded from tankers into the storage silos. From there it was fed via a screen to a dense phase pneumatic conveyor which fed into the storage vessel. This and the feed vessel were mounted on load cells and had a capacity of 6000 lb each. Coal left the feed vessel through two outlets each having a rotary valve, acting as a metering device, to regulate the flow into the conveying lines. The speed of the rotary valves could be varied by either local manual control or remotely by the output from the combustor bed temperature controller. The feed vessel was pressurised with nitrogen introduced just above each coal exit point and this pressure was controlled by a vent valve operating in conjunction with an automatic differential pressure controller. This maintained the feed vessel pressure at a constant level of about 5 psig above that of the combustor.

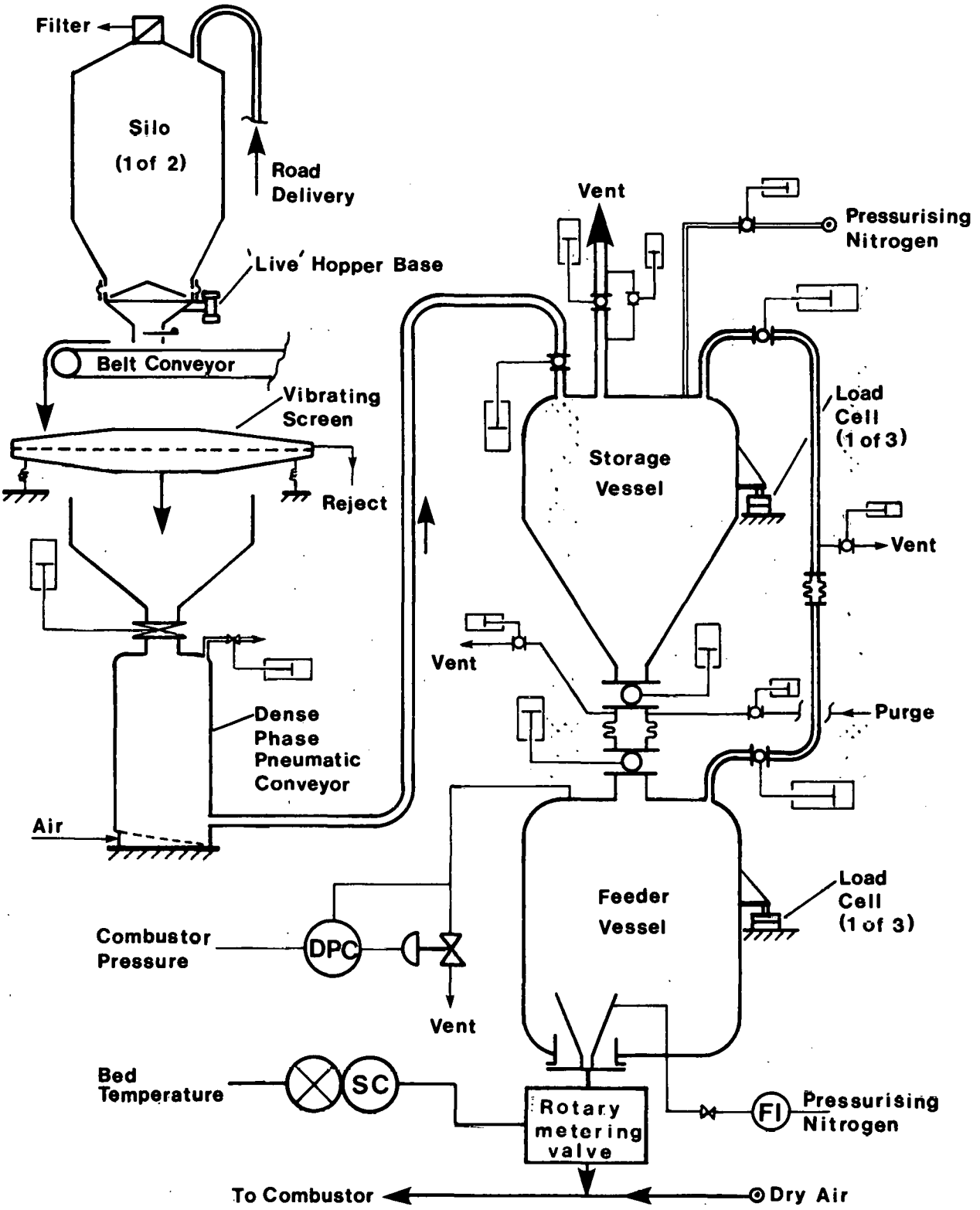

Fig.7 Coal Storage and Lock Hopper

The dolomite feed system (Fig. 8) was similar to the coal feed system and incorporated a single rotary valve supplying a separate feed nozzle. The feeder had a capacity of about 700 lb.

4.4 THE GAS CLEAN-UP SYSTEM

Hot gas cleaning was provided by a single cyclone which is shown schematically in Fig. 9. It was fabricated from Type 310 heat resisting steel and was housed in a 4.5 ft diameter pressure vessel located adjacent to the combustor. The pressure round the cyclone was equalised with the cyclone inlet pressure and thus the cyclone wall had only to withstand a small pressure differential. To reduce heat loss to a minimum, the space round the cyclone was loose-filled with expanded mica insulation.

The cyclone ash removal system is shown in Fig. 10. It consisted of a lock hopper system with a bag filter for final dust collection. Under normal operation the isolation valve separating hopper 'A' from hopper 'B' was open and dust collected in hopper 'B'. To discharge ash this valve was shut and the hopper 'B' vented through the collection bin/bag filter. The hopper 'B' discharge valve was then opened and the dust blown into the collection bin. The bin discharged into a drum in which each discharge could be weighed thus allowing the cyclone performance to be checked periodically. When discharging was complete hopper 'B' was repressurised with nitrogen to just below the hopper 'A' pressure and the isolation valve was opened.

To protect the combustor pressure control valve from erosive dust and excessive temperature the gases leaving the cyclone were first cooled directly with a water spray to saturation point and then cleaned in a stainless steel venturi scrubber. Water was removed from the gas in a cyclone and the gas left through the pressure control valve. To prevent acid corrosion in the wet pipe work and water cyclone, the pH of the water was controlled by the addition of ammonia introduced at the venturi scrubber.

4.5 INSTRUMENTATION AND CONTROL SYSTEM

A flow sheet/instrumentation diagram is shown in Fig. 11. Temperatures were measured using Type K mineral insulated thermocouples in association with chart recorders or the data logging system. Pressures and pressure differences were measured using standard process type pneumatic transmitters and chart recorders. Where

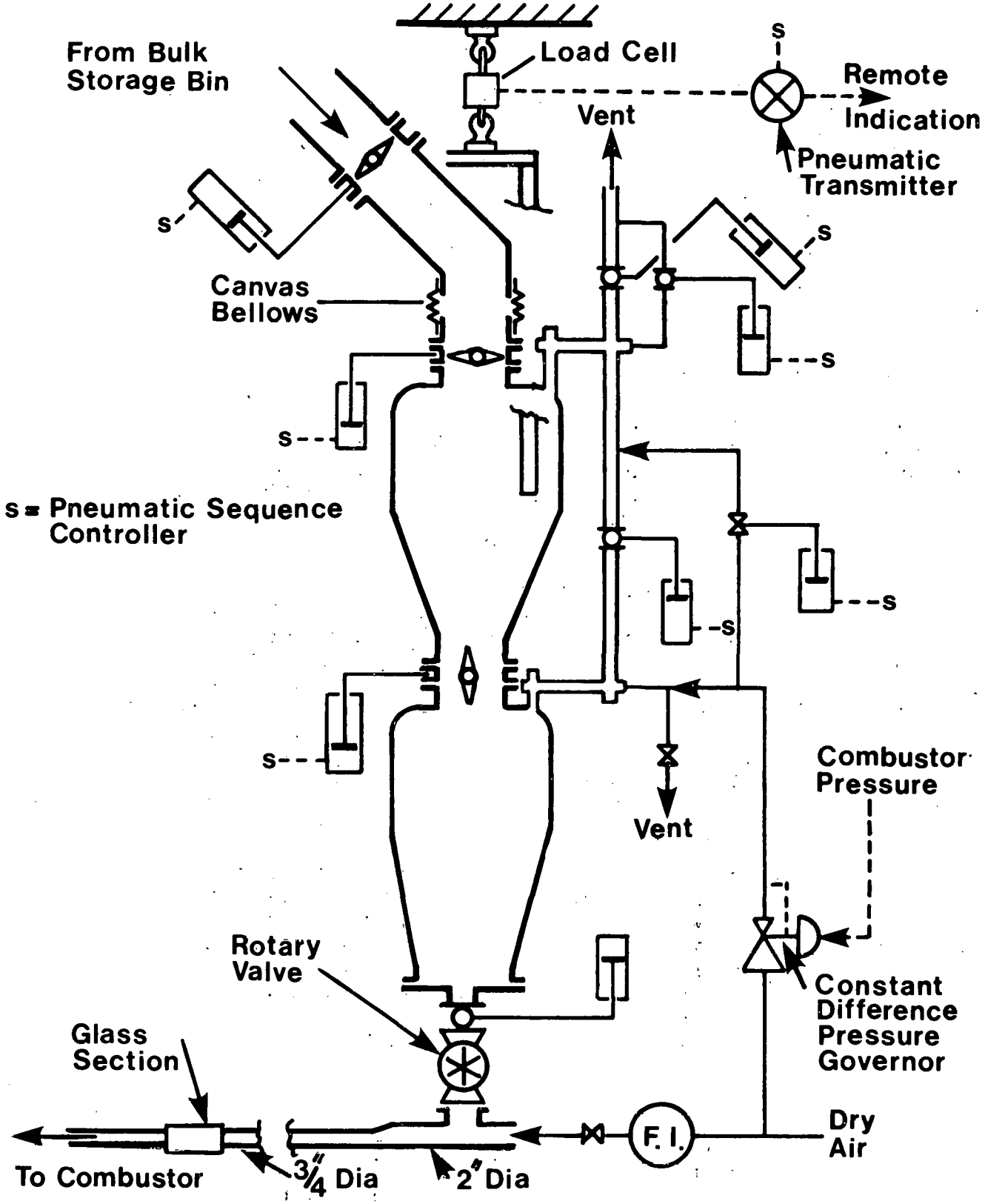

Fig. 8 Dolomite Feeder

D562

Dimensions
D = 20 inches
a/D = 0·65
b/D = 0·165
A/D = 0·30
h/D = 1·85
H/D = 3·88
B/D = 0·39
S/D = 0·65

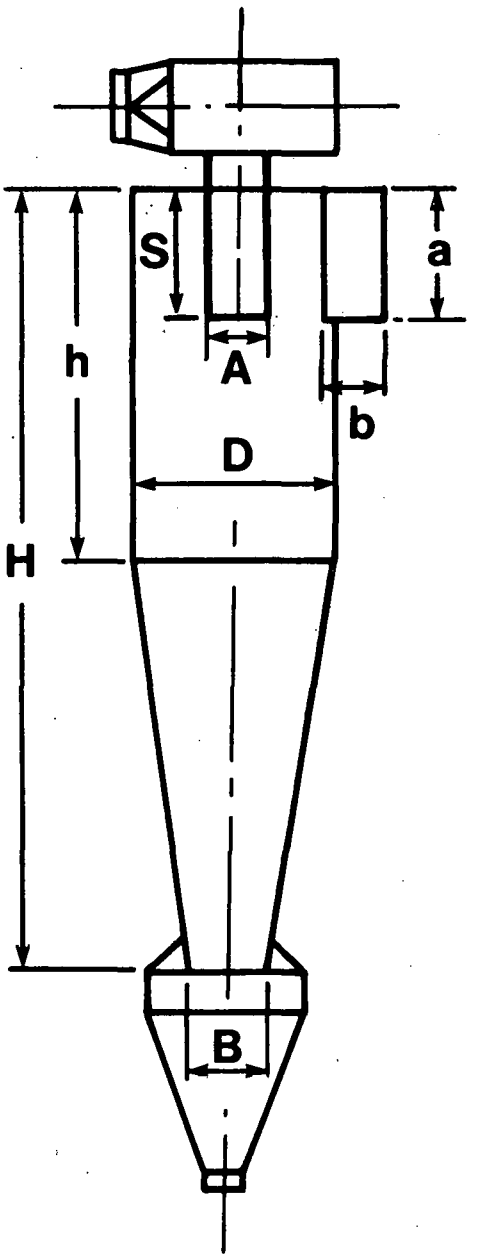

Fig.9 Cyclone dimensions and operating conditions

D543

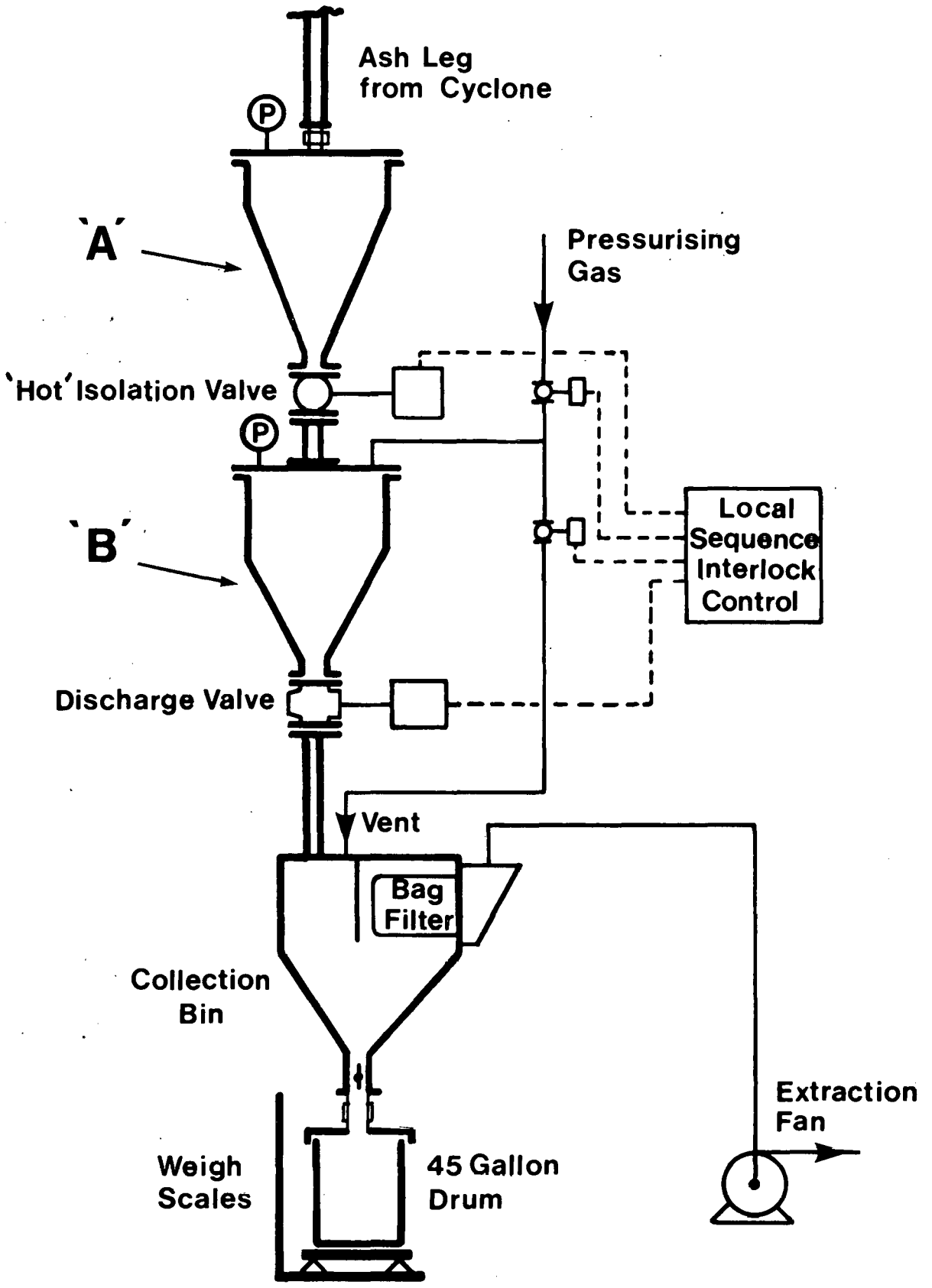

Fig. 10 Schematic of dust removal system

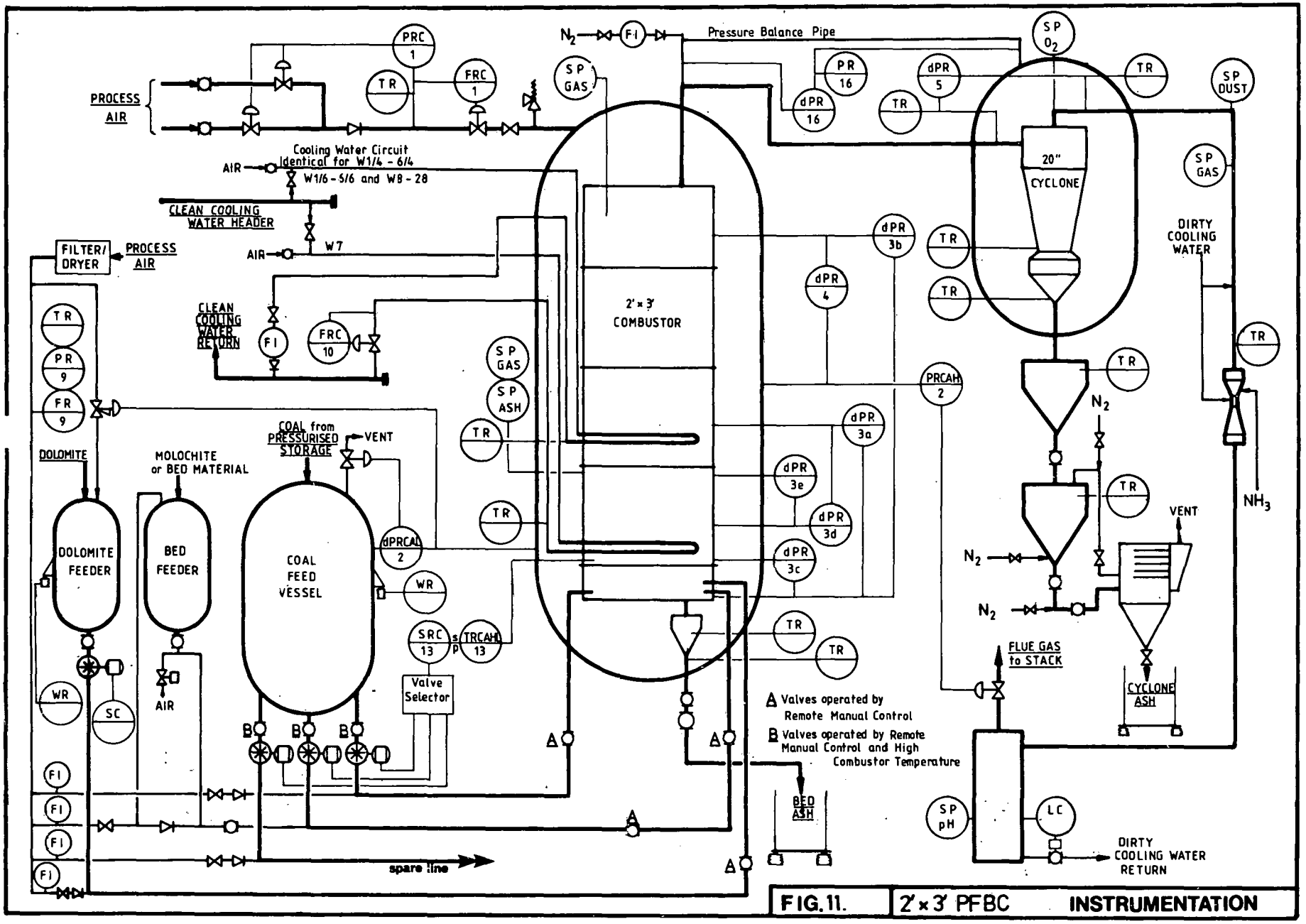

FIG. 11. 2' x 3' PFBC INSTRUMENTATION

D568A

it was required to data-log such signals they were converted to an electrical signal using strain-gauge type pressure transducers. Fluid flows were generally measured by orifice plates in conjunction with pneumatic transmitters and chart recorders. Again, these measurements were converted for data logging where required. All orifice plates conformed to British Standard 1042. Other flows, particularly the cooling water, were measured with variable area meters. Solids flows (coal and dolomite) were determined by changes in the respective load cell outputs with time.

The primary automatic controllers maintained combustor pressure, temperature and air input. The fluidising air leaving the compressed air receiver underwent two stages of pressure reduction: the first to provide a constant pressure supply and the second to provide flow control. Combustor casing pressure was maintained by modulation of the pressure let-down valve at the wet cyclone exhaust. Bed temperature was controlled by variation of coal rotary valve speed.

Secondary automatic controllers were used to control the differential pressure between combustor and

(i) coal feed vessel
(ii) dolomite feed vessel.

Dolomite feed was controlled manually by varying the rotary valve speed.

4.6 GAS AND SOLIDS SAMPLING

The gas sampling system is shown in Fig. 12. Gas was sampled from two points within the plant: the freeboard and the gas outlet from the cyclone (all the data analyses were based on the latter sample). Each stream was treated in a similar manner. It first passed through a primary ceramic fibre filter. Most of the flow was then vented directly to atmosphere and the remainder passed through a sintered metal filter followed by another ceramic fibre filter. The sample was dried in a Perma Pure permeation distillation dryer and delivered to a range of analysis instruments. The three stages of filtration minimised the possibility of contamination of the dryer. The constituents measured, and the detection methods used were as follows:-

(a) Oxygen - Paramagnetic
(b) Carbon dioxide - Infra-red
(c) Sulphur dioxide - Infra-red
(d) Carbon monoxide - Infra-red
(e) Oxides of nitrogen - Chemiluminescene

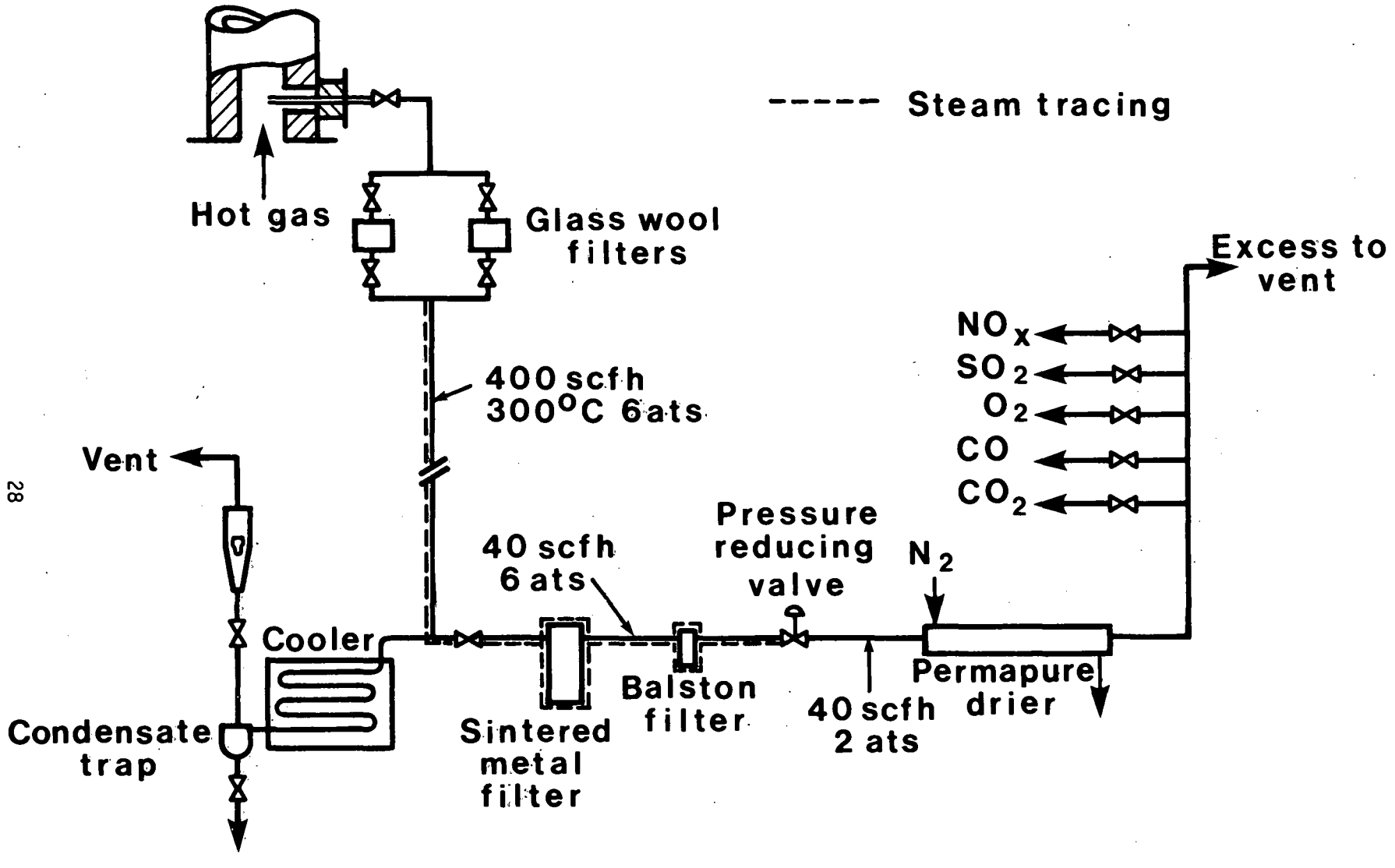

Fig.12 Diagram of system for sampling hot gases.

D564 A

Dust carried in the exhaust gases from the cyclone was sampled using a technique developed at NCB CURL and shown schematically in Fig. 13. Gas was withdrawn isokinetically through a sharp edged nozzle from the centre of the cyclone discharge duct, three duct diameters downstream from a half-area mixing baffle, cooled to (and maintained at) about 480°F and passed through a small cyclone and back-up filter. The gas was then cooled, dried and the flow measured by a variable area meter before being discharged to atmosphere.

Coal was sampled from the feed vessel offtakes (above the rotary valves) once every hour and bulked into a single sample over the period of a Test Section. Dolomite was sampled in a similar manner.

A gas/solids sampling probe (Fig. 14) was capable of traversing the fluid-bed between the wall and the vertical centre line, horizontally at a level approximately half-way up the tube bank. Traversing was achieved with a manually-powered chain drive. To avoid the problems associated with sliding seals, the probe was arranged to retract into an ancillary horizontal pressure vessel attached to the combustor pressure shell. Once the probe was in the fully retracted position, the ancillary pressure vessel could be isolated from the combustor and, after depressurisation, access to the probe inserts was possible. Separate probe inserts were used for sampling bed solids and for sampling gases. The former insert was an uncooled tube, whilst the latter was steam cooled. For sampling solids, the probe was advanced to the chosen insertion into the bed, using a nitrogen purge to keep the probe free of solids. Then, by adjustment of differential pressure the bed solids were allowed to collect in the bore of the probe insert. A ceramic fibre filter in the probe head was provided to prevent solids from entering the depressurising piping. The probe was immediately retracted into the ancillary pressure vessel to enable the bed sample to be recovered. In the gas sampling mode, gases from the fluid-bed passed through a sintered stainless steel insert at the probe tip and a ceramic fibre filter in the probe head. The filtered gases then flowed through a flexible stainless steel hose within the pressure shell, through the closure plate and then to the gas analysis instruments.

Temperature traverses were carried out by installing a Type K (chromel/alumel) stainless steel sheathed thermocouple in the solids sampling probe so that the junction was protruding 1 inch from the nose of the probe.

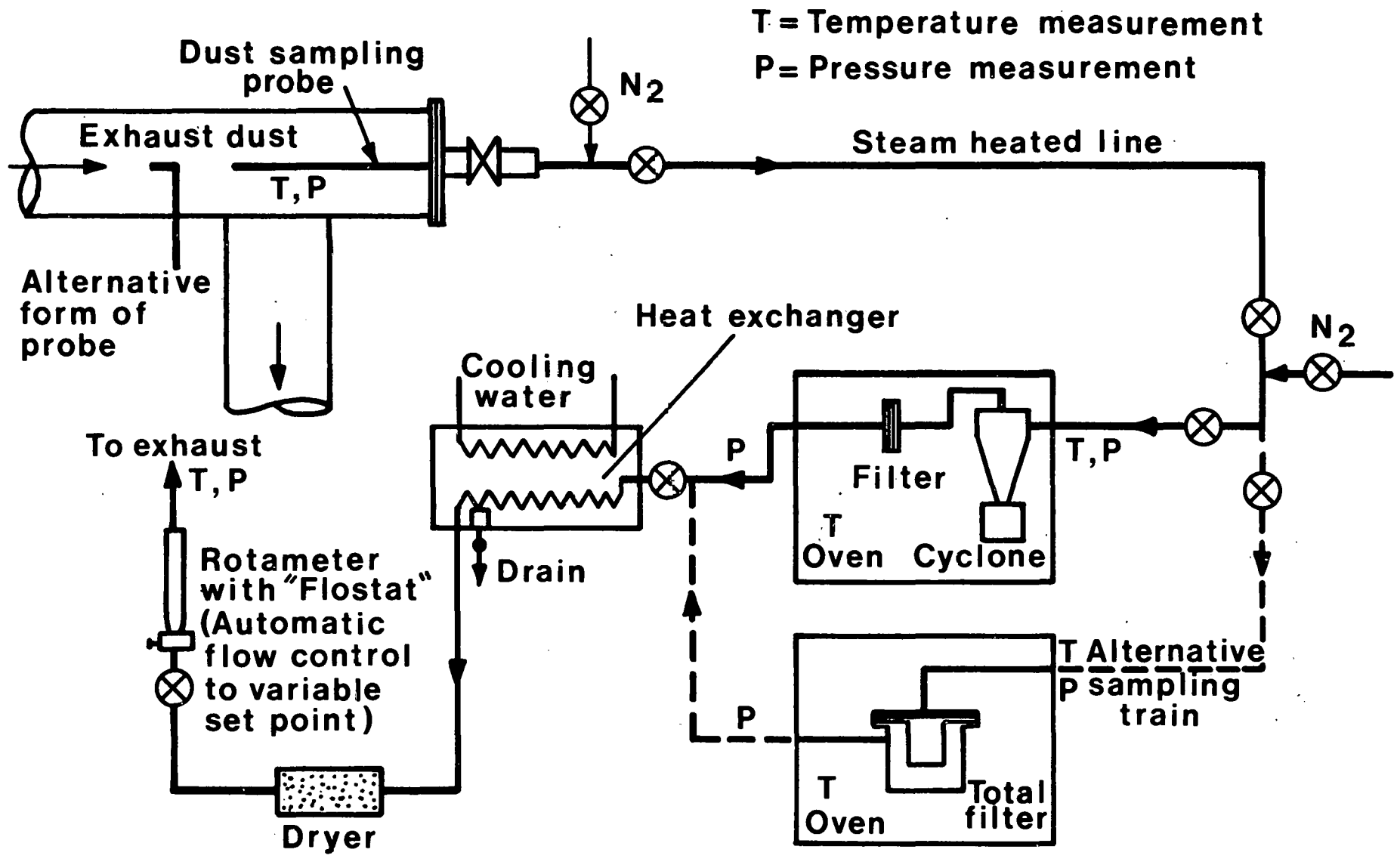

Fig.13 Arrangement of dust sampling systems

D565

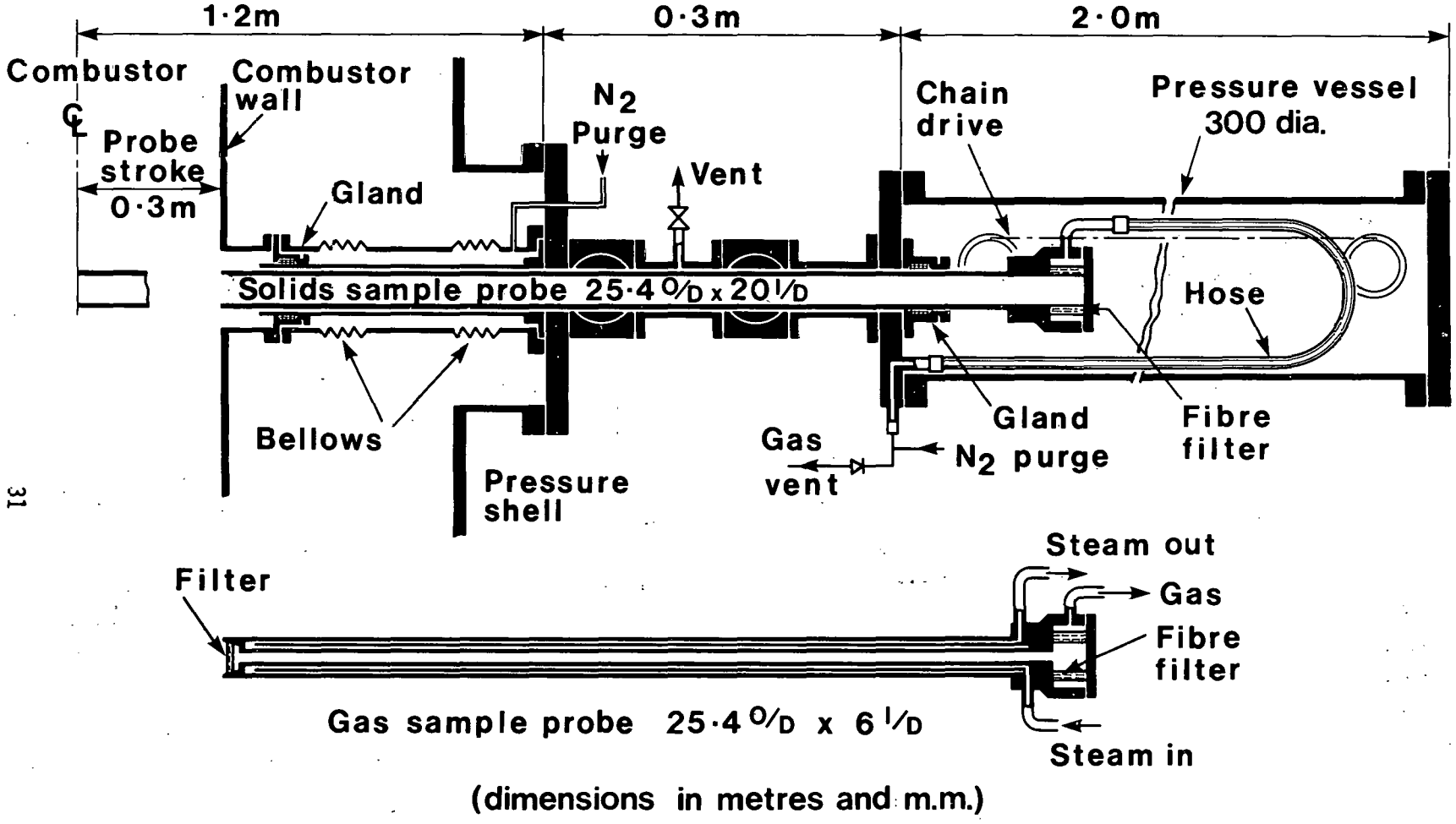

Fig.14 IN-BED SAMPLING PROBE

D567 A

4.7 ALARMS AND INTERLOCKS

The facility as a whole was equipped with alarms and interlocks to ensure safe operation. The major ones were as follows:-

(a) Combustor high temperature alarm and coal shut-off

(b) Combustor low temperature alarm

(c) Combustor high pressure alarm

(d) Coal-feed-to-combustor low differential pressure alarm and coal feed shut off.

The coal feed, dolomite feed and cyclone ash removal systems also were fully interlocked to prevent unsafe operation.

4.8 DATA ACQUISITION

Data-logged information was stored on punch tape for subsequent feeding into the computer system via a site terminal. The logging system could handle up to 100 temperature inputs and up to 50 other voltage measurements (e.g. converted pressures and flows). The logger normally scanned all channels once every 10 minutes but isolated scans could be obtained at other times and used in conjunction with the computer to provide immediate and comprehensive status reports. A micro computer, located on site, was linked to selected data points and provided a continuous visual display of important parameters such as air flow, combustor pressure and temperature, fluidising velocity, coal feed rate and dolomite feed rate.

5. COAL AND DOLOMITE DETAILS

The coal used throughout the programme was Ohio Glen Brook coal having the following general analysis:-

Table 1. Average analysis of Glen Brook coal

Moisture	"as fired"	- 3%
Ash	"	- 11-16%
Volatile matter	"	- 34%
Sulphur	"	- 2.8-3.6%
Chlorine	"	- <.08%
Swelling Number (British Standard)		- 5-7

Size distribution:-

% <3.35 mm	-	100
<1.7 mm	-	80-90
<0.25 mm	-	20-30
<0.063 mm	-	7-11

The coal was from the same shipment as that used in the recent 1000 hour test (Reports FE-3121-15a, b, c, d) and showed a similar variation in ash and sulphur contents.

There were sufficient supplies of Plum Run dolomite (Ohio) for only the first test, and the remaining two tests were carried out using a U.K. dolomite - Steetly, from the Whitwell quarry. Analyses of the two dolomites are given in Table 2.

Table 2. Analyses of dolomites

	Plum Run	Steetly
Moisture	0.0%	0.2%
$CaCO_3$	52.3%	50.4%
$MgCO_3$	43.4%	42.6%
Impurities	4.2%	6.8%
Size distribution:-		
% <3.35 mm	100	100
<1.7 mm	69	90-95
<0.25 mm	1	40-47
<0.063 mm	0.3	12

It will be seen that there was a major difference between the size distributions of the two stones.

6. RESULTS

6.1 PERFORMANCE DURING TRANSIENT CONDITIONS

The bed depth was changed 35 times in all, generally between about 9 ft and about 4 ft. Twenty occasions were concerned with commissioning the system and with lowering the bed rapidly in order to test the high temperature Kamyr isolating valve. On the remaining fifteen occasions the gas composition was monitored and results are summarised in Table 3. As with all the part-load investigations in this programme, only part of the tube bank was water-cooled, the remainder operating at bed temperature. It was possible, by admitting or shutting off water to different cooling tubes, to arrange for the amount of cooled surface to be varied and for it to be in different parts of the bed. Three main configurations were utilised as shown in Fig. 15. The total amount of cooled surface was such that, with the tube bank fully covered the excess air was approximately 50%. This meant that the amount of cooled surface was greater when operating at low bed temperatures. In configuration (a) the cooled surface was all below the 4 ft level so that as the bed depth was lowered only uncooled tubes were exposed. The excess air was therefore approximately the same at the end of the change. In configuration (b) the cooled surface was arranged to be evenly distributed throughout the bed height so that as the bed level was lowered, some cooled tubes were exposed and the excess air increased. In configuration (c) the cooled surface was arranged to be all in the top part of the tube bank so that as the bed level was lowered all the cooled tubes were eventually exposed and the excess air increased more than in (b).

The following points are relevant in interpreting Table 3, which is concerned only with configurations (b) and (c).

(1) When increasing bed depth with the bed temperature in automatic control, there was an increase in coal feed rate to compensate for the influx of cooler bed material and also to compensate as more cooled surface was immersed in the bed. This produced an overall reduction in excess air. The O_2 concentration went through a "trough" if the bed level was changed at a high rate - 0.4 ft/min or higher. At rates of change less than 0.2 ft/min, however, the automatic control loop maintained a matched increase in coal feed rate and there was a steady reduction in O_2 concentration, with no "troughs".

(2) When reducing bed depth with the bed temperature in automatic control, there was a steady increase in excess air as cooled surface became exposed to freeboard conditions.

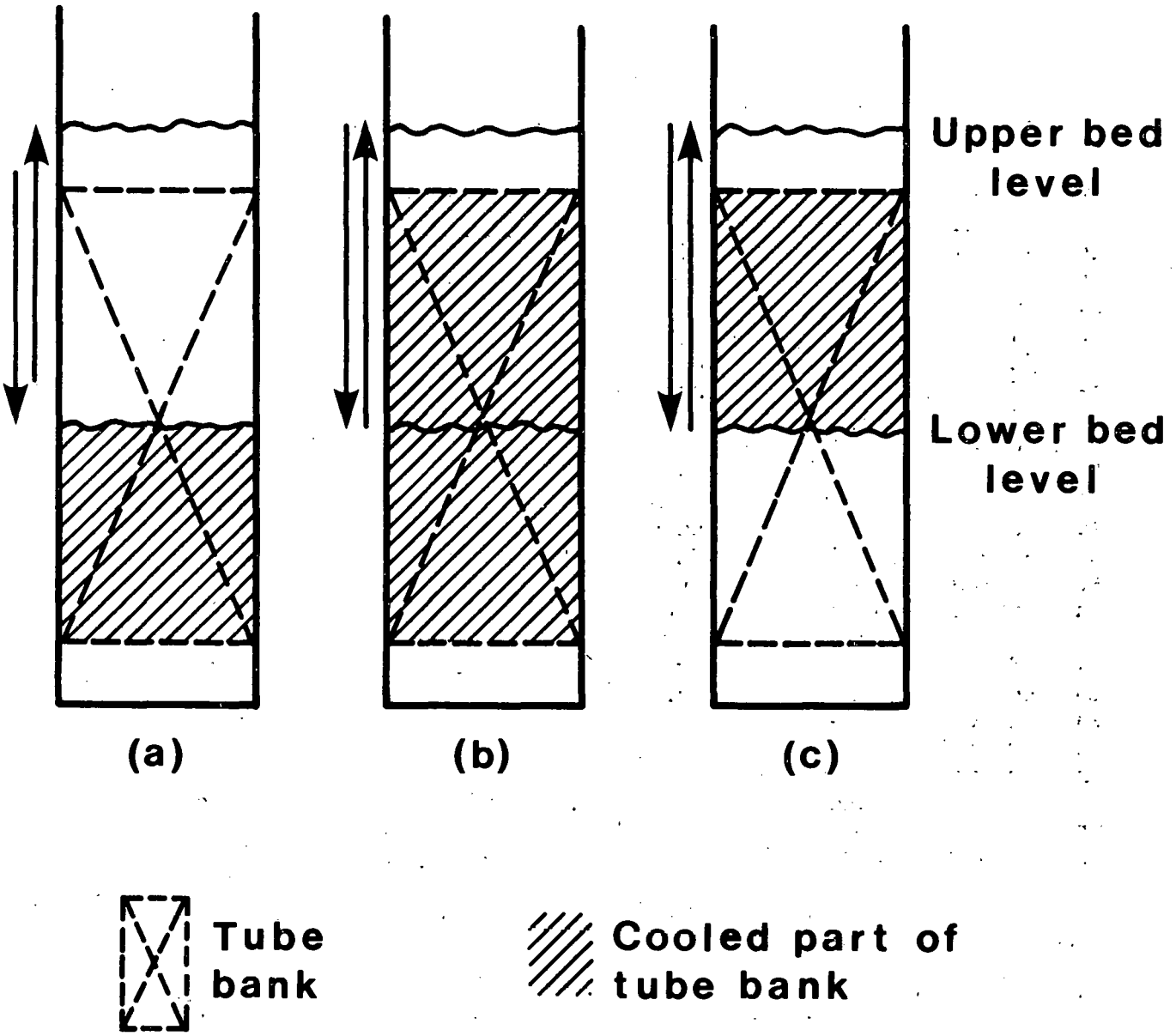

Fig.15 Different arrangements of cooled surface used in the programme

Table 3. Summary of changes during transient operation

Date	Time	Bed level change ft	Rate of change ft/min	Bed temp. °F	Heat** Transfer System	Change in			
						O_2 %	CO ppm	NO_x ppm	SO_2 ppm
10/29	1159	3.3 → 9.2	0.54	1400	(b)	11.5→ 4 →8.3	2500→140	-	420→520→320
10/29	1045	5.6 → 9.5	0.2	1400	(b)	9.8→ 7.5	600→160	200→250	330→390→300
10/29	1124	9.2 → 3.7	0.5	1400	(b)	7.5→11.5	160→2500	250→120	400→460
10/28	1657	5 → 9.5	0.2	1650	(b)	7.5→ 2.5→7.3		180→ 90→170	350→550→330
10/29	1436	4.9 → 9.7	0.2	1650	(b)	9 → 5.8→6.8	20→ 30→20	210→200	230→270→170
10/29	1612	4.4 →10	0.35	1650	(b)	10 → 5 →7	20→ 40→15	210→180→210	270→370→140
10/29	1344	9.6 → 4.6	0.25	1650	(b)	6.5→ 9.3	5→ 5	190→200	200→390→290
10/29	1549	9.8 → 4.1	0.48	1650	(b)	7 →10	20→ 20	200→210	170→390→280
10/29	1912	5.0 → 9.8	0.42	1650	(c)	12 → 5.5→7.3	10→ 30→ 5	220→160→230	140→270→100
10/29	2231	4.6 → 9.4	0.27	1650	(c)	11.3→ 6.3→7.5	5→ 30→ 5	210→220	180→290
10/30	0046	4.5 → 9.3	0.44	1650	(c)	11.8→ 4 →7.5	5→ 30→ 5	210→175→220	160→370→150
10/29	2119	9.5 → 4.5	0.31	1650	(c)	7.5→11.5	20→ 30→10	230→200	170→380→200
10/29	2332	9.7 → 4.3	0.45	1650	(c)	6.3→12	5→ 10	220→180	180→350→190
10/29	1746	4.7 → 9.5	0.18	1430→1640*	(b)	8.1→ 5	230→350→10	220→180→220	250→400→610
10/29	1707	9.7 → 4.8	0.29	1640→1470*	(b)	7 →13.8→8.3	5→200	210→230→220	140→260

* Pressure was changed from 35 psig (at 4.7 ft) to 75 psig (at 9.5 ft) and vice-versa whilst bed depth and temperature were changing.

** See Fig. 15 for arrangement of cooling surface.

D697

(3) On two occasions bed temperature (at an overall rate of about 10°F min) and pressure (at a rate of about 2 psi/min) were altered simultaneously with bed depth. The pressure was changed by locking the pressure reducing valve in position and altering the set point for air flow at the same time as the set point on the temperature controller, at one minute intervals. Fluidising velocity was maintained approximately constant. This sequence of operations simulated, as nearly as possible in the absence of a gas turbine, load changing in a combined cycle plant. Although the absolute pressure level was lower than would occur in a gas turbine, the 2 to 1 change in pressure with load was similar to that which would occur with a two-shaft gas turbine.

The data in Table 3 show that:

(a) With 50% excess air as the datum, increasing bed depth from a minimum at 0.4 to 0.5 ft/min did not reduce the excess air below about 12%. This minimum excess air existed for only a few minutes and caused a minor excursion in CO if the bed temperature was high, a momentary reduction in NO_x emission and a momentary increase in SO_2 emission.

(b) At a bed temperature of 1400°F, decreasing the bed depth resulted in CO emission increasing from 140 ppm (v/v) at 9 ft bed depth to 2500 ppm at 3.8 ft bed depth as shown in Fig. 16.

(c) At 1650°F bed temperature, the CO emission was about 10 ppm and varied little with bed depth. The relationship between gas composition and bed temperature is summarised in Fig. 17 for a bed depth of 9.5 ft and a constant amount of bed cooling surface (i.e. excess air decreased as temperature increased). This shows that CO emission was strongly dependent on bed temperature and not on O_2 concentration (providing there was excess O_2 available). NO_x emissions increased slightly as the bed temperature decreased. This coincided with an increase in O_2 concentration, but as is discussed more fully in Section 6.2.3, it seems that temperature was the main influence.

(d) Typical results obtained when changing bed temperature, bed depth and pressure simultaneously are shown in Fig. 18. The initial starting point was a shallow bed of 4.9 ft depth, low bed temperature of 1440°F and pressure of 32 psig. As a result, the initial CO and SO_2 emissions were high at 250 ppm and 220 ppm respectively.

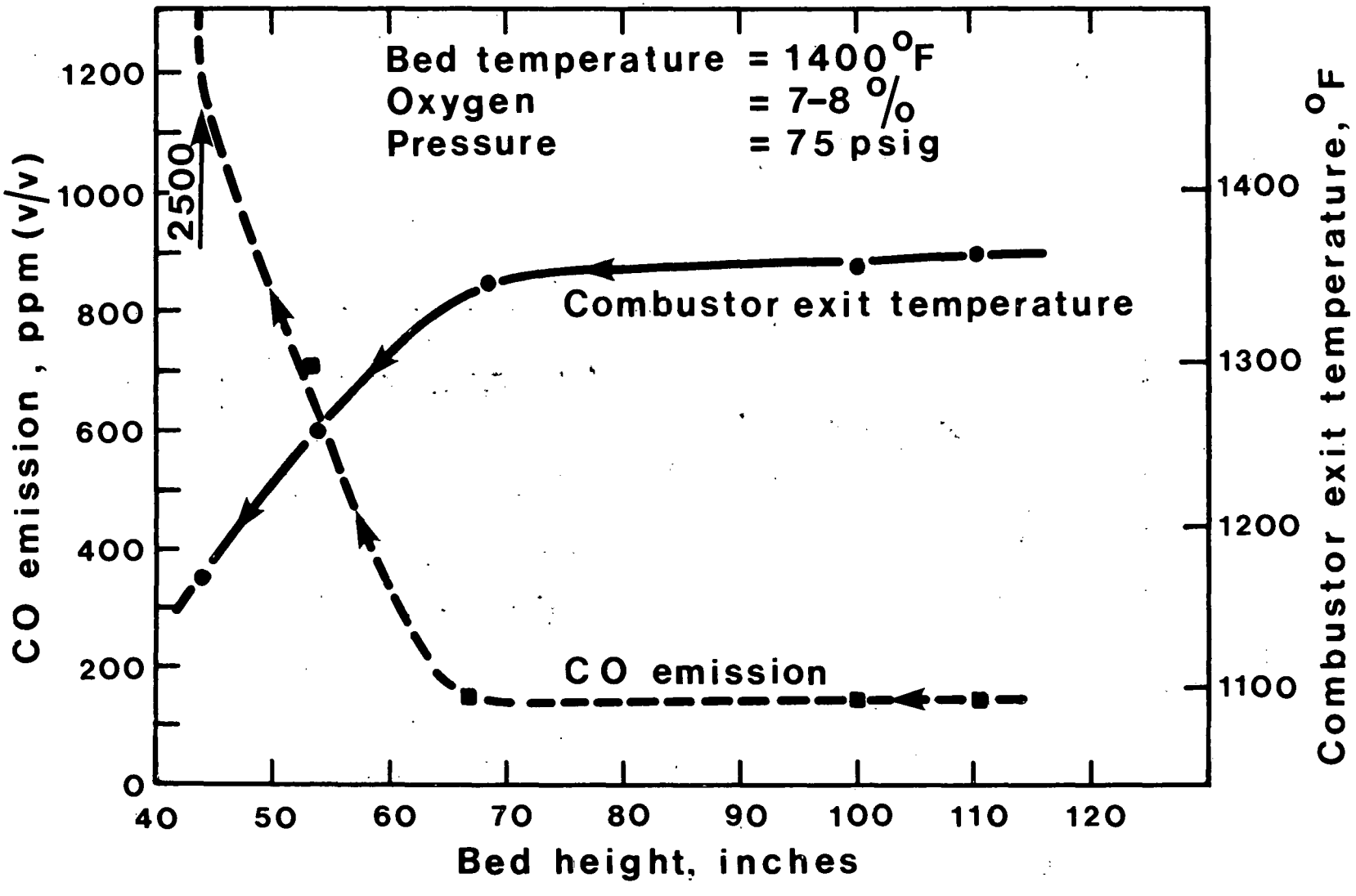

Fig.16 Effect of reducing bed height on CO emission

D609

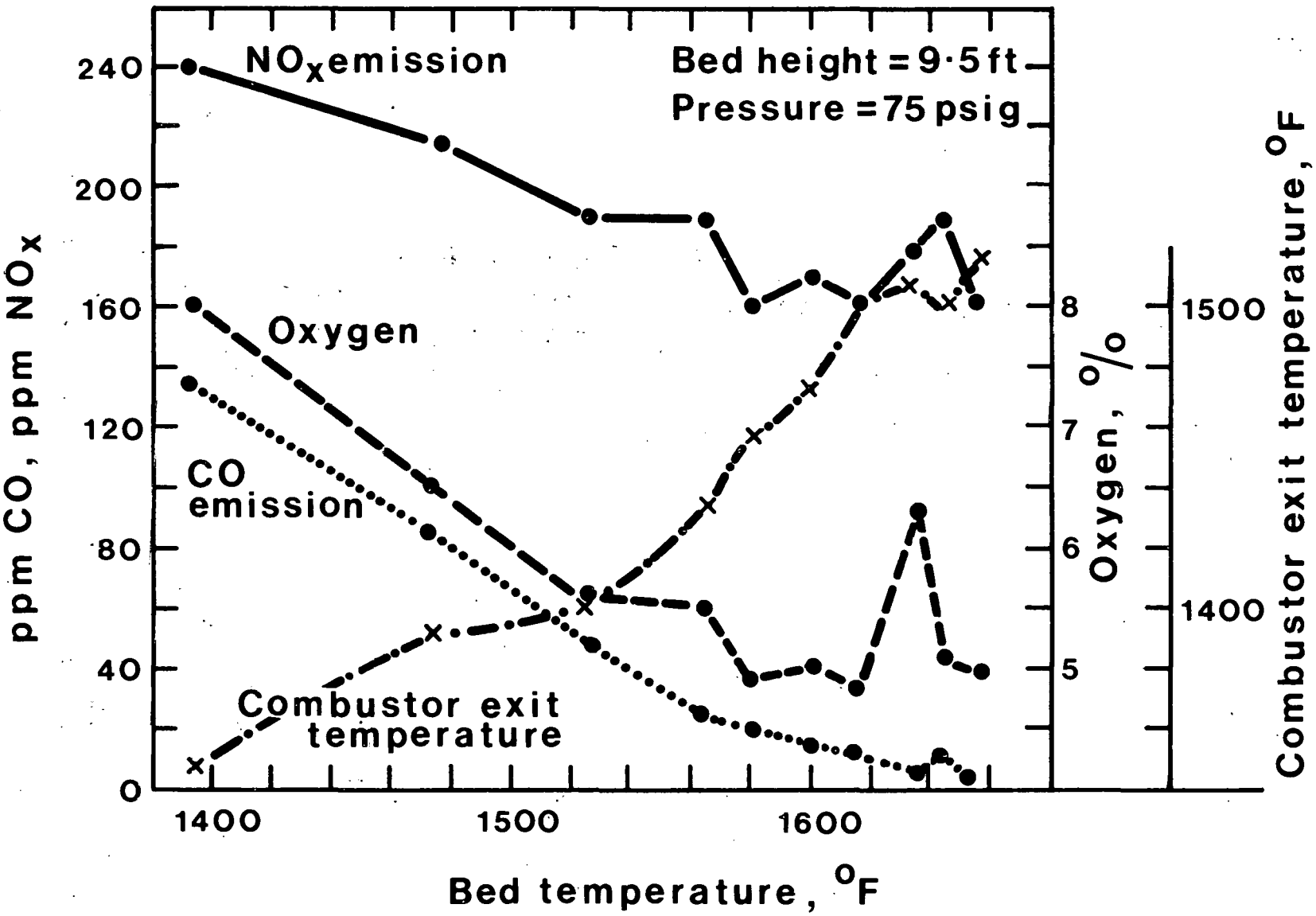

Fig.17 Effect of increasing bed temperature

D610

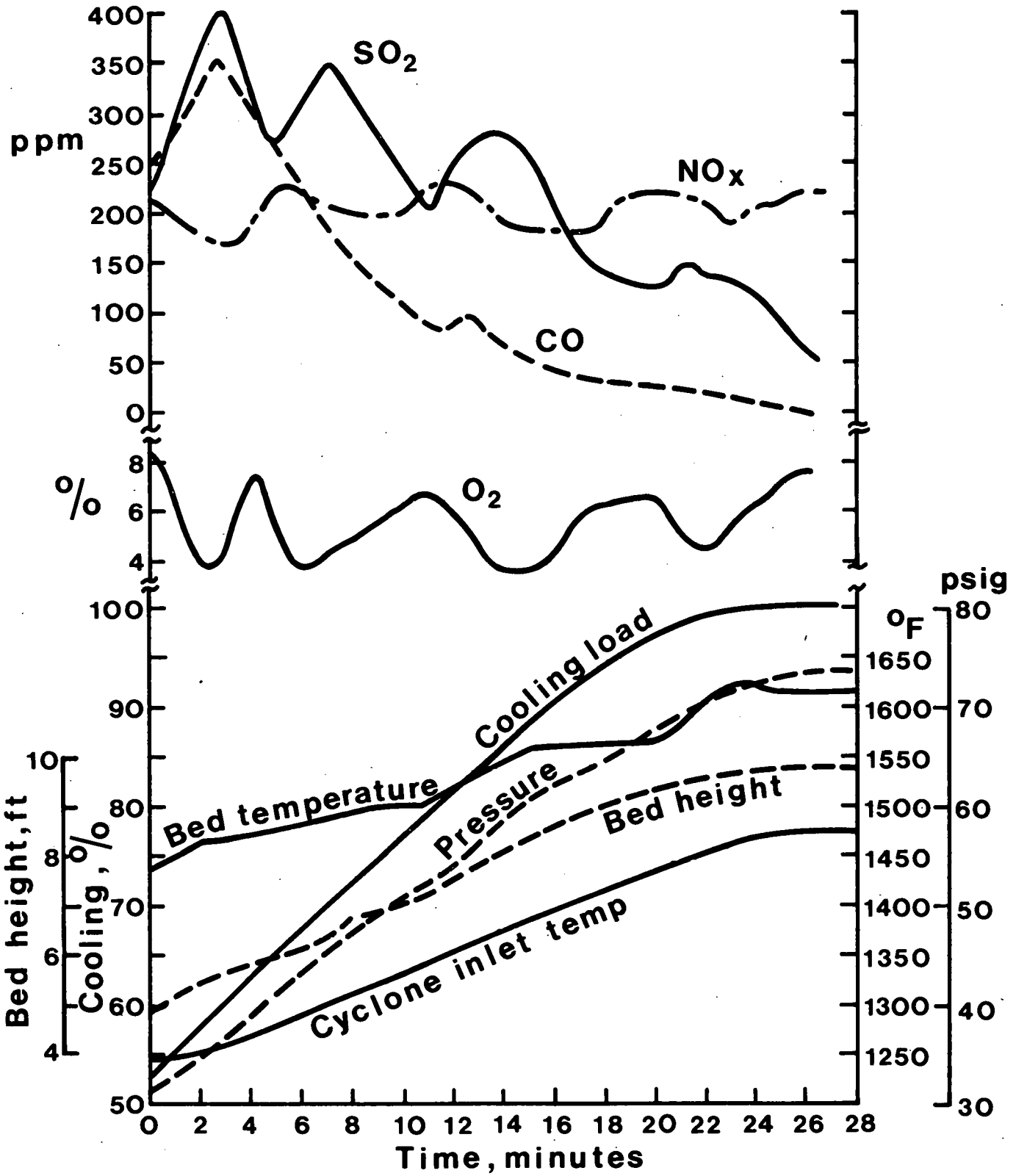

Fig.18 Changes during a load increase

D623

As the air flow (and therefore the pressure), bed temperature and bed depth were increased, the coal feed rate had to increase by many times. This increase was accomplished by a mixture of steady increases (to match increases in airflow and cooled bed material) and step increases (to match increases in bed temperature and in cooling load as water-cooled circuits were covered by the increasing bed depth).

The step changes produced rapid changes in O_2 concentration in the flue gas. The excess air was 65% at the start of the load change and 50% at the end, passing through a minimum of 20% on the way.

The initial increase in coal feed rate was sufficient to increase the CO and SO_2 emissions momentarily to a peak of 350 and 400 ppm respectively. Thereafter, the effect of bed height was dominant in reducing the emissions to final values of 10 and 50 ppm respectively. The effect of further rapid increases in coal feed rate could still be detected by peaks in SO_2 emission and troughs in O_2 concentration.

NO_x emission changed in sympathy with changes in O_2 concentration, but with no significant change in start-to-end conditions. At first sight this might be thought to be at variance with the experience in (c) above, but it must be remembered that in Fig. 18 the increase in coal feed rate was very large and the NO_x emission in $lb/10^6$ Btu was decreasing as the load increased.

All the changes indicated in Fig. 18 were reproduced from charts with the exception of the changing cooling load. Thus the rates of increase of bed height and pressure were reasonably steady, whilst the increase of cyclone inlet temperature was extremely steady. The cooling load increased in a step-wise fashion as water-cooled circuits became immersed in the bed. No attempt is made to show this in Fig. 18, a straight line being drawn between the initial and final cooling loads.

Conclusion: It has been demonstrated that load can be altered in a rapid and controlled manner by changing combinations of bed depth temperature and pressure. Although load changes caused some transients in gas composition, these were not sufficient to cause operational difficulties.

The most important practical change was the reduction in O_2 concentration which occurred when the bed height was increased at a rapid rate. The

extra energy required to reheat the incoming bed material resulted (in the most extreme case) in a temporary drop in excess air from 65% to 12%. In a full-scale plant the loss of heat from the stored bed material would be much lower and the excess air "trough" when increasing load would not be as pronounced. Nevertheless, it seems prudent to design full-scale plant for a "full load" excess air of not less than about 50% when using bed depth as a load control parameter.

It was not practicable to cover all possible combinations of variables in this series of tests. When a specific commercial (or demonstration) plant is designed, with specific gas turbine and steam conditions (and therefore specific load-following conditions), it may be necessary to reproduce the exact part-load transients on the Leatherhead rig.

6.2 OPERATION AT STEADY-STATE CONDITIONS

During the programme a number of test sections were carried out at different bed depths, bed temperatures, and with or without cooled surface in the freeboard*. These represented possible part-load operating conditions. Details and analyses for each of these test sections have already been reported in Documents Fe-14129-2, 4 and 5, and will not be repeated here. The operating conditions and some of the main results are given in Table 4.

6.2.1 Combustion

A feature of part-load operation was that some combustion took place in the freeboard, the extent of which increased as the bed temperature and bed depth were reduced and which was inhibited when cooled coils were exposed in the freeboard.

Combustion in the freeboard was monitored by temperatures measured at various positions in the combustor. Thermocouples were inserted through the walls to a depth of 3 inches. Measurements in the bed were probably reasonably accurate, but measurements in the freeboard would have been subject to radiation errors. Nevertheless, it is believed that the measurements reflected the general pattern of combustion.

Typical temperature distributions are shown in Fig. 19 for what might be termed a maximum load condition of high bed temperature and deep bed, and in Fig. 20 for a minimum load condition of low bed temperature and low bed depth with some cooling in the freeboard.

---

* "Freeboard is defined traditionally as the space between the top of the bed surface and the gas exit. In these experiments, depending on the bed level and the arrangement of cooled surface, the freeboard could contain (a) no tube bank; (b) an uncooled tube bank or (c) a partially-cooled tube bank.

Table 4. Summary of steady-state operating conditions and main results.

Test/Section		1/1	1/2	1/3	1/4	2/1	2/2	3/1	3/2	3/3
Duration	h.	15	17	11	4	17	10	20	20	18
Bed temperature	°F	1460	1630	1405	1635	1400	1400	1630	1385	1650
Fluidising velocity	ft/s	3.7	3.9	3.8	3.9	4.0	4.1	4.1	2.5	4.1
Inlet pressure	psig	74.5	74.5	74.5	74.5	74.8	74.7	75.6	75.3	75.5
Bed depth	ft	4.1	8.8	8.7	9.1	5.8	6	4.3	4.2	8.8
Bed density	lb/ft^3	48	43	45	44	40	40	38	49	40
Freeboard cooling		No	-	-	-	No	Yes	Yes	Yes	-
Arrangement of cooling surface (Fig. 15)		(a)	(b)	(b)	(b)	(a)	(b)	(b)	(b)	(b)
Combustor exit temp.	°F	1510	1530	1375	1555	1460	1330	1140	1155	1515
Total air flow	lb/h	9400	9260	10100	9360	10490	10800	9710	6530	9340
Coal feed rate	lb/h	680	640	740	825	755	730	635	455	600
Dolomite feed rate	lb/h	215	230	255	255	215	215	190	185	210
Ca/S mol ratio		1.65	1.7	1.6	1.55	1.4	1.4	1.6	2.35	2.05
Bed retention	lb/h	195	166	202	101	124	124	64	118	53
Elutriation	lb/h	93	95	129	151	209	209	201	121	177
Excess air	%	53	62	57	29	57	62	59	50	54
Gas analysis (dry, by volume)										
O_2	%	7.5	8.2	7.8	4.9	7.8	8.2	8.0	7.2	7.6
CO_2	%	11.8	11.4	11.5	14.4	11.7	11.2	11.2	12.0	11.6
CO	ppm	-	-	-	-	90	240	45	220	5
SO_2	ppm	310	150	310	200	635	615	375	140	55
NO_x	ppm	160	170	230	170	190	210	205	295	190
SO_3	ppm	3	1.2	3.5	-	-	-	-	-	-
Combustion efficiency	%	97.8	99.0	96.7	97.8	97.1	95.8	96.0	95.3	99.0
Sulphur retention	%	86	93½	87	93	71	71½	79	92	96½
Time constant	s	-	700	-	-	380	-	280	450	700

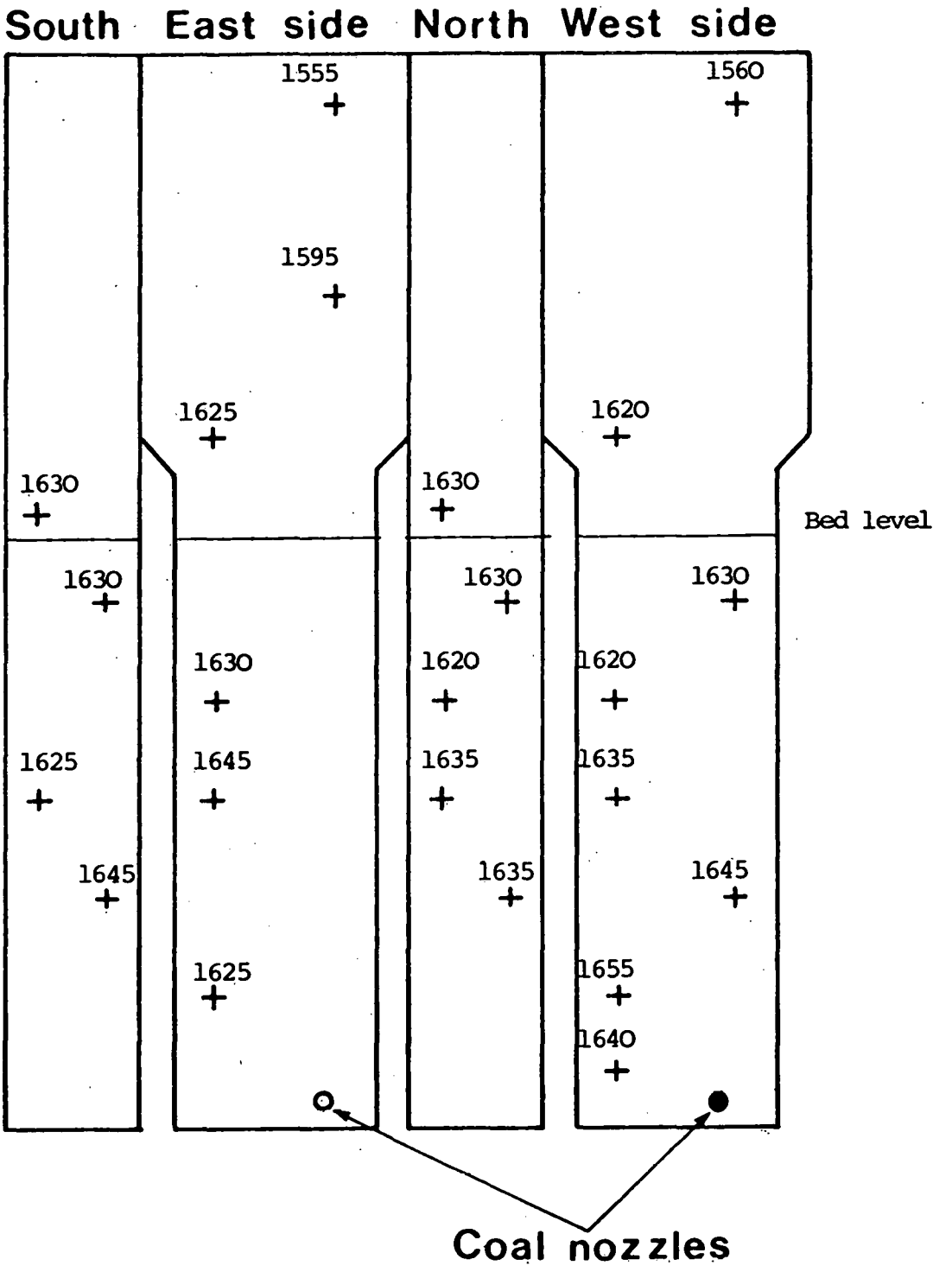

+ Thermocouples project 3 inches into the bed or freeboard at these positions. Numbers are temperatures in °F.

Fig. 19. Temperature distribution
High bed temp. Deep bed.

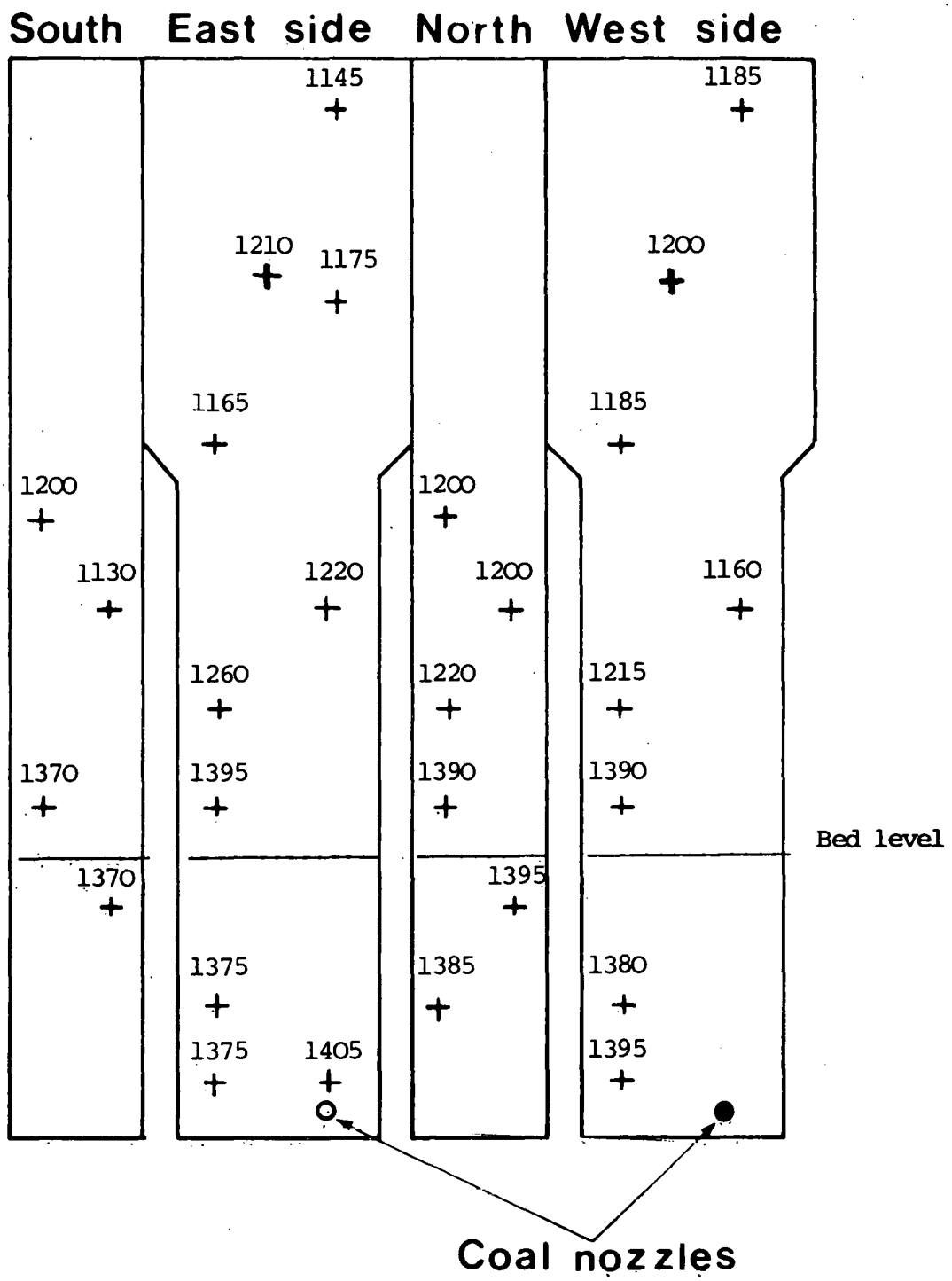

+ Thermocouples project 3 inches into the bed or freeboard at these positions. Numbers are temperatures in °F.

Fig.20 Temperature distribution
Low bed temperature. Shallow bed

D535

From distributions such as those shown in Figs. 19 and 20, composite diagrams have been produced (Figs. 21 and 22) which show the variation in the freeboard temperature for each of the test conditions.

It will be seen from Figs. 21 and 22 that the temperature distribution within the bed was substantially uniform (±20°F). Although this was not as uniform as the distribution obtained in the 1000 hour programme with the tapered bed, it still represents an isothermal reactor.

The temperature distribution in the freeboard depended very much on the operating conditions. With a bed temperature of c. 1640°F and a bed depth of 9 ft, the freeboard temperature fell steadily with distance above the bed surface. At this condition it can be assumed that there was very little, if any, combustion in the freeboard. The drop in temperature (about 100°F) was due to the heat losses through the combustor freeboard casings. This condition will be referred to as the datum in the following discussion.

Reducing the bed temperature to c.1400°F from the datum reduced the temperature drop in the freeboard from 100°F to c.25°F and for three to four feet above the bed surface the temperature was the same as, or slightly exceeded, that in the bed, i.e. some freeboard combustion was taking place.

Reducing the bed temperature to c.1400°F and the bed depth to 4 ft (with the exposed tubes in the freeboard being uncooled) resulted in substantial freeboard combustion with peak temperature rising to 170°F above the bed temperature before declining slightly due to heat losses. Actually, this was not one of the conditions listed in Table 1. Attempts to operate steadily at this condition were abandoned because of the dangers of combustion in the cyclone and because it was apparent that at temperatures below about 1460°F a reduction in bed temperature was accompanied by an increase in off-gas temperature (and vice versa). This is a situation which would make control of gas turbine plant extremely difficult.

Combustion in the cyclone actually occurred when the combustor had been operating at 1400°F bed temperature and 5 ft deep bed for a few hours. There was a rise in temperature across the cyclone of 50°F instead of the usual 10°F drop and this situation could be overcome only by increasing the bed depth to 6 ft.

It was therefore concluded that minimum load conditions (at 4 ft/s, 50% excess air, 6 bar) with no freeboard cooling would be 1400°F bed temperature and 6 ft deep bed or 1460°F bed temperature and 4 ft deep bed. At both these conditions, the maximum freeboard temperature

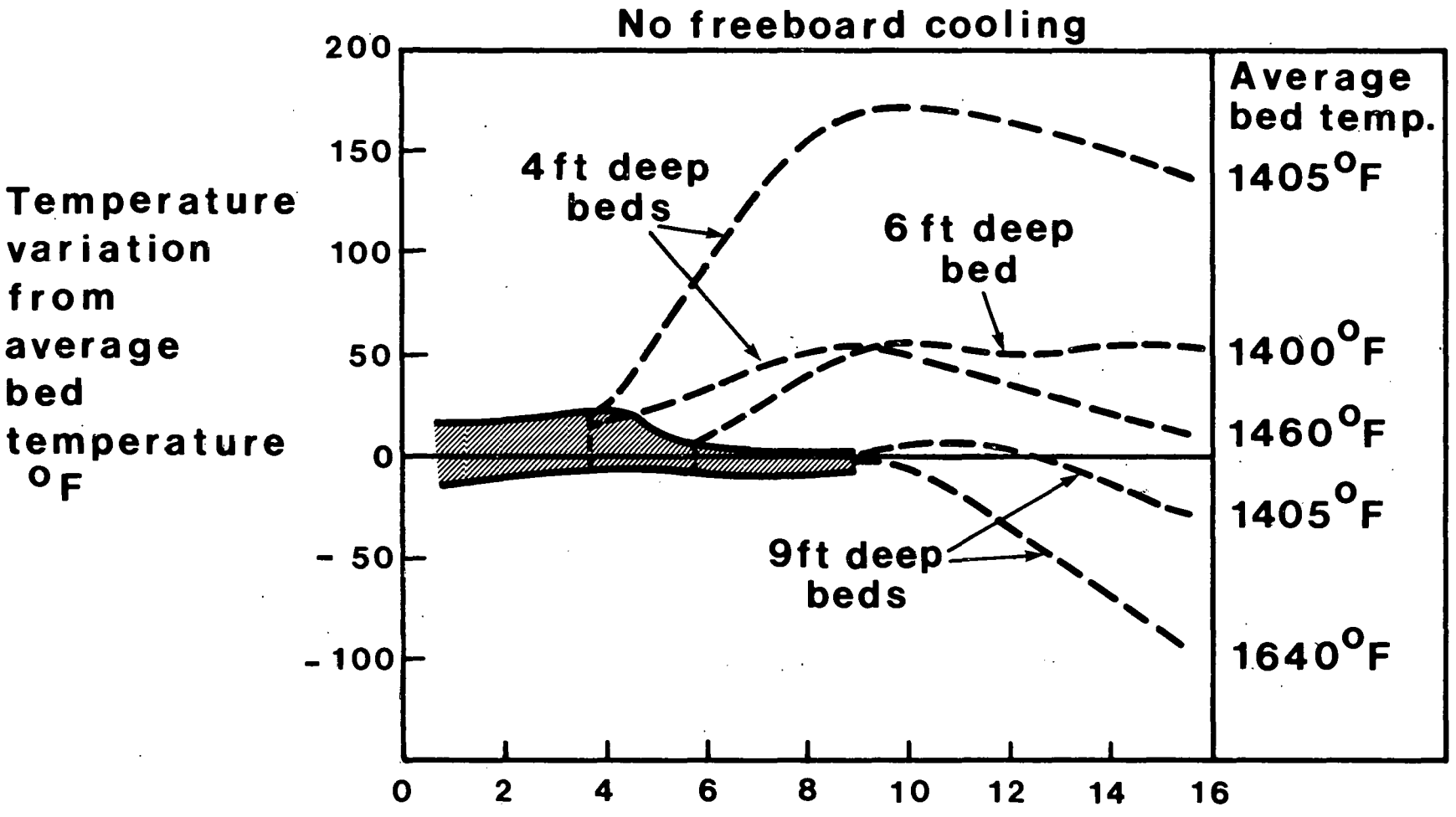

Shaded area indicates spread of temperatures within the bed

Fig.21 Variation of temperature with height above distributor : freeboard uncooled

D650

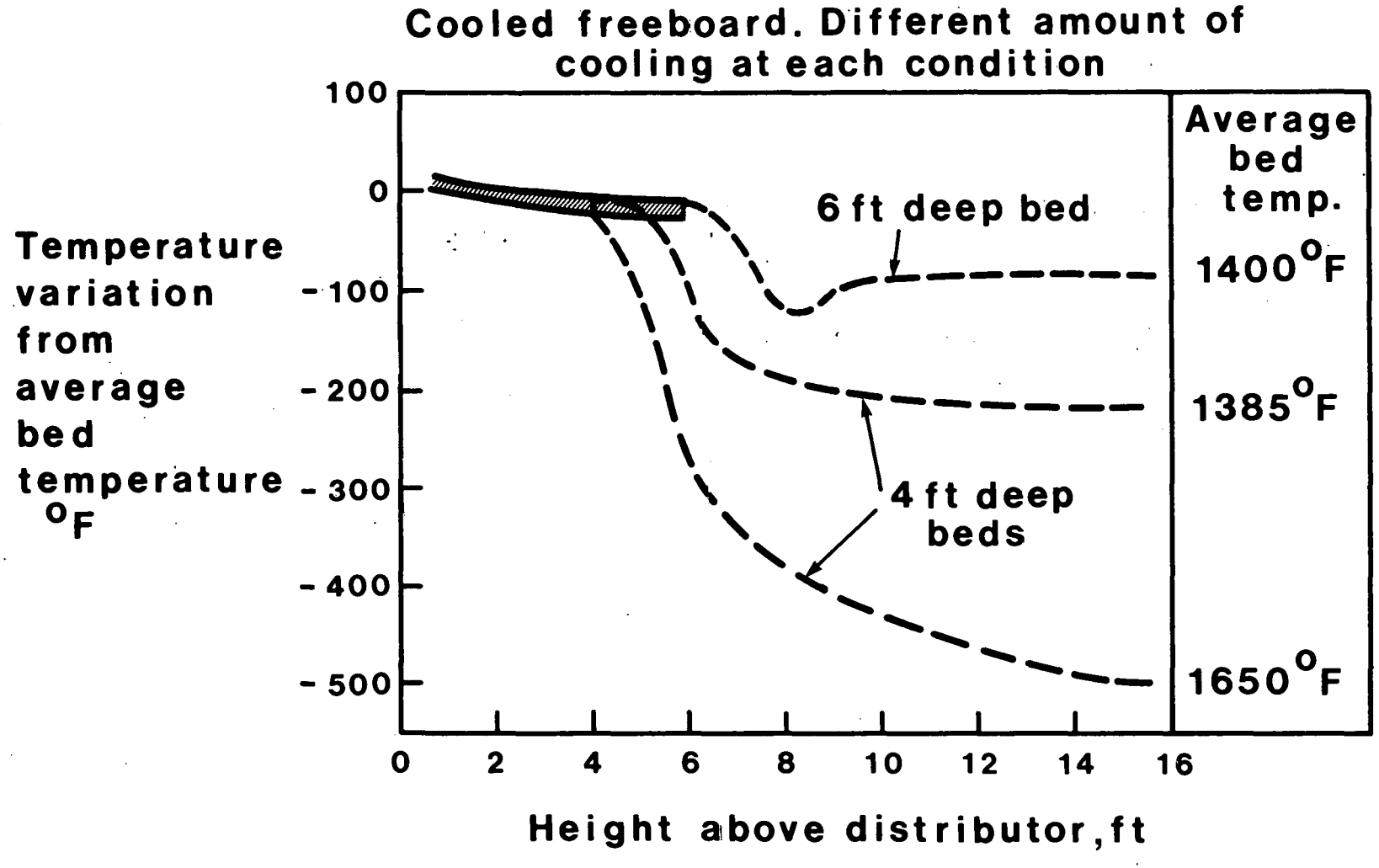

Fig.22 Variation of temperature with height above distributor: freeboard cooled

D651

was 50°F higher than the bed temperature. There was less combustion in the freeboard at 1460°F/4 ft than at 1400°F/ 6 ft.

Subsequently a more systematic investigation into the relationship between bed and freeboard temperatures at a bed depth of 4 ft was carried out. The bed temperature was lowered progressively over a period of several hours. Excess air was maintained approximately constant by adjusting the amount of in-bed cooling. The way in which the cyclone inlet temperature varied is shown in Fig. 23.

With cooled tubes in the freeboard, combustion above the bed was suppressed. The drop in temperature through the freeboard depended on how much cooling surface was activated. Distributions are shown in Fig. 22, but they are not comparable in the same way that data in Fig. 21 are comparable, because different amounts of cooled surface were used at each condition. In the case of the 4 ft deep beds, the cooled surface was adjusted to give a cyclone inlet temperature of about 1150°F - a typical turbine inlet temperature at low load.

Combustion efficiency. The combustion efficiency at each condition is given in Table 4. There was a relatively large variation in efficiency - from 95% to 99% - but because of the number of variables involved, it is not easy to decipher any trends. The data have been rearranged in Table 5 below to help clarify the effect of the different variables:-

Table 5. Effect of variables on combustion efficiency

Bed depth	(Gas residence time)	Bed Temp.	Freeboard cooling	Freeboard combustion	Combustion efficiency
Deep	(2s)	High	None	"No"	99.0
Deep	(2s)	High	None	"No"	97.8*
Low	(1s)	Low	None	"Yes"	97.8
Low	(1.5s)	Low	None	"Yes"	97.1
Deep	(2s)	Low	None	"No"	96.7
Low	(1s)	High	Yes	"No"	96.0
Low	(1.5s)	Low	Yes	"No"	95.8
Low	(1.75s)	Low	Yes	"No"	95.3

* 25% excess air

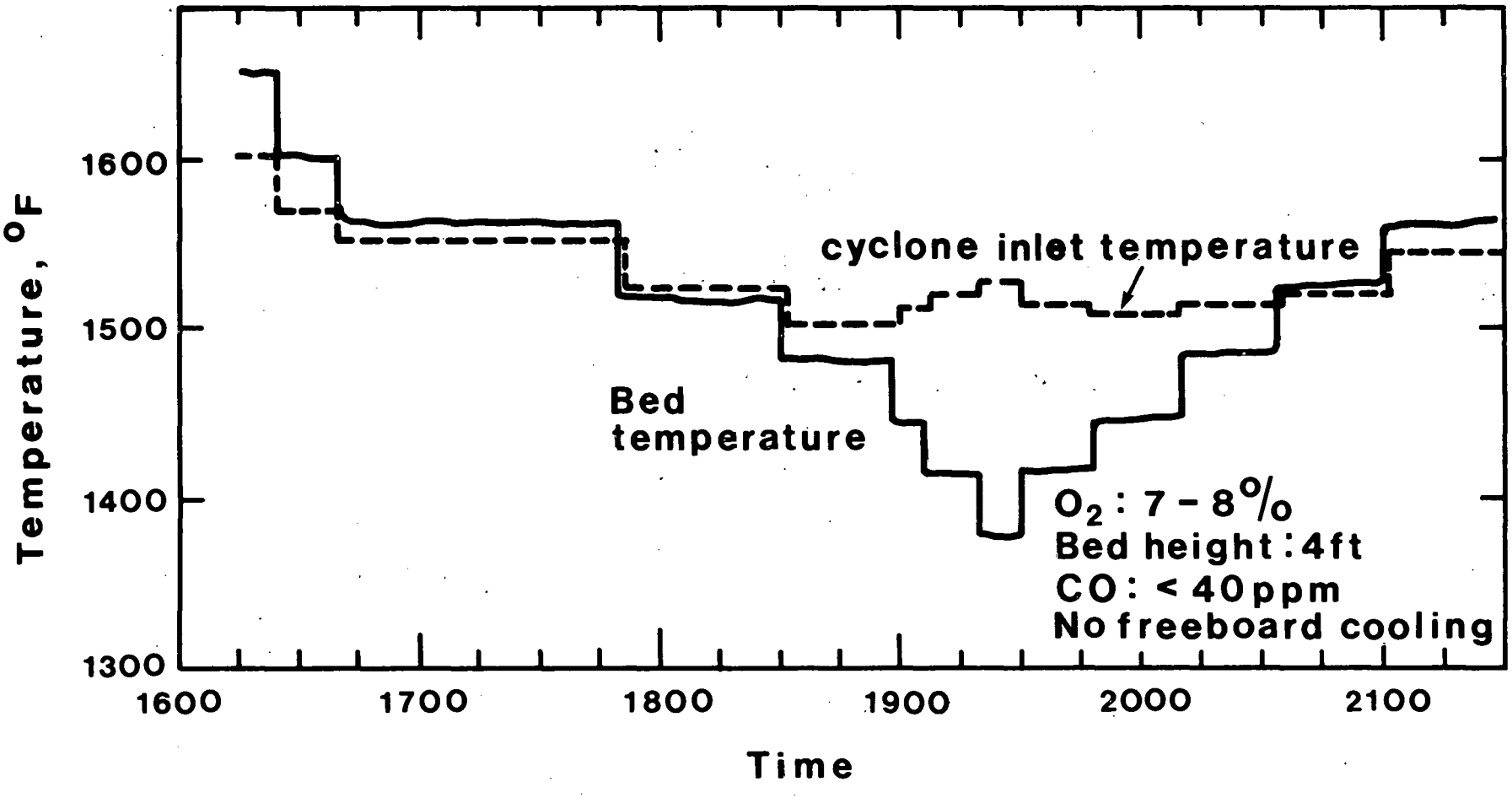

Fig.23 Freeboard combustion investigation

D628

In Table 5, the existence of freeboard combustion is divided arbitrarily into "No" or "Yes" according to whether any temperature in the freeboard was lower or higher than the bed temperature. Examination of Table 5 shows that the combustion efficiency decreased as the gas residence time (almost synonymous with bed depth in these tests) and bed temperature decreased - as might be expected. Suppressing combustion in the freeboard also had a significant effect on combustion efficiency.

The loss of combustion efficiency was due entirely to the elutriation of unburnt carbon. Carbon monoxide concentrations were about 5 ppm (v/v) at the datum conditions. Decreasing the bed depth to 4 ft, and suppressing freeboard combustion increased CO concentrations to about 50 ppm. Operating at low bed temperature, low bed depth and also suppressing freeboard combustion increased the CO emissions to about 250 ppm. None of these CO concentrations has any significant effect on combustion efficiency.

Empirical correlation for predicting combustion efficiency. Over the last five or six years the Leatherhead combustors have been operated over a wide range of conditions of bed area, excess air, fluidising velocity, bed depth, bed temperature, freeboard temperature and coal type. An empirical correlation has been developed:-

$$1-\eta = \frac{A^{0.5}}{R\, t_b\, t_f^{0.33}(1+X)} \exp\left[\frac{2535}{T_b}\right] \exp\left[\frac{-3.67(T_f-T_b)}{T_b}\right]$$

Where η = fractional combustion efficiency
A = bed area per coal feed nozzle (ft^2)
t_b = gas residence time in the bed (s)
t_f = gas residence time in the freeboard (s)
X = fractional excess air
T_b = bed temperature (^oR)
T_f = combustor exit temperature (^oR)
R = a derived coal reactivity factor

It should be noted that the correlation contains no pressure term since all the data were generated at about 6 atmospheres. There is also no term for coal feed size, although this is partly implicit

through the influence of fluidising velocity on t_b and because coal feed size is usually chosen to suit the velocity.

The form of the correlation was based on some 65 sets of data obtained using very similar US coals (Illinois No. 6, Illinois No. 5 and Glen Brook). This enabled the value of R to be derived. The form was then used to obtain values of R corresponding to six other fuels which have been tested in the Leatherhead combustors. Details are given in Appendix 1.

The correlation is compared with observed data in Fig. 24. Most of the data are derived from work sponsored directly or indirectly by DOE (and its predecessors) and are identified separately. Values of the parameters used were A - 0.785 ft^2 (in a 12 inch dia combustor) to 9 ft^2; t_b - 0.2s to 3.6s; t_f - 0.6 to 7.4s; x - 0.2 to 3.0; T_b - 1750^oR to 2200^oR; T_f - 1580^oR to 2200^oR.

A separate comparison of the observed and calculated combustion efficiency for data from the 1980 programme is shown in Fig. 25.

Values of R used in the correlation are shown in Fig. 26, plotted as a function of the oxygen content in the fuel, which is one of the parameters normally used for indicating the coal type.

Combustion with a single coal nozzle. In one of the test sections (Test 3/3), all the coal was fed through one nozzle. The objectives were (i) to investigate the effects of increasing the heat input per coal nozzle (i.e. the ratio of bed area/number of coal nozzles) and (ii) to provide a datum for future programmes in which it is hoped to feed "run of mine" coal to a single point in the bed. Coal was fed through the nozzle marked "dolomite" in Fig. 3 and the dolomite through one of the coal nozzles (i.e. the duties of the dolomite and one of the coal nozzles were interchanged for this test).

The temperature distribution with a single coal nozzle is shown in Fig. 27. It will be seen that there is a zone around the nozzle in which bed temperatures are up to 90^oF higher than the average in the remainder of the bed.

Although the temperature distribution was not as uniform as with two coal nozzles, there were no detrimental effects on combustion efficiency, sulphur retention or NO_x emission.

6.2.2 Sulphur retention

Sulphur retention data are given in Table 4. Because of the number of variables involved the data have been processed further to facilitate

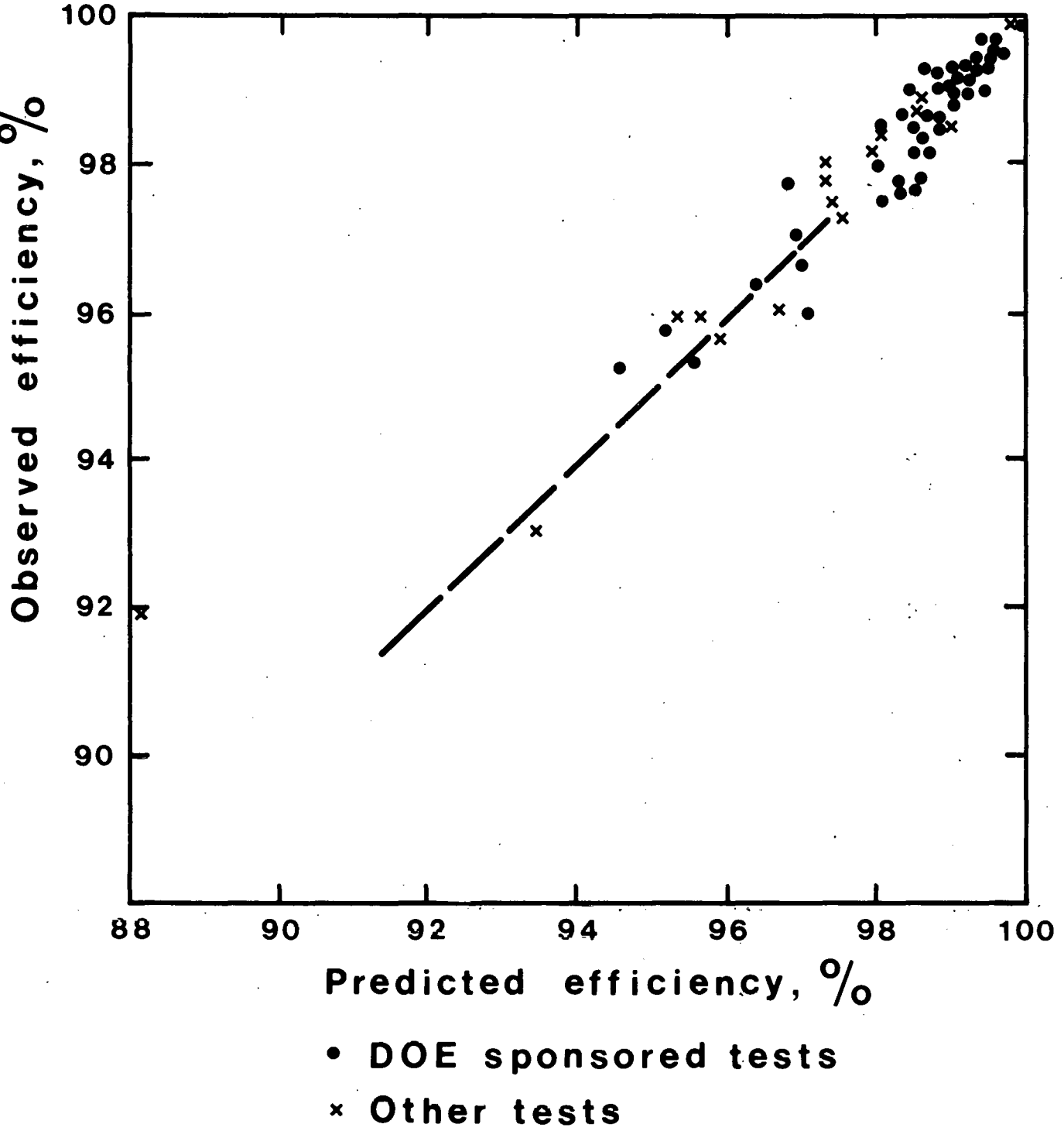

Fig.24 Observed v predicted combustion efficiency

D659

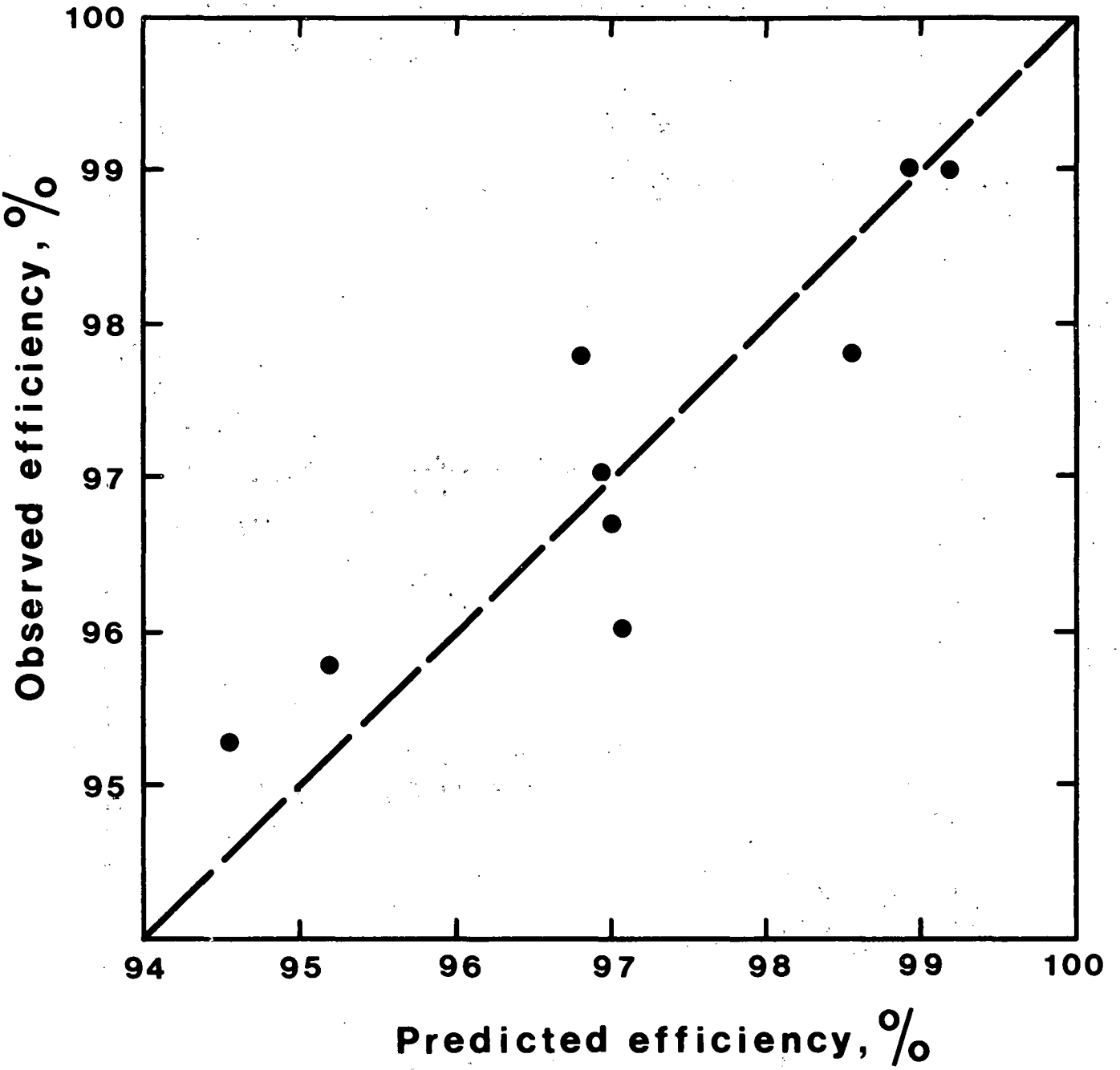

Fig.25 Observed v predicted combustion efficiency (1980 programme)

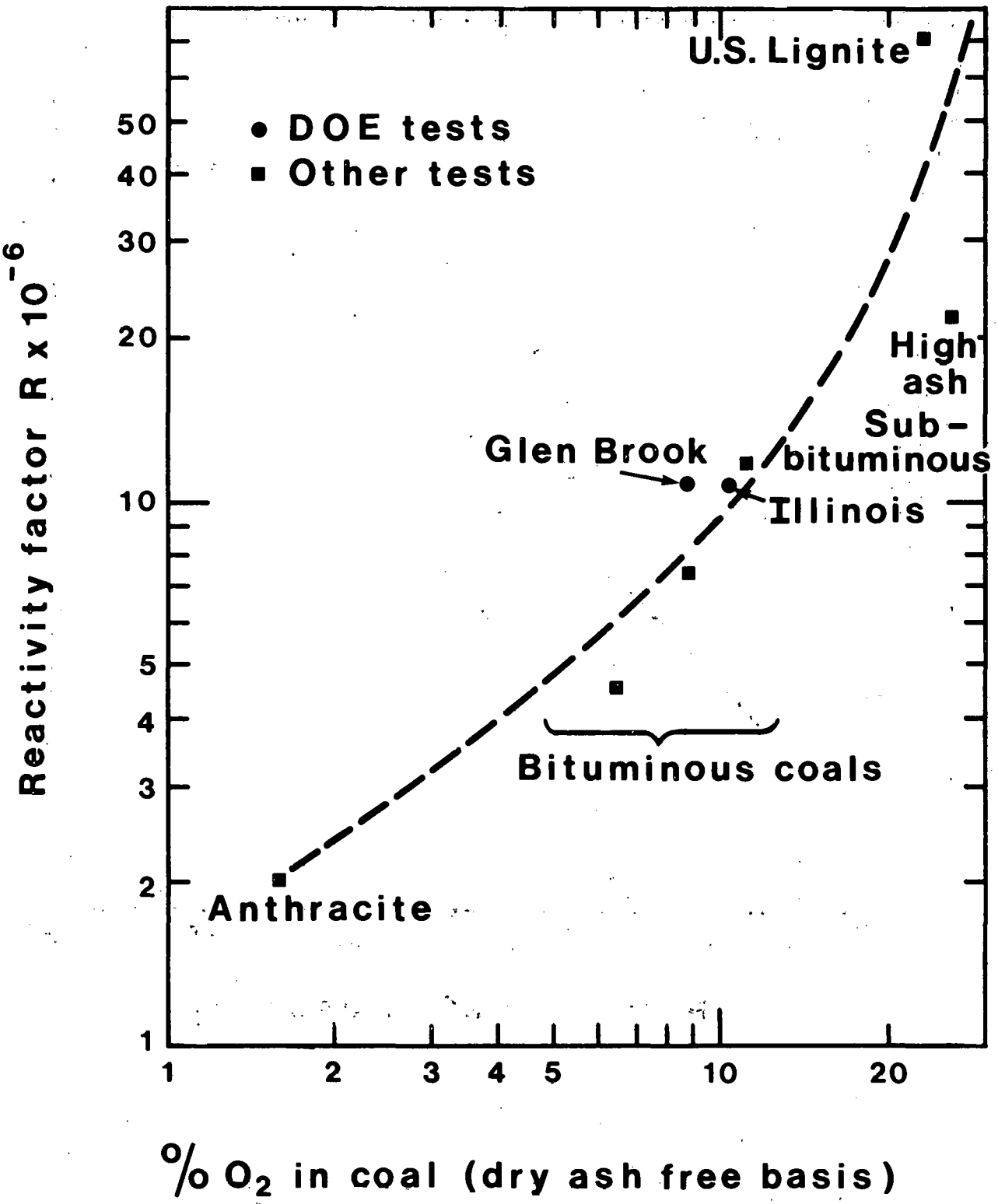

Fig. 26 Relation between coal oxygen content and reactivity

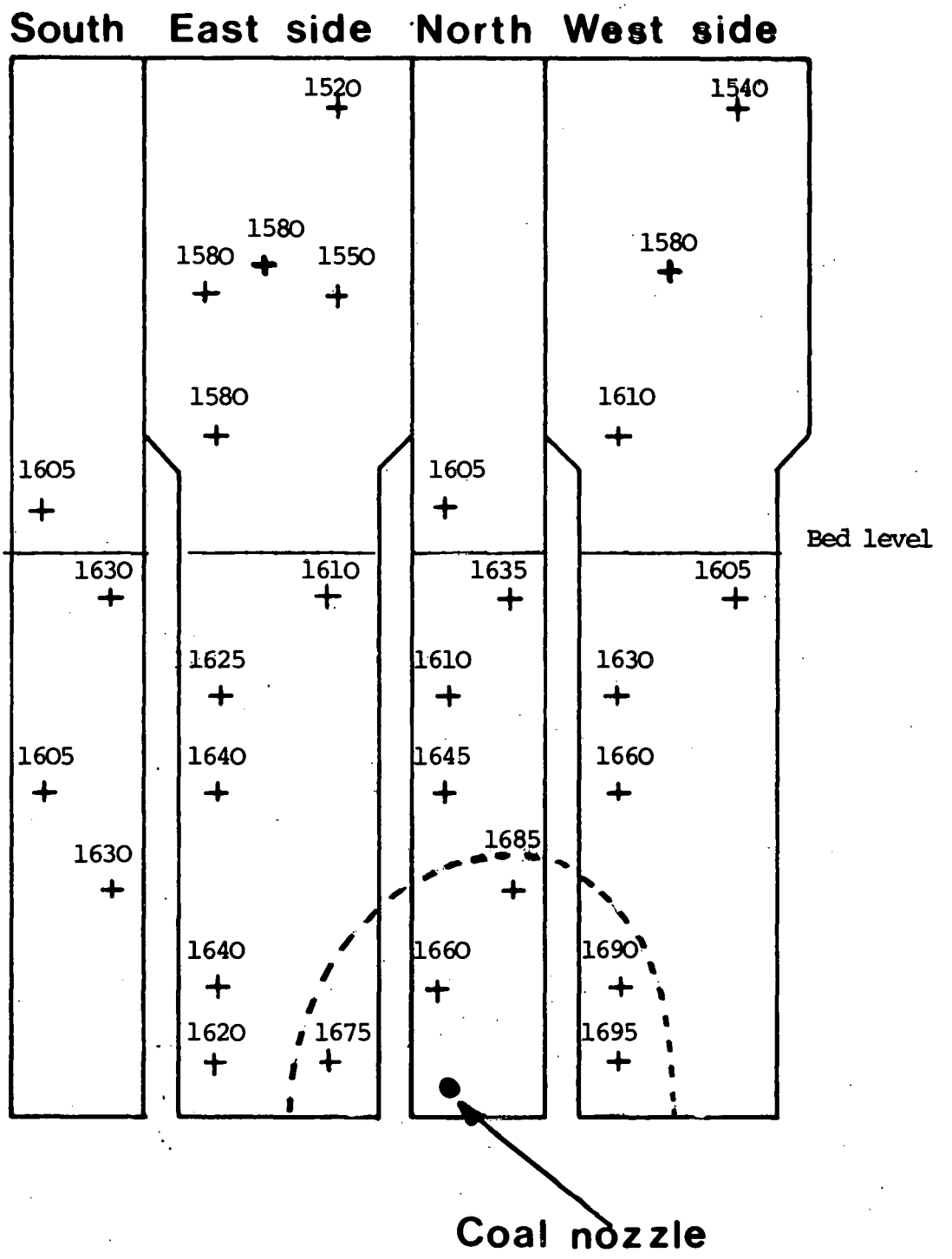

+ Thermocouples project 3 inches into the bed or freeboard at these positions. Numbers are temperatures in °F.

Fig. 27 Temperature distribution
Single coal nozzle

comparison and results are shown in Table 6 where the data have been normalised to common conditions of superficial gas residence time in the bed (2.3s) and of Ca/S mol ratio (1.7) using the following procedures (Ref. 1).

$$R/(100 - R) = at$$
$$\ln(1-R/100) = -b\,C$$

where R = sulphur retention $= 100\left[1-\frac{\text{Sulphur emitted as } SO_2}{\text{Total sulphur in coal}}\right]$ %

C = Ca/S ratio $= \frac{\text{mols calcium in dolomite input}}{\text{mols sulphur in coal input}}$

t = gas residence time $= \frac{\text{Bed depth}}{\text{Fluidising velocity}}$

Fig. 28 shows a plot of sulphur retention against Ca/S ratio for the data normalised to a common gas residence time of 2.3s and Fig. 29 shows a plot of sulphur retention against gas residence time for the data normalised to a common Ca/S ratio of 1.7. There is a clear effect of bed temperature which is emphasised in the bottom line of Table 6 where sulphur retention is normalised to a residence time of 2.3s and a Ca/S ratio of 1.7. Allowing for experimental error, there is a clear division between results at high (1630-1650°F) and low (1385-1405°F) bed temperatures. An exception was Test 1/1 which appeared to give too high a sulphur retention for the operating conditions. However, the bed temperature for this test was higher than the remainder of the low temperature tests, and there was significant combustion in the freeboard. Similarly, the results from Test 3/1 suggest that cooling the freeboard may have reduced the sulphur retention slightly.

Table 6. Sulphur retention

Test		1/1	1/2	1/3	1/4	2/1	2/2	3/1	3/2	3/3
Bed temp.	°F	1460	1630	1405	1635	1400	1400	1630	1385	1650
Combustor exit temp.	°F	1510	1530	1415	1555	1460	1330	1140	1155	1515
Gas residence time (t)	s	1.1	2.2	2.3	2.3	1.5	1.5	1.0	1.7	2.2
Ca/S mol ratio (C)		1.65	1.7	1.6	1.55	1.4	1.4	1.6	2.35	2.05
Measured sulphur retention	%	86	93.5	87	93	71	71.5	79	92	96.5
Retention normalised only to t = 2.3s	%	93	94	87	93	79	79.5	89.5	94	96.5
Retention normalised only to C = 1.7	%	87	94	88	95	78	78.5	81	84	94
Retention normalised to t = 2.3s and C=1.7	%	93.5*	94	88	94.5	85	85.5	91	87	

Ref.1 National Coal Board "Reducing emissions of sulphur oxides, nitrogen oxides and particulates by using fluidised combustion of coal". Report to US Environmental Protection Agency Ref. DHB 060971, Sept. 1971.

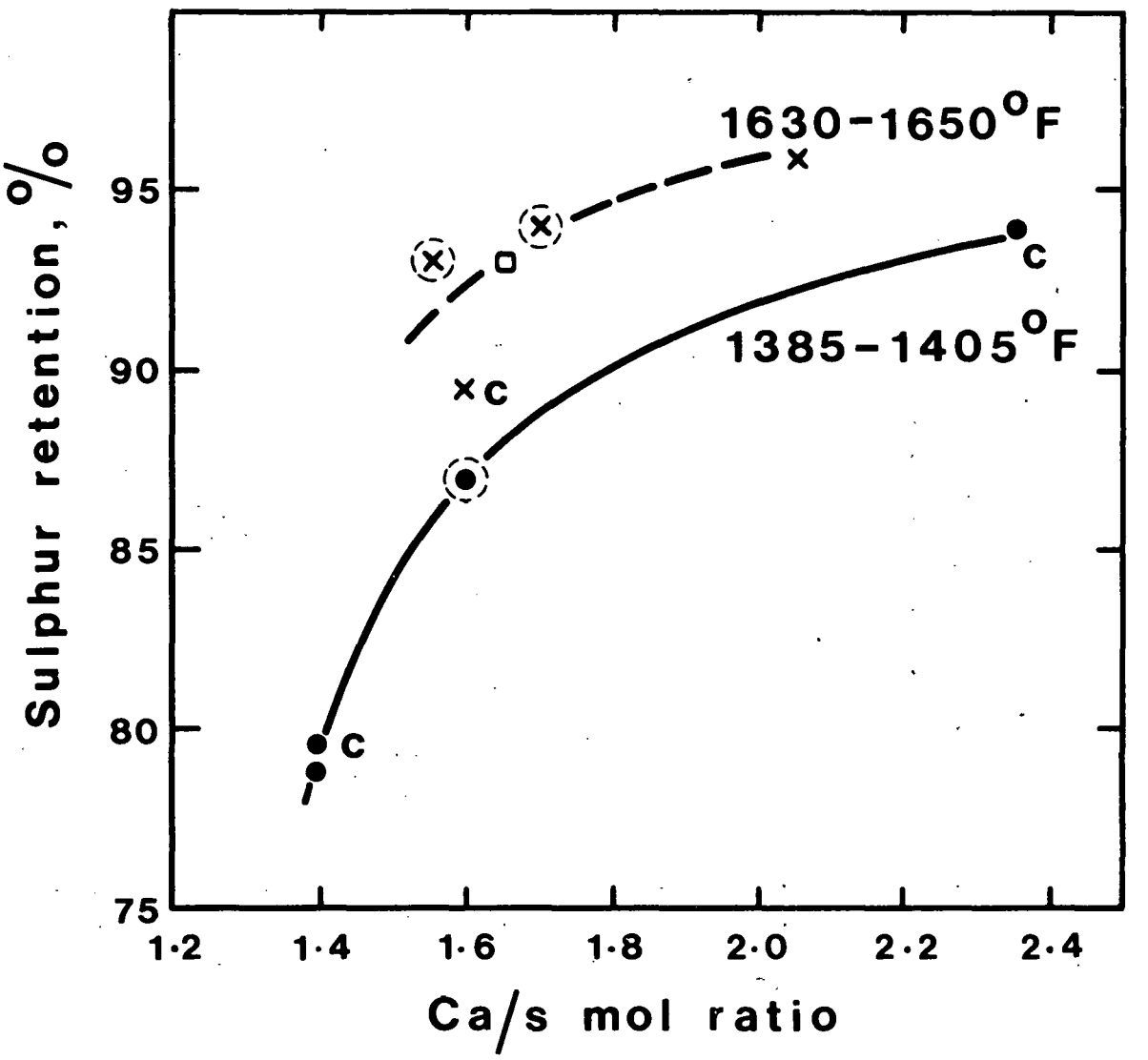

Data normalised to 2·3s gas residence time

- ⊙ ● 1385-1405°F bed temperature
- ⊗ × 1630-1650°F bed temperature
- ▫ 1460°F bed temperature
- ▫⊙⊗ Plum run dolomite. All other data with Steetly (U.K.) dolomite
- c Cooled freeboard

Fig.28 Variation of sulphur retention with Ca/s ratio and bed temperature

D649

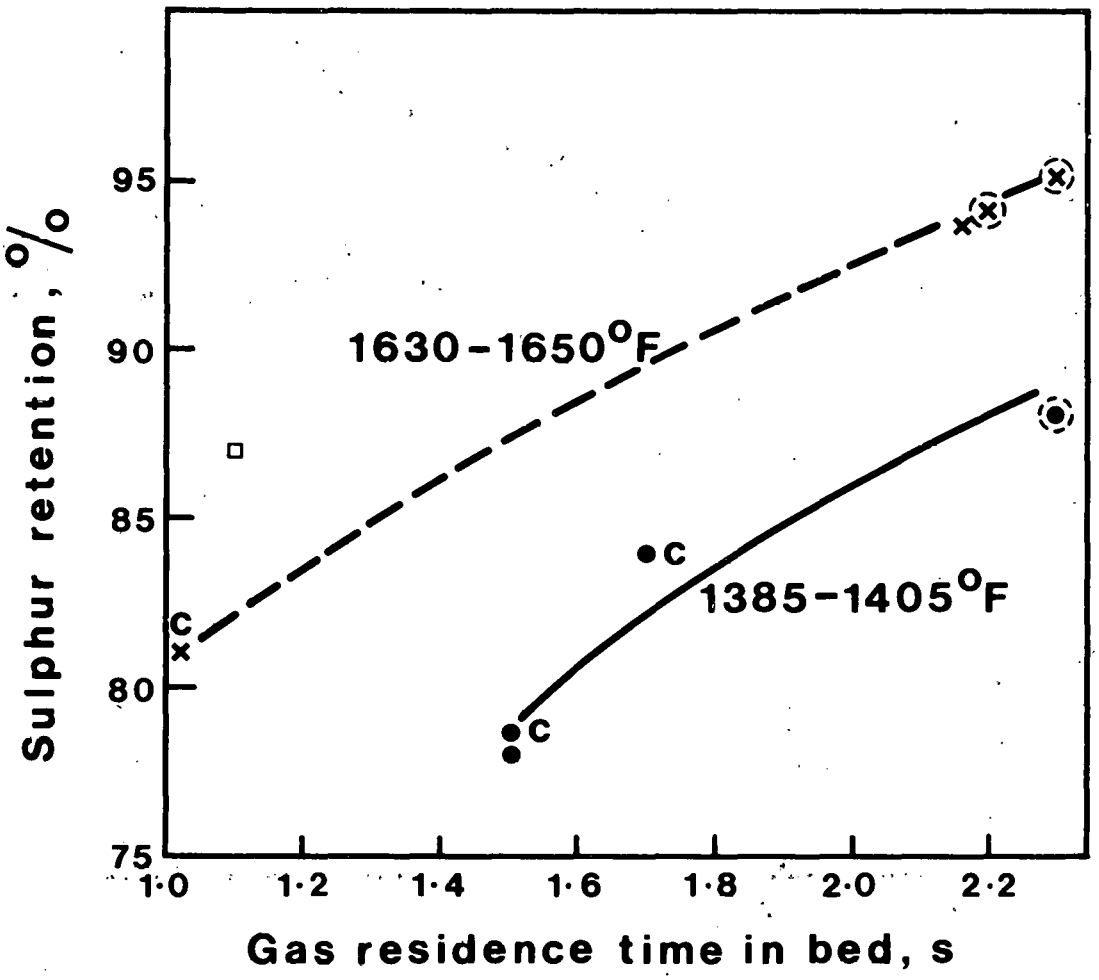

Data normalised to Ca/s ratio of 1·7

- ⊙ • 1385-1405°F bed temperature
- ⊗ × 1630-1650°F bed temperature
- □ 1460°F bed temperature
- □ ⊙ ⊗ Plum run dolomite. All other data with Steetly (U.K) dolomite
- c Cooled freeboard

Fig.29 Variation of sulphur retention with gas residence time and bed temperature

The effect of bed temperature was probably also partly due to the fact that at the low bed temperature the $CaCO_3$ component of the dolomite was only partially calcined and even the $MgCO_3$ calcination may have been incomplete (see Section 6.2.3). It is shown in Ref. 2 that the extent of calcination (α) of a $CaCO_3$ particle can be expressed as a function of $(p_e-p_c)/p_e$

where p_e = equilibrium partial pressure of CO_2 (atmospheres)
= $1.18 \times 10^7 \exp(-34230/T)$ (Ref. 3)

and p_c = prevailing CO_2 partial pressure (atmospheres)

Data on calcination conditions are given in Table 7 and Fig. 30.

Table 7. Bed calcination conditions

Test		1/1	1/2	1/3	1/4	2/1	2/2	3/1	3/2	3/3
Calcination of Ca	%	56	99	49	81	55	56	97	47	97
Sulphation of Ca	%	46	58	51	52	69	68	65	49	62
p_e	atm	0.21	0.91	0.14	0.72	0.12	0.12	0.98	0.11	1.05
p_c	atm	0.71	0.68	0.69	0.86	0.70	0.67	0.67	0.72	0.70
$(p_e-p_c)/p_e$		-2.38	0.25	-3.9	-0.19	-4.83	-4.58	0.32	-5.55	0.33

The value of p_c used in Table 7 and Fig. 30 was the partial pressure of CO_2 in the off-gas. This is, of necessity, a compromise. The CO_2 partial pressure in a fluidised bed is essentially zero below the coal feed point, increasing to the value in the off-gas as the bed surface is approached. Thus the effective value of the parameter $(p_e - p_c)/p_e$ lies between unity (corresponding to zero CO_2) and the values given in Table 7. This, together with the possibility of direct sulphation of the carbonate explains the apparent anomaly of partial rather than zero calcination at negative values of $(p_e - p_c)/p_e$.

The calcination situation is complicated further when the material elutriated from the bed is considered. Table 8 compares calcination/sulphation data for material remaining in the bed and for material collected by the cyclone.

It will be seen that the change from Plum Run to Steetly dolomite*

---

* For reasons outside the control of the contractor, there was only sufficient Plum Run dolomite remaining from a previous contract for Test 1. However, the enforced change in dolomite produced much useful information.

Ref. 2. T.R. Ingraham and P. Marier, Can.J.Chem.Eng. 1963, 41, 170-173.

Ref. 3. N.H. Ulerich et al, EPRI Report No. FP-426, August 1977.

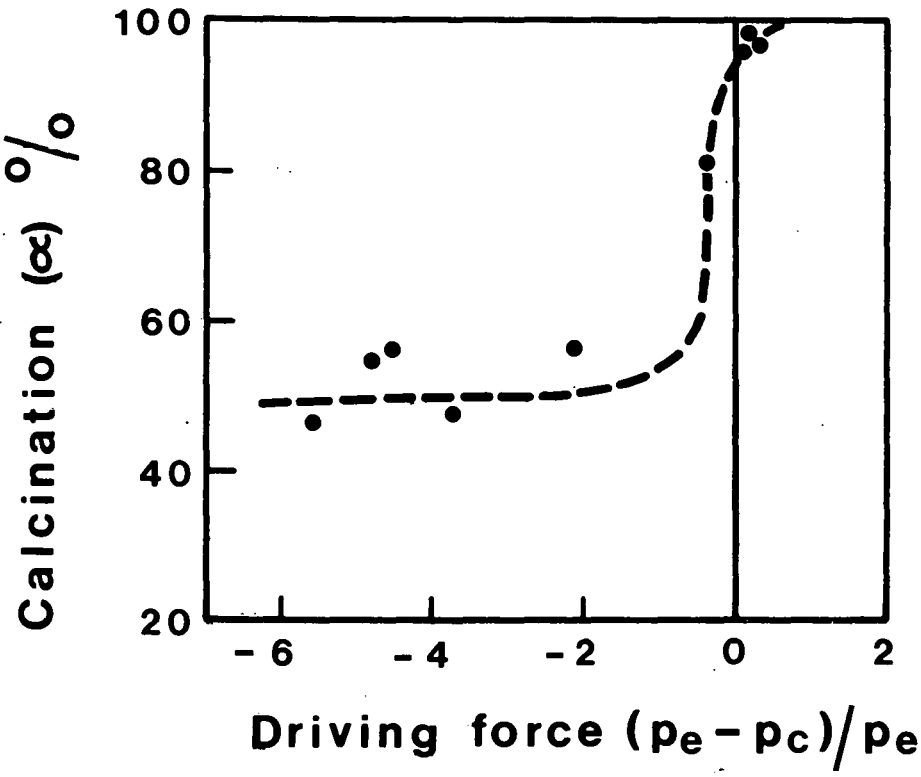

p_e = equilibrium partial pressure of CO_2

p_c = actual partial pressure of CO_2

Fig.30 Effect of CO_2 partial pressure on calcination in bed

produced a major change in the composition of the elutriated dust with a major reduction in the calcination and sulphation reactions. This may have been due to a lower reactivty for the Steetly dolomite (although the reactivities of either dolomite are not known) or it may have been a result of the much wider size distribution of the Steetly dolomite. Whereas only 10% of the Plum Run was elutriated, up to 65% (depending on operating conditions) of the Steetly dolomite was elutriated.

Table 8. Comparison of calcination/sulphation data for in-bed and elutriated dust

Test	1/1	1/2	1/3	1/4	2/1	2/2	3/1	3/2	3/3
Calcination in bed %	56	99	49	81	55	56	97	47	97
Calincation in elutriated dust %	46	81	51	86	0	0	25	0	71
Sulphation in bed %	46	58	51	52	69	68	65	49	62
Sulphation in elutriated dust %	55	51	67	68	23	24	36	19	32
Dolomite	----Plum Run ----				-----Steetly (U.K.)---				
Size, max	3350 μm				3350 μm				
median	c.1400 μm				c.400 μm				

Anticipating the discussion on elutriation in Section 6.4, it can be postulated that elutriated dolomite material can arise from three sources:-

(1) degradation of the partially-sulphated dolomite in the bed. This is normally a small amount and results in an elutriated material which is similar in calcination and sulphation to that remaining in the bed although the superfines (i.e those not collected by the cyclone) tend to be fully sulphated, indicating that these superfines are formed by abrading the surface of bed particles.

(2) rapid elutriation of any fine dolomite in the input with little reaction occurring. The amount of this material depends on the size distribution of the feed.

(3) decrepitation of the feed, i.e. the break up of material due to an initial thermal shock and to the rapid evolution of CO_2 from the stone. This tends to produce an elutriated material which

has a low sulphation level with a calcination level depending on the calcination conditions in the bed. It is not easy to distinguish between mechanisms (2) and (3).

Examination of Table 8 shows that for Plum Run dolomite, the reactions in the bed material and in the elutriated material were similar indicating that mechanism (1) probably predominated. The amount of Plum Run material which was elutriated was small. For Steetly dolomite, the amount of material elutriated was considerably higher. The low calcination and sulphation levels suggest that mechanisms (2) or (3) were predominant. Conditions of low temperature with low residence times in the bed (Tests 2/1, 2/2 and 3/2) or high bed temperature but with low residence time and low freeboard temperature (Test 3/1) did not calcine the elutriated material to any great extent; whereas high bed temperature with low residence time (Test 3/3) produced a much greater degree of calcination.

In view of the difference between Steetly and Plum Run in the composition and quantity of the elutriated dolomite, it may be no more than coincidence that there appeared to be no difference in the overall sulphur retention performance.

6.2.3 Half calcination of dolomite. It is generally assumed in fluidised combustion where bed temperatures are in excess of 750°C (1400°F) that the half-calcination of dolomite

$$MgCO.CaCO_3 \rightarrow MgO.CaCO_3 + CO_2$$

is carried to completion.

However the chemical analyses of bed material and of elutriated material often exhibit characteristics which are inconsistent with this assumption. More CO_2 may be present than can be accounted for as $CaCO_3$ alone (e.g. Test 2 - cyclone dusts) or the amount of sulphur and CO_2 present may be more than can exist with the calcium present (e.g. Test 2 : bed material). These observations are consistent with incomplete half-calcination where some of the CO_2 may still be in combination with magnesium as $MgCO_3$. These inconsistencies are usually apparent only at low bed temperatures (≈1400°F) and, with elutriated material, are more pronounced in conjunction with a heavily-cooled freeboard. Recent work (Ref. 4) has shown that the half-calcination reaction can be slow and in an effort to confirm the hypothesis that half-calcination of dolomite

---

Ref. 4. Half-Calcination of Dolomite at high pressures: Kinetics and structural changes, C.L. Steen et al, Environmental Science and Technology, 14, (5), May 1980, p.588.

may be incomplete, the extent of CO_2 evolution at 1110°F was measured in the laboratory from a sample of cyclone dust (Test 2/1). At this temperature, CO_2 would emanate mainly from the dissociation of $MgCO_3$ rather than $CaCO_3$. It was found that some 15% of the CO present in the sample was evolved at this temperature, indicating the presence of $MgCO_3$.

6.2.4 NO_x emissions

At the datum conditions of deep bed and high temperature, NO_x emission was about 0.32 lb/10^6 Btu, which agrees with data obtained elsewhere at about 50% excess air. Relevant information for each test section is summarised in the following Table:-

Table 9. NO_x emissions

Test		1/1	1/2	1/3	1/4	2/1	2/2	3/1	3/2	3/3
NO_x concentration	ppm	160	170	230	170	190	210	205	295	190
NO_x emissions	lb/10^6 Btu	0.29	0.32	0.42	0.25	0.32	0.37	0.37	0.50	0.34
O_2 concentration	%	7.5	8.2	7.8	4.9	7.8	8.2	8.0	7.2	7.6
Bed temperature	°F	1460	1630	1400	1630	1400	1400	1630	1400	1650
Exit temperature	°F	>1500	>1500	1410	>1500	1460	1330	1140	1160	>1500
Bed depth	ft	4	9	9	9	6	6	4	4	9

Examination of Table 9 shows that there was a tendency for the NO_x emissions to be higher when bed or freeboard temperatures or bed depths were low, suggesting that reduction of NO to N_2 (which is now well established as one of the reactions proceeding at the same time as the production of NO) is influenced by the bed and freeboard conditions. Although too many variables are involved to make quantitative deductions, the data - taken in conjunction with a limited number of measurements within the bed and at the bed surface as discussed in Section 6.3 - support the following hypothesis:-

(1) The amount of NO produced initially from the fuel N_2 is relatively large and is not strongly influenced by bed temperature.

(2) Subsequent reduction of this NO depends on the residence time in the bed (i.e. on the bed depth) and on the prevailing temperatures.

6.2.5 SO_3 emissions

During Test 1, SO_3 concentrations in the exhaust gas were monitored continuously by staff from the Marchwood Engineering Laboratories (MEL) of the U.K. Central Electricity Generating Board. The technique consisted of extracting a continous sample from a location downstream of the cyclone, passing it through a solution of iso-propyl-alcohol and analysing for SO_3 by the barium-chloranilate reaction (Ref. 5). The emissions measured through the test are given in Fig. 31 and averaged values for the test sections are given in Table 4. Emissions were generally less than 4 ppm (v/v), although higher values (8 to 15 ppm) were observed during two periods. The first of these occurred at the beginning of the test and coincided with a period when the emission of SO_2 was high (up to 700 ppm). The second occurred during the period between Section 2 and 3 when frequency response testing was being carried out on the combustor and the coal input was being varied rapidly.

As had been noticed in a previous programme (Ref. 6) a transient peak of 20-30 ppm of SO_3 was measured immediately following plant shut down, thought to be due to desorption as metal and refractory cooled down.

6.2.6 Alkali emissions

Measurements of the alkali (Na and K) vapour content of the gases were made in five test sections, generally in duplicate determinations. A sample of the gas downstream from the main cyclone was passed through a train consisting of a small cyclone and two electrostatic precipitators. After sampling 500 to 1000 litres of gas over a period of about 2 hours, the cyclone and precipitators were washed out, the washing filtered and the filtrate analysed for Na and K.

The results showed concentrations of 1.0±0.4 ppm (w/w)* Na and 1.3±0.9 ppm K. Although the sample was deliberately made non-isokinetic, some dust was collected. The above figures therefore include the soluble part of the dust collected. Previous work has shown that the dust has a solubility of about 20%. Analysis of the sample residues showed that the solids collected had concentrations of 0.6±0.4 ppm Na and 2.7 ±2.1 ppm K, i.e. the soluble concentrations were relatively small.

No effect of operating conditions, in particular of bed temperature, could be detected.

Table 10 shows the distribution of alkali throughout the system

---

Ref. 5. CEGB Publication, SO_3 monitor, Hanover Fair Brochure, April 1977.

Ref. 6 Pillai K.K. and Wood P., 1000 hour test programme in a pressurised fluidised bed facility, Final Report to US DOE Vol. II, FE-3121-15-C, 1980.

* ppm (w/w) = wt. of Na or K per 10^6 parts by weight of gas.

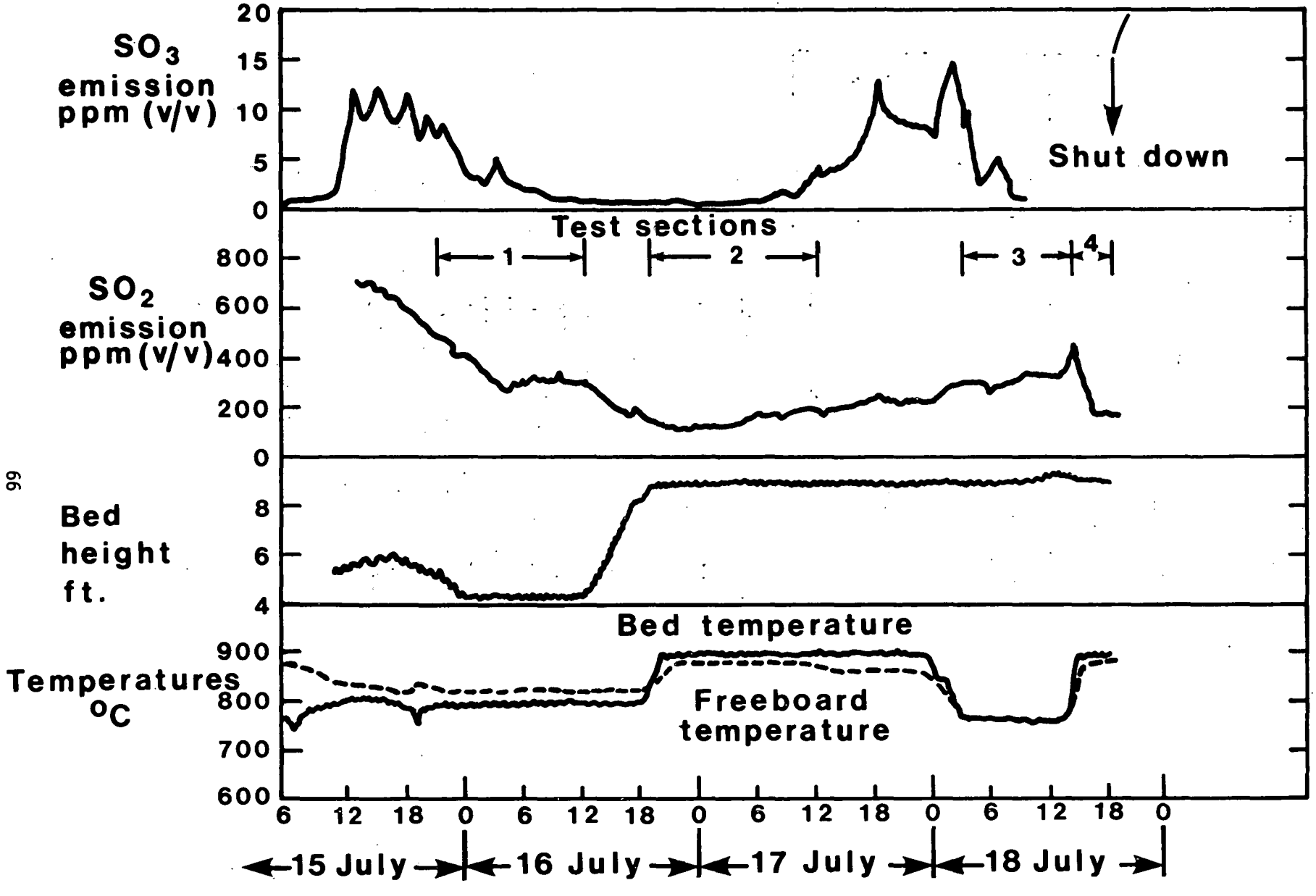

Fig.31 SO_3 emission history

D548

Table 10. Distribution of alkali in parts by weight per million parts of dry gas and (% of input)

	Na	K	Cl
Input In coal	20.2±3.1 (55%)	146.2±21.6 (92%)	42.6±12.5 (72%)
In dolomite	16.2±3.7 (45%)	12.5± 2.7 (8%)	16.4± 4.6 (28%)
Output			
From bed overflow	10±4.1 (25%)	43±13.2 (23%)	5.4± 3.8 (c.9%)
Dust collected by cyclone	25.6±6.5 (65%)	125±17 (68%)	8.9± 6.9 (c.15%)
Dust escaping cyclone	3±0.9 (8%)	13.1±3.6 (7%)	0.3± 0.2 (c.0.5%)
Vapour	1±0.4 (2%)	1.3±0.9 (1%)	*

* Not determined, but obviously contained most of the input chlorine.

Note that the total measured output is greater than the input due to sampling and analytical errors.

6.2.7. Conclusions. Operation at part-load conditions (low bed depth and/or low bed temperature) resulted in a lower combustion efficiency than the 99% obtained at "full load" conditions. The amount of combustion occurring in the freeboard increased at part-load, but was inhibted when the freeboard was cooled by exposed cooling tubes. With a bed temperature of 1400°F, bed depth of 4 to 6 ft and combustor exit temperatures of 1150 to 1350°F, the combustion efficiency was 95 to 96%. It may be necessary to install a fines recycle loop in commercial plants if prolonged operation at part load is required. At low bed temperatures and low bed depths the CO concentration in the exhaust increased from 5 ppm (v/v) to 90 ppm and increased further to c.250 ppm when the freeboard was cooled.

Operation at part-load resulted in a lower sulphur retention, the latter falling from 95% at full-load to less than 80% at low bed temperature and bed depth.

NO_x emissions were typically 0.3 lb/10^6 Btu with an apparent tendency to increase slightly as the load was reduced.

SO_3 concentrations in the exhaust gases were in the range 4 to 15 ppm (v^3/v). Occasional values of 20-30 ppm were measured and it is clear that many more measurements need to be made before it can be sure that "back-end" corrosion will not be a problem in commercial plant.

6.3 IN BED SAMPLING

The probe described in Section 4.6 and shown in Fig. 14 was used to obtain solids samples for analysis and to carry out gas-sampling and temperature traverses. The traverses were carried out at a height of 5 ft above the distributor and along a line extending 12 inches into (i.e. up to the centre) of the combustor. Thus, depending on the bed depth, the traverses were either across the splash zone or within the bed.

After some teething problems, the probe operated satisfactorily. Accurate data appeared to be produced, but interpreting some of this data (particularly gas composition) was difficult, if not impossible. This was because conditions along a 12 inch line cannot be considered representative of conditions across an area of 6 ft^2. In this respect, the investigations are best considered as having shown that in-bed sampling is possible in a two-casing, pressurised fluidised bed. To have obtained representative data on the Leatherhead combustor would have meant traversing from one wall to the other across at least two positions, and preferably three, at the same height above the distributor.

With the above limitations in mind, the data will now be described.

Table 11 gives the analyses of the solids samples taken in different test sections operating with bed depths greater than 5 ft. The corresponding analyses of the samples of bed material taken from the normal bed offtake (through the distributor) at approximately the same times are also included. During Test 1/3, a duplicate traverse was carried out approximately 30 minutes after the first. The results show that there was no significant difference between the analyses of solids taken from different positions in the bed and it is probably reasonable to conclude that the whole of the bed had substantially the same (solids) composition for any particular set of operating conditions.

Gas sampling traverses from Test 3 are reproduced in Figs. 32 and 33. The results are plotted as deviations from the gas concentration at the combustor exit (cyclone outlet) as a function of distance:-

(1) The O_2 and CO_2 analyses all indicated a high excess air near the wall. In Test 3/3 the O_2 and CO_2 analyses indicated a zone between about 4 inches and 12 inches which was lower

Table 11 Solids samples traverses within the bed.

Test		½				1/3				1/4				2/1					3/3				
Distance from wall, inches		2	7	12	*	2	7	12	*	2	7	12	*	2	4	8	12	*	2	4	8	12	*
C	%	0.06	0.07	<0.05	<C.05	<.05 <0.05	<0.05 <0.05	<0.05 <0.05	<0.05	<0.05	0.09	0.05	<0.05	-	-	-	-	-	<0.05	<0.05	<0.05	<0.05	<0.05
CO_2	%	0.80	0.80	1.05	0.4	11.4 11.4	11.4 11.7	12.9 11.6	12.4	10.5	9.3	7.7	7.8	-	-	-	-	-	0.45	0.45	0.75	0.75	0.85
CaO	%	33.6	33.5	33.3	32.6	30.6 30.6	30.5 30.7	30.8 30.4	31.0	31.5	31.8	32.3	32.3	22.1	22.0	21.5	22.3	21.9	30.5	31.3	30.6	32.1	31.6
Fe_2O_3	%	2.8	2.9	2.9	2.8	2.5 2.3	2.4 2.3	2.4 2.3	2.0	2.2	2.2	2.2	2.0	-	-	-	-	-	-	-	-	-	-
Na_2O	%	0.24	0.19	0.21	0.11	0.12 0.09	0.25 0.09	0.15 0.09	0.09	0.09	0.09	0.15	0.09	-	-	-	-	-	-	-	-	-	-
K_2O	%	0.33	0.33	0.34	0.32	0.30 0.30	0.30 0.31	0.34 0.30	0.27	0.30	0.32	0.31	0.29	-	-	-	-	-	-	-	-	-	-
SO_3	%	25.8	26.0	26.0	27.1	22.9 22.7	23.0 22.7	23.0 22.6	22.6	22.8	23.3	23.7	23.9	19.9	20.0	19.5	19.7	20.2	27.8	27.9	27.8	27.4	27.8
Cl	%	0.03	0.02	0.03	.04	0.04 0.03	.04 .04	0.03 0.04	0.06	0.04	0.04	0.04	0.04	-	-	-	-	-	-	-	-	-	-
Size distribution																							
% <3.350mm		100	100	100	-	100 100	100 100	100 100	-	100	100	100	-	100	100	100	100	100	100	100	100	100	100
<2.80 mm		99.6	99.6	99.5	-	99.5 99.4	99.4 99.2	99.1 99.2	-	99.3	99.3	99.5	-	-	-	-	-	-	-	-	-	-	-
<2.36 mm		96	95	96	-	96 95	96 94	95 95	-	94	94	95	-	-	-	-	-	-	-	-	-	-	-
<1.70 mm		80	78	80		81 75	80 74	77 78	-	74	73	76	-	93	93	93	94	94	83	77	78	82	88
<1.18 mm		61	54	60	-	60 55	60 53	56 58	-	51	51	53	-	-	-	-	-	-	-	-	-	-	-
<0.85 mm		43	35	41	-	40 37	40 34	37 40	-	33	33	34	-	-	-	-	-	-	-	-	-	-	-
<0.50 mm		15	12	14		14 12	14 11	11 14	-	11	10	11	-	22	22	23	24	25	27	19	21	25	28
<0.25 mm		0.1	0	0.1	-	0.2 0.1	0.1 0.1	0.1 0.1	-	0.1	0.1	0.1	-	0.5	0.4	1.5	0.4	0.4	0.4	0.4	0.2	0.5	0.7
<0.15 mm		0	0	0	-	0.1 0	0 0	0 0	-	0	0.1	0.1	-	0.2	0.2	0.2	0.2	0.2	0.2	0.2	0.1	0.3	0.4
Surface mean dia. mm.		0.79	0.87	0.81	-	0.80 0.86	0.81 0.88	0.86 0.82	-	0.90	0.90	0.86	-	-	-	-	-	-	-	-	-	-	-

* Analysis of samples taken from the normal bed offtake (through the distributor) at approximately the same time as the traverses.

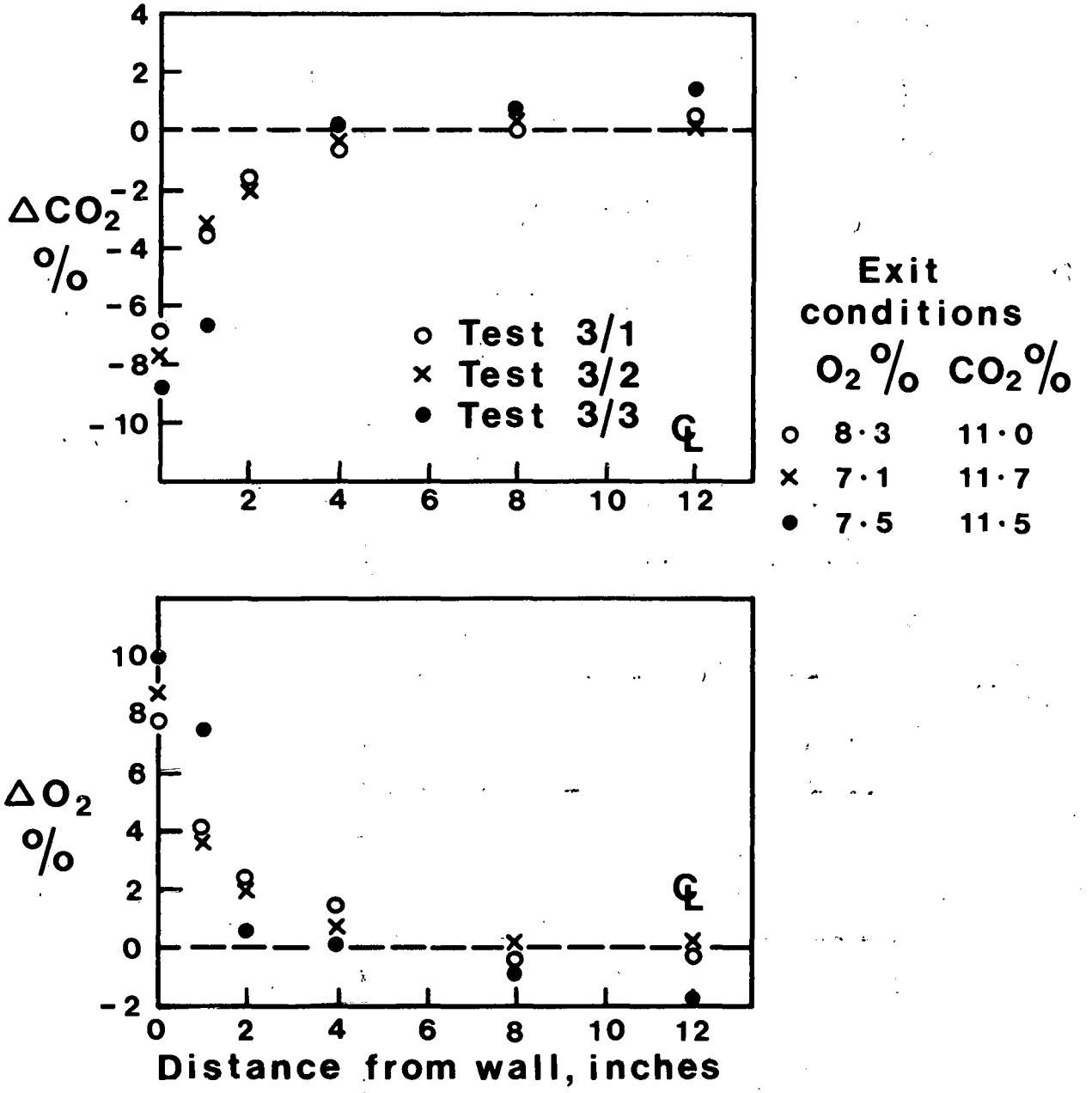

$\Delta O_2, CO_2 = (\text{measured } O_2, CO_2 - \text{exit } O_2, CO_2)\ \%$

Note:- Traverses in 3/1, 3/2, were in splash zone; in 3/3 was in bed.

Fig.32 Variation in gas composition at 5ft level

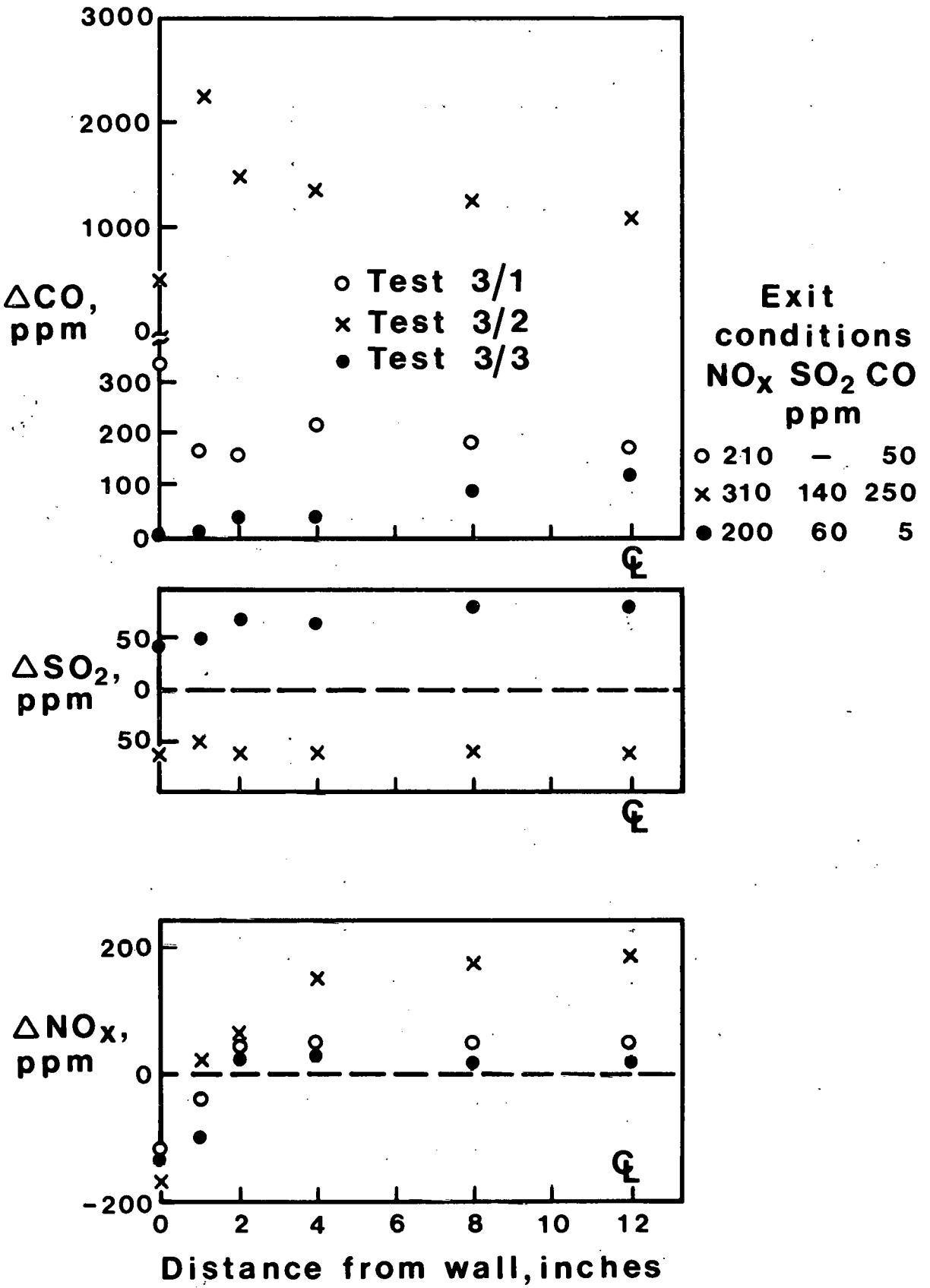

Fig.33 Variation in gas composition at 5ft level

in excess air than the combustor exit. This was the test in which a single coal nozzle was used at a different position (in plan view) to the two coal nozzles used in all the other tests. Presumably the traversing line was, coincidentally, along a zone somewhat richer in coal constituents.

(2) Appreciable CO levels (up to 2500 ppm) were measured in Test 3/2 and they were considerably higher than at the combustor exit. This test was at a low bed temperature. CO levels were also higher along the traversing line than at the combustor exit in Tests 3/1 and 3/3 - at high bed temperature - although the CO concentrations were considerably lower than in Test 3/2.

(3) NO_x concentrations were also higher along the traverse line (except near the wall) than at the combustor exit. This was particularly so in Test 3/2, where levels of 500 ppm were measured.

(4) SO_2 concentrations on the traverse line were greater than at the combustor exit in Test 3/3, but lower in Test 3/2. (No SO_2 measurements were made in Test 3/1).

(5) Gas concentrations in the bed fluctuated rapidly. O_2 varied by ±1.3%; CO_2 by ±1.8% and CO by ±70 ppm in Test 3/3. These fluctuations were an order of magnitude greater than the fluctuations at the combustor exit. Large parts of the gas analysis train were common to both samples (samples were withdrawn through the same drying and analytical equipment alternately from the in-bed sample probe and the combustor exit probe) although there was rather more opportunity for damping of fluctuations in the combustor exit sample. Fluctuations when traversing across the splash zone in Tests 3/1 and 3/2 were less than in Test 3/3.

No useful conclusions can be drawn from the gas sample traverses because of their possibly unrepresentative character - as described earlier.

Temperature traverses were carried out with bed depths and temperatures of 9 ft and 1640°F; 6 ft and 1400°F; 4 ft and 1400°F (i.e. across the splash zone). Except for a region within 1 inch of the wall, the temperature distribution was uniform to within ±10°F when traversing in the bed. There was rather more variation (±20°F) when traversing in the splash zone. Temperature appeared to fall by about 30 to 40°F between the 1 inch insertion and the wall. The probe could not be positioned more accurately than about ±0.5 inches relative to the wall.

6.4 ELUTRIATION

Examination of Table 4 shows that there was a major change in the elutration pattern after Test 1, with much more material being elutriated in Tests 2 and 3. (Test 1/4 is ignored, because it was of too short a duration for equilibrium to have been established). This increase was due to the use of a much finer dolomite.

The results have encouraged a reappraisal to be made of all the elutriation data obtained on the Leatherhead rig over the past few years with the intention of providing a general empirical method of predicting the amount of elutriation. In view of the complexities of the process there seems little likelihood of a theoretical model being available in the forseeable future.

When carrying out mass and heat balances on the Leatherhead rig it has been the practice to carry out sufficient analyses to enable the elutriation of coal ash and dolomite to be differentiated. This forms the basis for the present analysis. In order to avoid ambiguity both the coal ash and the dolomite are based on a sulphate-free, CO_2-free basis, and the "inert" content of coal ash and dolomite is defined as

$$(100 - \%\ H_2O - \%\ Cl - \%\ \text{elemental carbon} - \%\ CO_2 - \%\ SO_3)\%$$

Material elutriated from a bed is mainly composed of particles smaller than that size for which the gas velocity - at the prevailing temperature and pressure - is the terminal or free-fall velocity. This critical size is termed the "elutriable" size and "fines" are defined as that material smaller than the elutriable size. "Fines" in the solids feeds are elutriated rapidly. Some of the remaining material is reduced in size in the bed to something smaller than the elutriable size after which it is also rapidly elutriated. Processes causing size reduction include attrition, thermal shock and calcination, and are not amenable to any general treatment.

6.4.1 Elutriation of dolomite. As already described in Section 6.2.2 elutriation of dolomite "inert" can occur by three mechanisms:-

(1) rapid elutriation of any input dolomite which is finer than the elutriable size. Fig. 34(a) shows the relationship between the proportion of elutriable dolomite "inert" in the feed and the proportion actually elutriated. Data were taken from 25 test conditions and details are given in Appendix 2. Fig. 34(a) shows a clear correlation, with the fraction actually elutriated being generally 5 to 20% higher than the elutriable fraction in the feed. This bias is mainly a result of size reduction processes in the bed, which are due to

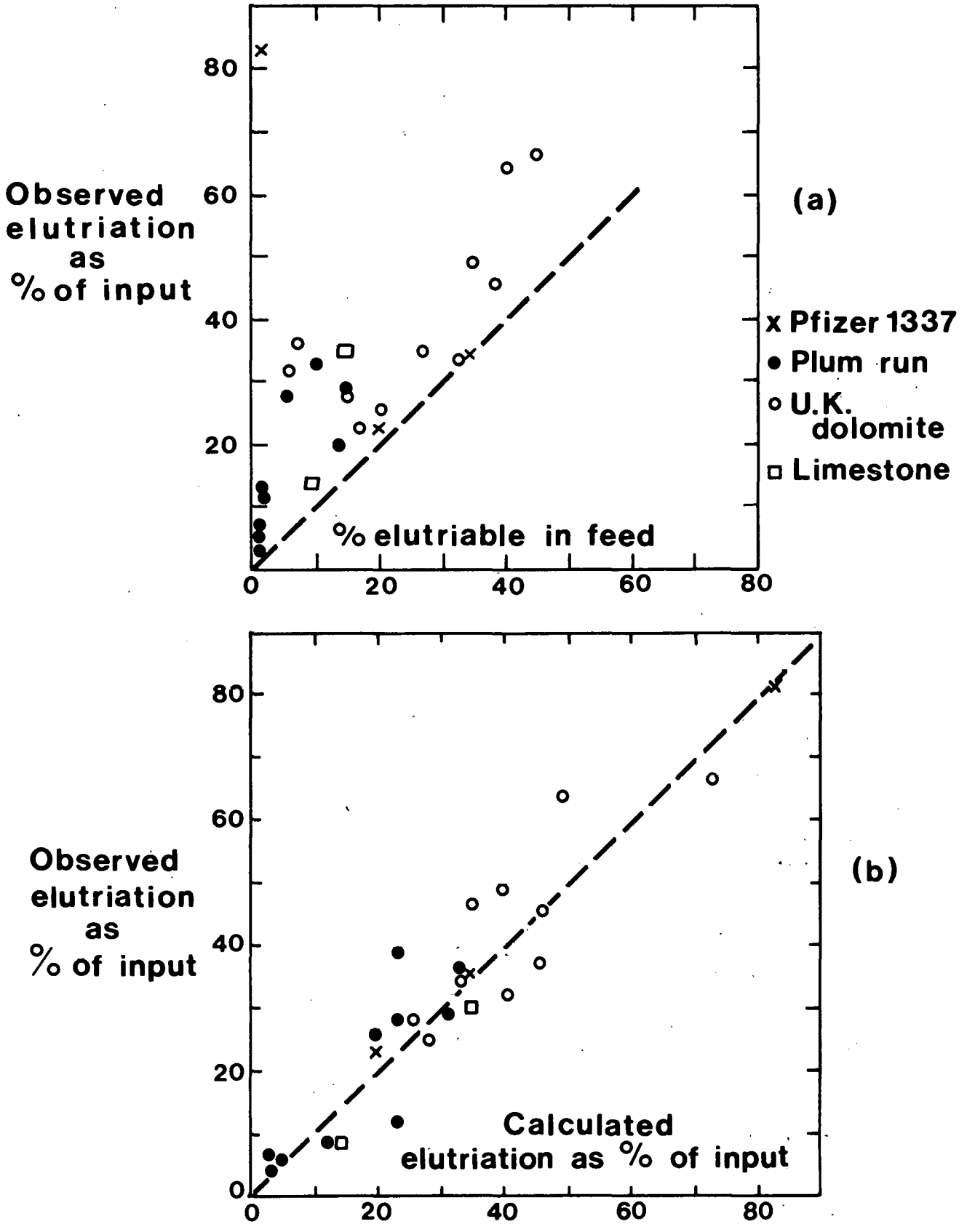

Fig.34 Elutriation of sorbent

(2) decrepitation of the incoming particles due to the sudden evolution of carbon dioxide and to shock heating of the particle

(3) attrition and abrasion of particles in the bed, enhanced by the fact that calcination converts the hard stone into soft, easily breakable material, but hindered by sulphation which hardens the particle.

It is reasonable to suppose that mechanism (2) will be proportional to the rate of feed of dolomite and to some function of the rate of calcination in the bed. Mechanism (3) will depend on the amount of dolomite material in the bed and on some function of the velocities in the bed. (This function is often assumed to be $U - U_{mf}$). The data from the 25 test conditions are reproduced in Appendix 2, where it is shown that the amount of fines produced by mechanism (2) is small in PFBC and can be neglected. It is also shown that the "best fit" to mechanism (3) requires a function $(U - U_{mf})^n$ where $n = 3$. However, a simpler relationship is shown in Fig. 35 where r is the rate of production of fines in the bed (defined as the difference between the observed elutriation and the elutriable quantity in the feed and W is the weight of dolomite material in the bed. It would appear that attrition and abrasion are negligible at values of $(U - U_{mf})$ lower than about 2.5 ft/s. It must be remembered that because most of the elutriated dolomite arises from the elutriable part of the dolomite feed, almost any correlation to account for fines production in the bed will be effective.

Using Fig. 35 together with the amount of elutriable material in the dolomite feed produces a calculated value of elutriation which is in close agreement with the observed value, as shown in Fig. 34(b).

6.4.2 Elutriation of coal ash. Fig. 36 plots the amount of coal ash elutriated against the elutriable amount in the feed, using the data given in Table A3 of Appendix 2. The upper diagram plots the amount fo coal ash elutriated against the amount elutriable in the coal feed - assuming that the ash size distribution is the same as the coal size distribution. It is clear from Fig. 36(a) that there is no real correlation between the two parameters, with 40 to 70% more being elutriated than would be expected from the coal size distribution.

It is well-known that the size distribution of the coal ash is finer than that of the coal and that the extent of the difference depends on how much "stone" is included in the material. The relationship between the size of the coal and the ash particles for Glen Brook coal is shown in Fig. 37. This was produced by ashing a sample of coal in in a laboratory furnace at 1650°F and determining the resulting size distribution. Fig 36(b) shows the revised relationship for Glen Brook

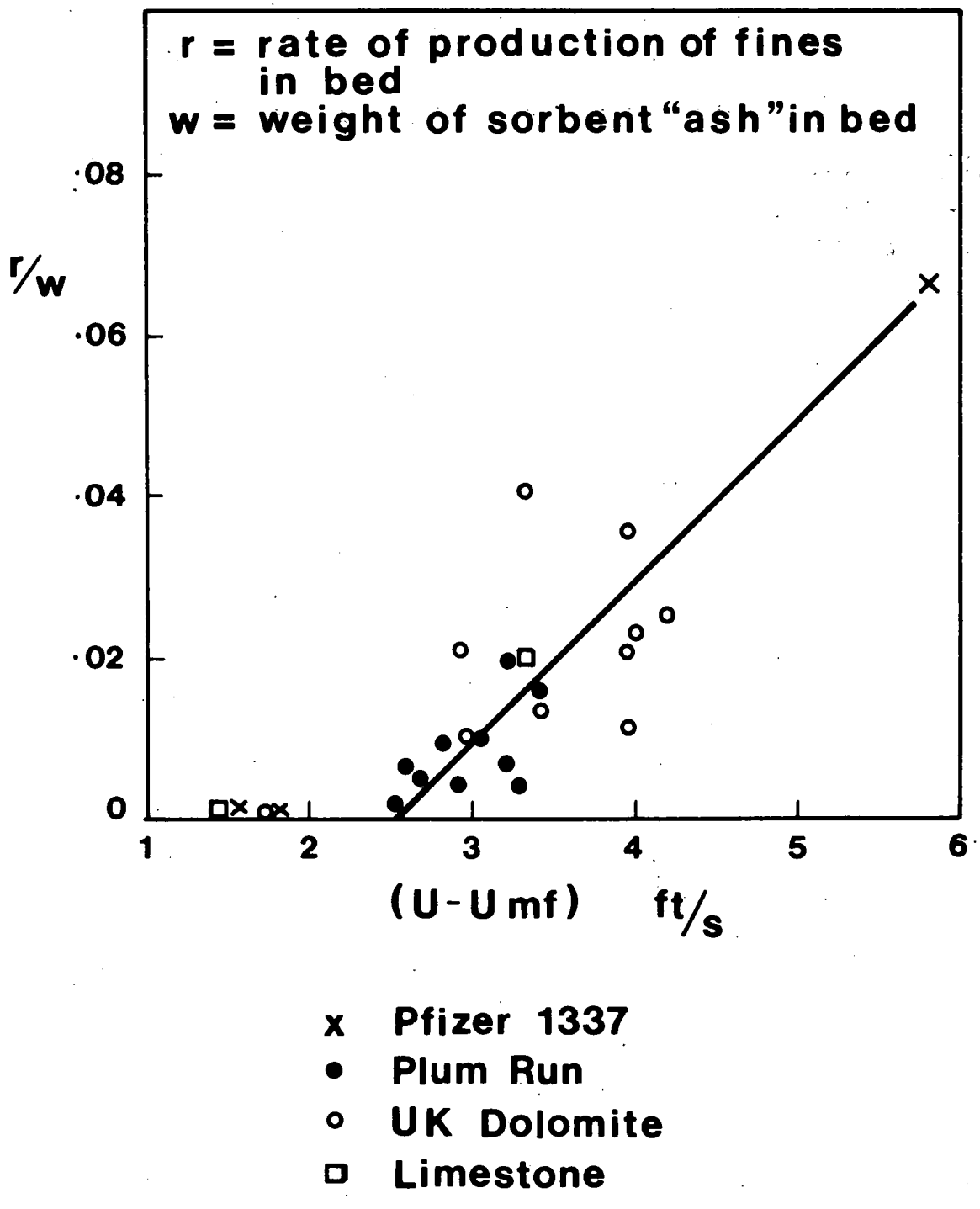

Fig.35 Sorbent "fines" production in bed

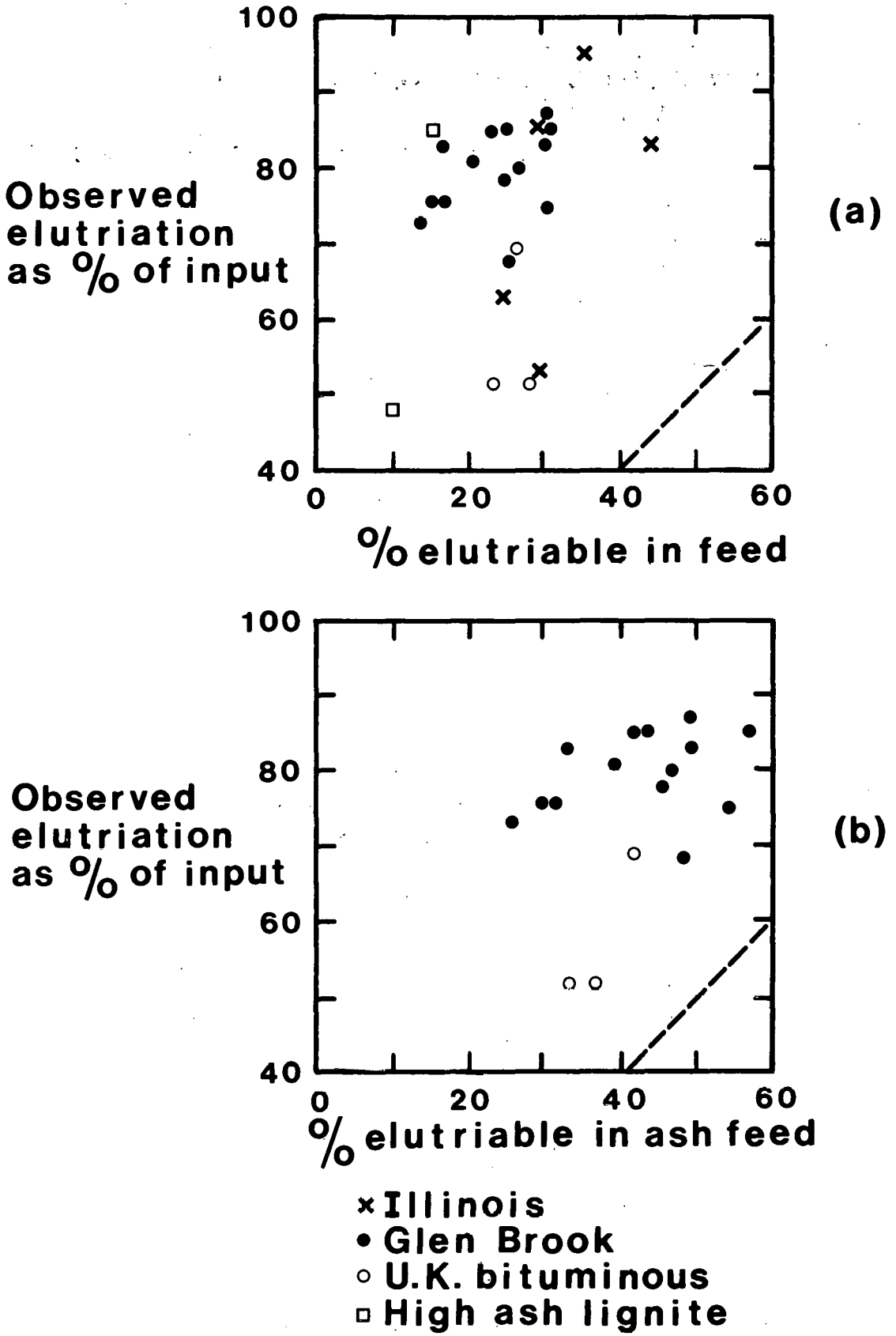

Fig.36 Elutriation of coal ash

D654

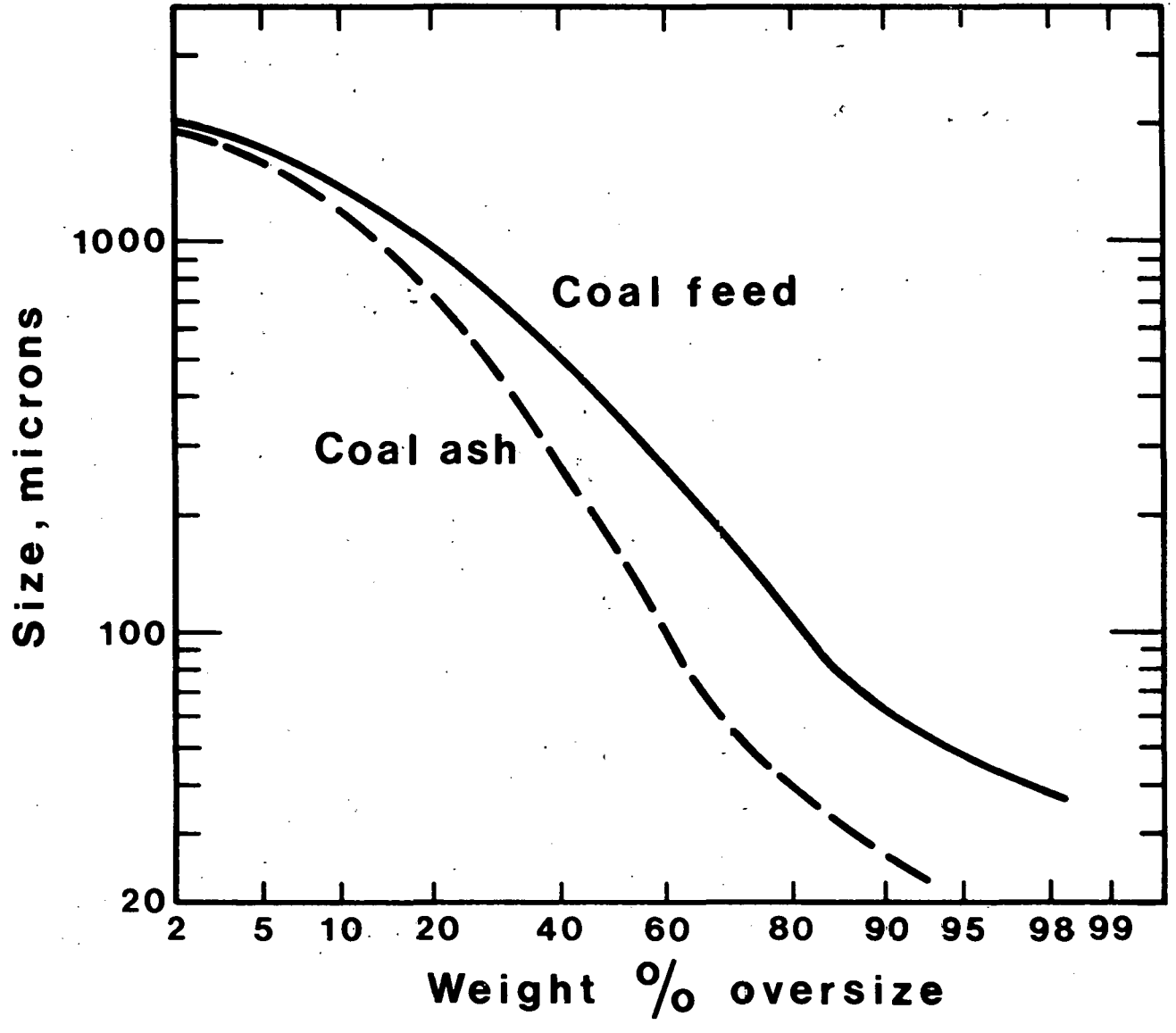

Fig. 37 Size distributions of coal and ash from Glen Brook coal

D648

coal ash between the amount of coal ash elutriated and the amount elutriable in the coal feed - based on the coal ash size distribution of Fig. 37. Also included are data for the U.K. bituminous coal - the only other coal for which ashing data are available.

From Fig. 36(b) it can be seen that 20 to 50% more is being elutriated than would be expected from the coal ash size distribution. Clearly, unlike dolomite, a substantial part of the elutriated fines is produced by size reduction processes in the bed.

As for dolomite, the rate of fines production in the bed can be expected to depend on the amount of coal ash in the bed and on the fluidising velocity. It can also be expected to depend on the hardness of the coal ash, which can vary from coal seam to coal seam and also can vary with the mining technique. There is not enough coal ash remaining in the bed to enable rate of fines production to be evaluated from the experimental data in the same way as for the dolomite. However, a general correlation between the total amount elutriated and the fluidising velocity is shown in Fig. 38. A reasonable correlation exists for Glen Brook and Illinois coal. The high ash sub-bituminous coal produced similar amounts of elutriation (although sub-bituminous coals, in general, might be expected to produce more), but the U.K. bituminous coal - which was known to contain more "stone" than the U.S. coals - resulted in less elutriation.

It is suggested that Fig. 38 can be used for design purposes to predict the amount of coal ash which will be elutriated when burning Eastern U.S. coals. In broad terms, 60% will be elutriated at 2.5 ft/s fluidising velocity, and 80% at 4 ft/s.

6.4.3 Size distribution of elutriated material. The size distributions of the elutriated material for the nine test conditions in the 1980 programme were remarkably uniform, as is shown by the hatched area in Fig. 39. This is in spite of the facts that the size distribution of the feed varied considerably, that the amount of material elutriated varied considerably and that the velocity varied from 2.5 ft/s to 4 ft/s. The elutriated dust was somewhat finer than dust elutriated at a fluidising velocity of 6.5 ft/s in the same combustor and somewhat coarser than the dust elutriated during the previous 1000 hour programme. At the moment there are insufficient data to be able to predict the size distribution.

6.4.4 Conclusions. The work carried out over the last few years has confirmed that factors controlling the amount of elutriation from a

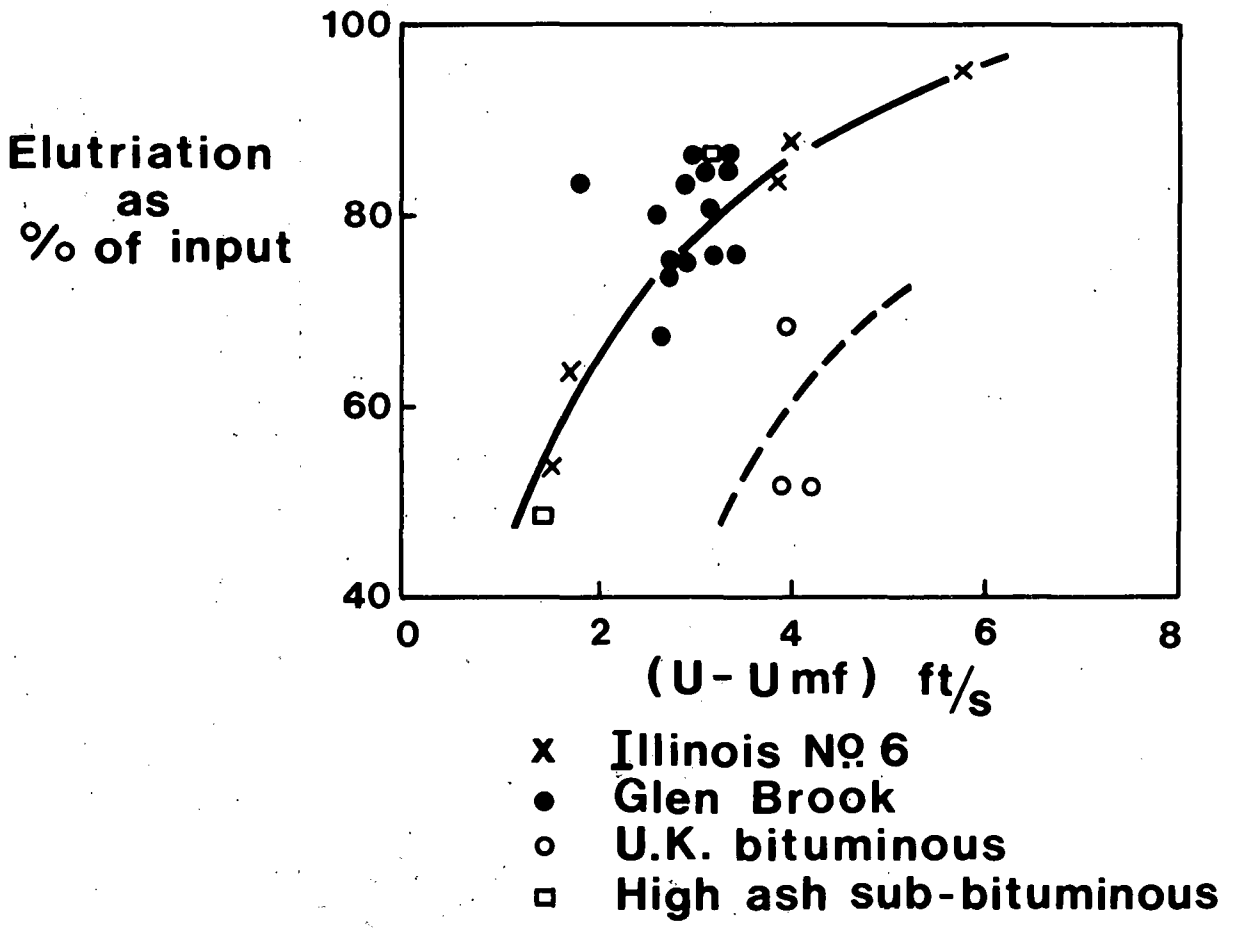

Fig.38 Elutriation of coal ash v fluidising velocity.

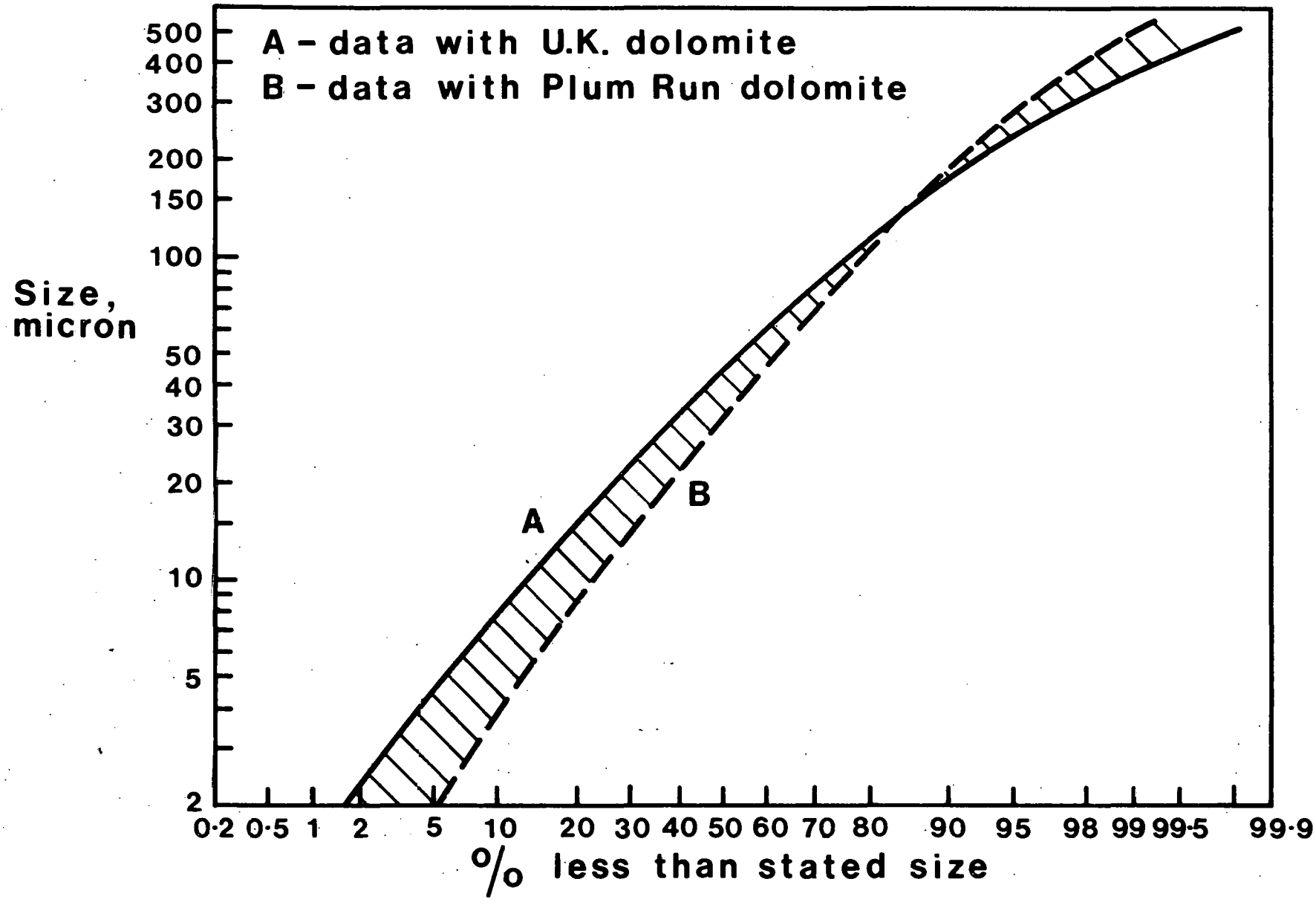

Fig.39 Size distribution of elutriated material

D662

pressurised fluidised bed are complex. The proportion of dolomite elutriated depends primarily on the proportion of elutriable material in the feed with a small additional amount being produced by attrition in the bed. Attrition depends mainly on the fluidising velocity. Coal ash elutriation arises from both the proportion of elutriable material in the feed and from attrition in the bed, which in turn depends on the fluidising velocity and the nature (hardness) of the adventitious ash associated with the coal.

Using the information given above it is possible to make an approximate estimate of the amount of dolomite and coal ash which will be elutriated (bearing in mind that the changes in weight due to calcination and sulphation have to be allowed for), but it is desirable that pilot-scale tests should be carried out where reasonably precise design data are required.

6.5 HEAT TRANSFER

Measurements of heat flux were made at part-load conditions simulated in different ways:-

(1) at different bed depths and temperatures (steady state conditions)

(2) whilst varying the bed depth (other parameters - except excess air - being held constant).

Measurements were also made with a constant bed depth of 4 ft and constant bed temperature whilst varying the amount of cooling in the freeboard. The increase in heat (coal) input required to maintain a constant bed temperature was a measure of the heat being abstracted by the freeboard tubes from the bed itself.

6.5.1 Heat transfer to immersed tubes. Heat fluxes were measured at irregular intervals during the three tests, attempting to cover as many conditions of bed temperature and bed depth as possible. Figs. 40 and 41 show some of the heat transfer coefficients as a function of height above the distributor for different temperature bands. Each diagram shows a characteristic rise in heat transfer coefficient through the first few rows of the tube bank, followed by a more gradual or negligible rise in the remainder of the tube bank. This change in coefficient is due possibly to bubble break-up in the first few rows of the tube bank with a consequent reduction in particle/tube contact time.

Fig. 40 shows that there was a slight reduction in heat transfer coefficient with lower bed temperature. This effect is masked in

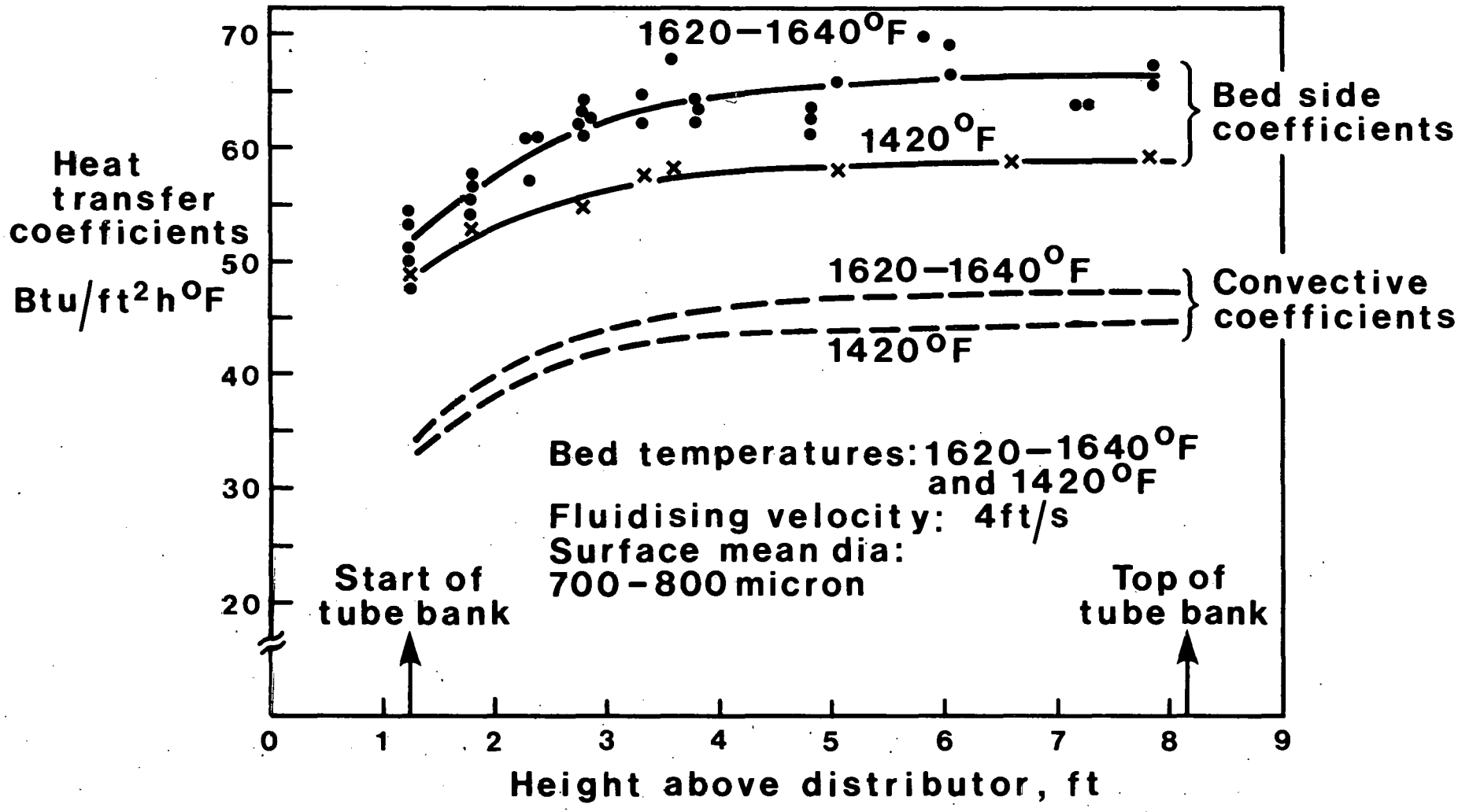

Fig.40 Heat transfer to immersed tubes: Bed depth 9ft.

D657

Fig. 41 because the lower bed temperature test was carried out at a lower fluidising velocity (2.5 ft/s instead of 4 ft/s) and there was a consequential reduction in the size of the bed material (from about 750 μm to 600 μm).

Heat transfer coefficients as a function of bed temperature (ignoring the tube bank "entry effect) are shown in Fig. 42. The convective (or conductive) component is obtained from the relationship

$$h_c = h_b - 0.8\sigma \left\{ \frac{T^4_b - T^4_m}{T_b - T_m} \right\}$$

where h_c = convective coefficient
h_b = bed-to-tube coefficient
T_b = bed temperature
T_m = metal surface temperature (calculated from water flow rates and measured heat fluxes)
σ = Stefan Boltzman constant

The convective component shows a slight increase with increase in bed temperature. This increase is roughly equal to the increase in gas conductivity, although this may be coincidental.

6.5.2 Heat transfer in the "splash" zone. Data were obtained in two ways:-

(a) under steady-state conditions the heat transfer coefficients to the "freeboard" circuits were measured. Several sets of data were obtained at slightly different bed depths in the range of 4 to 5 ft and at different bed temperatures.

(b) as the bed depth was slowly increased, the heat transfer coefficients were measured at discrete time intervals. This had the effect of changing the position of each cooling circuit relative to the bed surface as time progressed.

Data are plotted in Fig. 43 as a fraction of the heat transfer coefficient which occurred to the tubes when immersed. One row (row 27) at one condition has been separately identified (by a cross) to illustrate the manner in which the heat transfer coefficient varied. Other rows (11, 15, 19, 22 and 25) produced a similar series of points. The equation of the line through the experimental points can be expressed as:

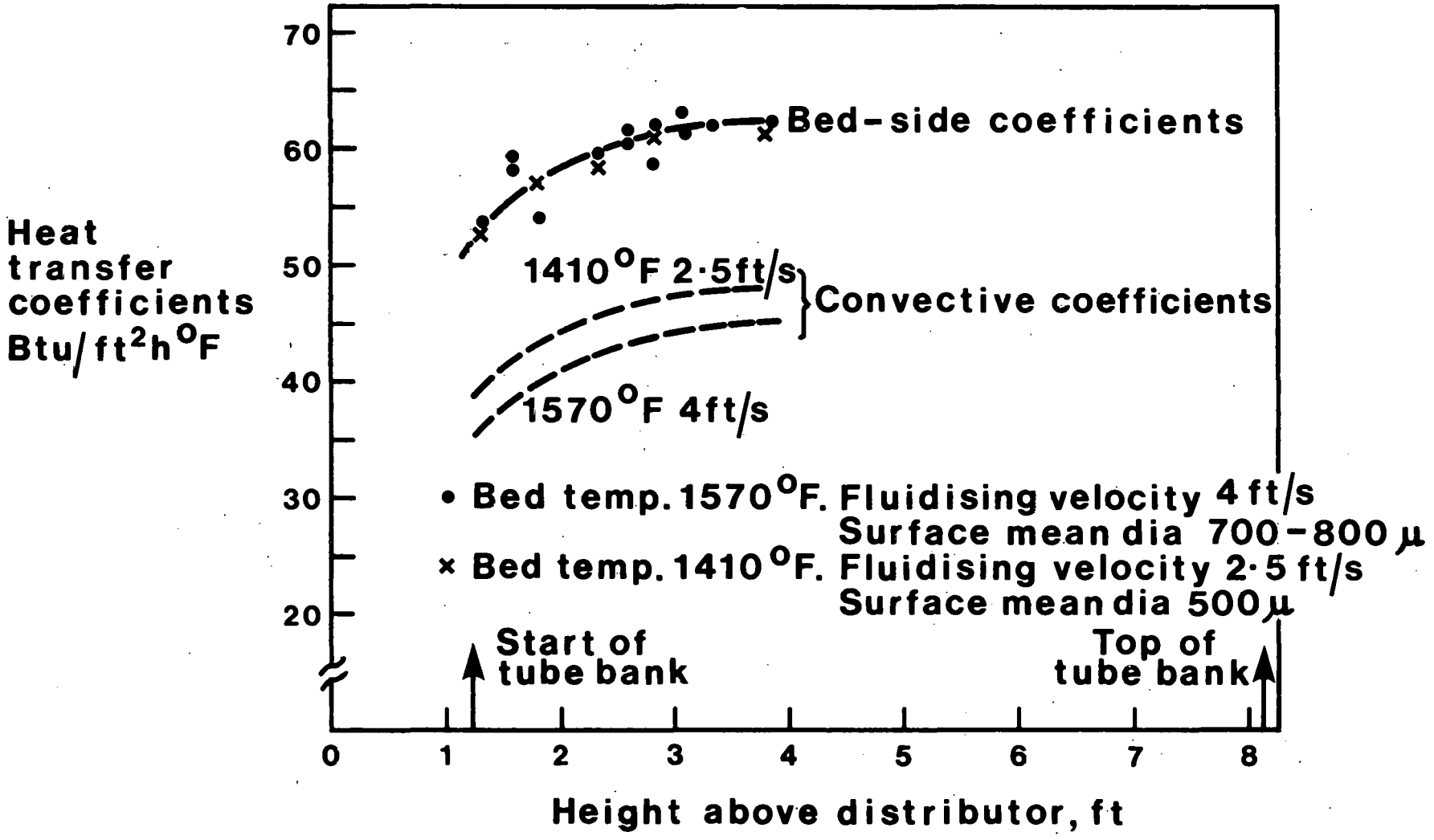

Fig.41 Heat transfer to immersed tubes: Bed depth 4·2ft

D663

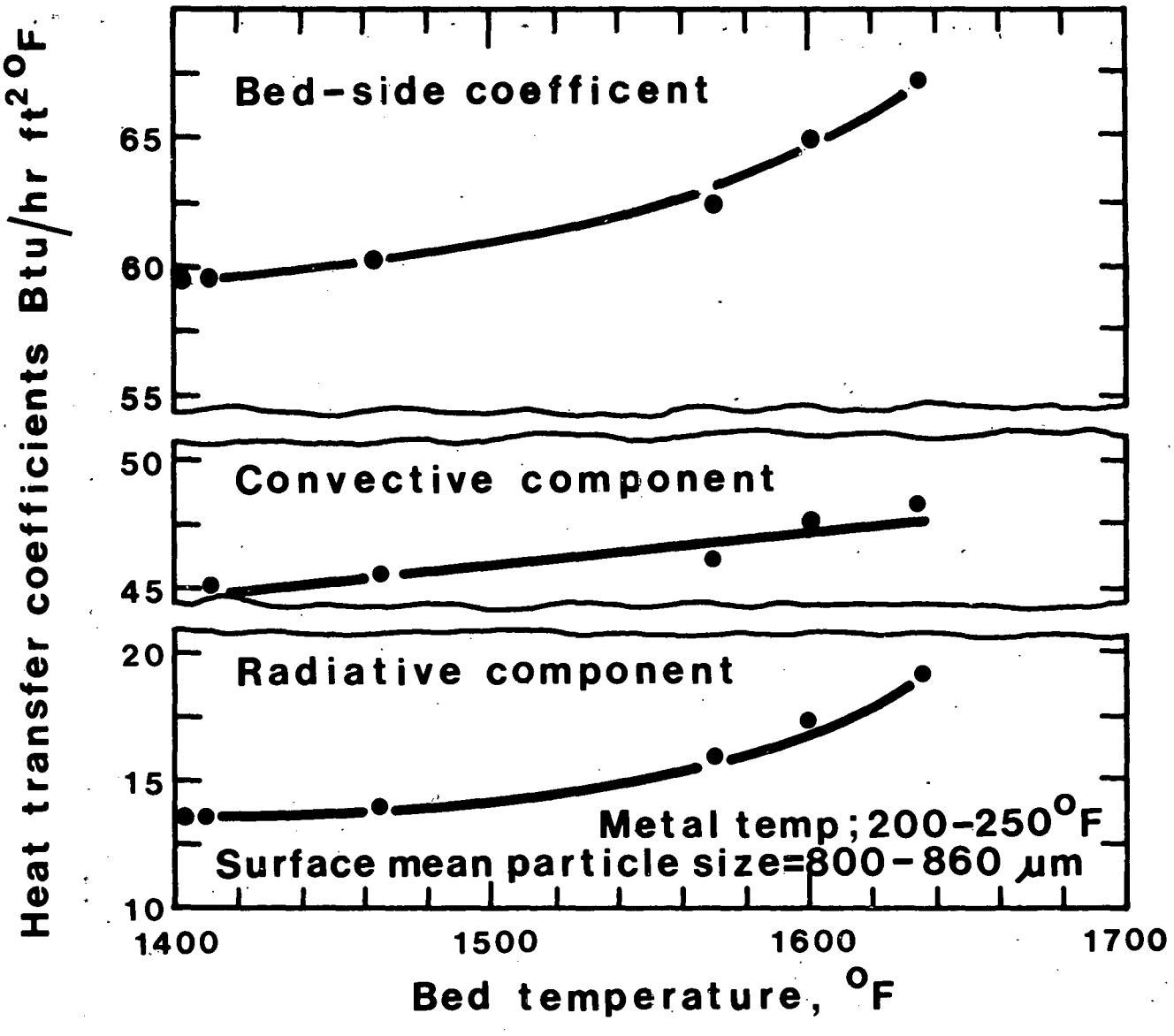

Fig.42 Effect of bed temperature on immersed tube coefficients

D589

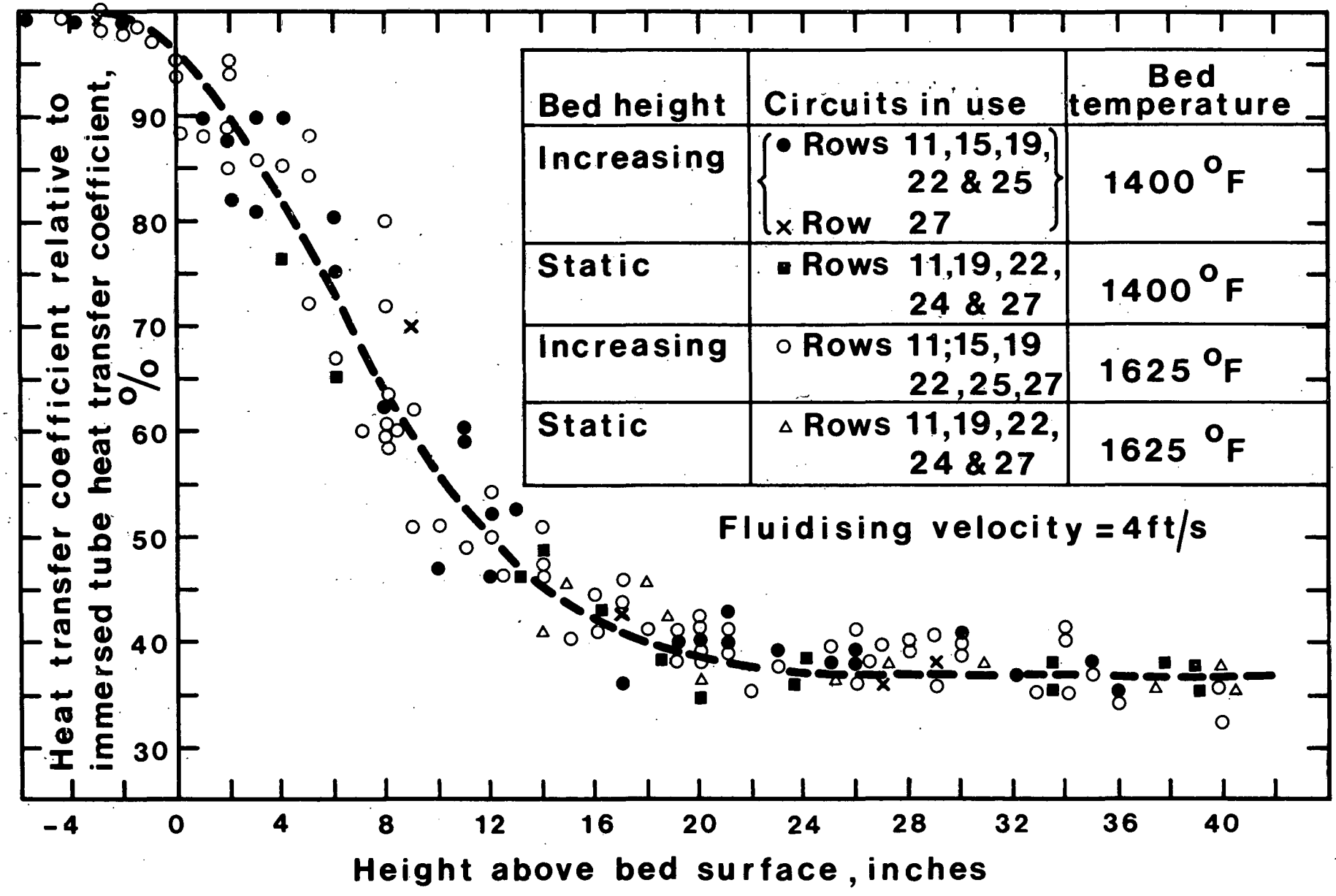

Fig.43 Freeboard heat transfer coefficients

D590

$$\frac{h}{h_b} f = 0.38 + 0.62 \exp(0.007014(H+3)^2$$

where H is the position above the bed surface in inches.

The maximum heat transfer coefficients in the bed appeared to occur slightly below the bed surface. However, the position of the bed surface is calculated from pressure drop measurements which ignore any change in bed density near the splash zone. The position of the bed surface is, therefore, somewhat imprecise.

No attempt was made to calculate the radiative component of heat transfer in the "splash zone", and hence to isolate the convective component. The calculated "convective plus radiation" coefficient for a clean gas was 15 Btu/ft^2 h $^{\circ}$F at a gas temperature of 1400 $^{\circ}$F, i.e. about 22% of the in-bed heat transfer coefficient. This, however, must be an under estimate since the presence of solids (about 10,000 ppm were being elutriated) would enhance both the convective and the radiative heat transfer. Measured heat transfer rates to the highest rows at the lowest bed heights indicated a minimum freeboard coefficient of about 38% of the in-bed coefficient.

In calculating the heat transfer coefficients in the splash zone the local temperatures were taken from appropriate distributions, such as that shown in Fig. 44 which applies to one of the set of data plotted in Fig. 43. Temperatures were measured by thermo-couples inserted to a depth of about 3 inches at various positions on the combustor walls.

6.5.3 Heat transferred from the bed to the "splash zone". Some of the heat abstracted in the freeboard originates from the bed itself and is conveyed into the freeboard region as "splashing" bed material. This material cools down as it gives up its heat in the freeboard and then exerts a cooling load on returning to the bed. To maintain constant bed temperature therefore requires a higher coal feed rate - all other conditions being equal - when freeboard cooling is present.

Any cooling surface in the freeboard receives heat in the following forms:-

(1) by conduction/convection from splashing bed material

(2) by convection from the dirty gas flowing past it, and

(3) by radiation from the surrounding environment.

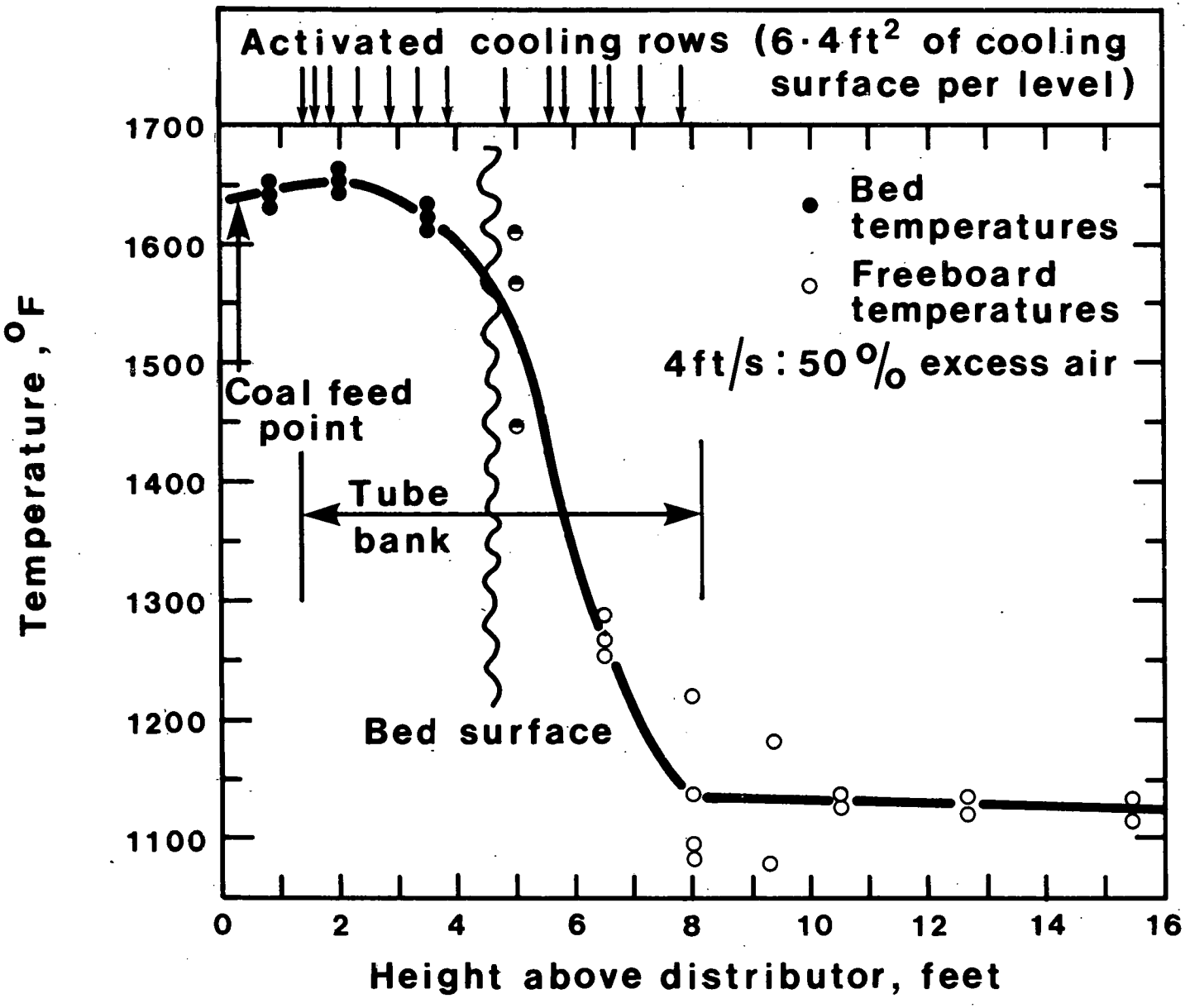

Fig.44 Combustor temperature profile with heavily-cooled freeboard.

Two method were used to determine the proportion of heat abstracted in the freeboard due to splashing:-

(a) Oxygen variation. With a bed depth of 4 to 5 ft, rows of cooling tubes in the freeboard were activated or shut off singly, and the resultant change in oxygen content of the flue gas was monitored (automatic coal feed rate control being exercised to maintain constant bed temperature). The increase or reduction in heat input to the bed was quantified assuming complete combustion of carbon to carbon dioxide, thus:

$$\Delta Q = \Delta m_{O_2} \times 5438 \text{ Btu/lb}$$

where ΔQ = heat transfer due to splashing (Btu/h)

Δm_{O_2} = change in mass flow rate of free oxygen in the gas (lb/h)

(b) Heat balance. Considering the temperature profile in the freeboard enabled approximate heat balances to be constructed around the region containing single rows of cooling surface, thus

Heat transfer due to splashing = heat absorbed by cooling tube
- heat lost by gas
- heat losses through combustor walls.

The procedure required that gas temperature profiles be determined by interpolation and was subject to large uncertainties.

Fig. 45(a) gives the data obtained by the above two methods. An exponential reduction in the splashing heat transfer with height is apparent. Agreement between the two methods is good, but it is thought that the analysis by the direct method (oxygen variation), was more accurate even though very small oxygen variations were being measured at the top of the splash zone.

Fig. 45(b) details the contribution made by splashing to the total heat transfer coefficient in the freeboard. It is evident that in this case, the effects of splashing were significant for up to 24 inches above the bed surface. The existence or otherwise of cooling surface in this region will have obvious implications for bed temperature, coal feed rate and excess air level. The height of the splash zone appears to be independent of bed temperature but is likely to increase with increasing velocity.

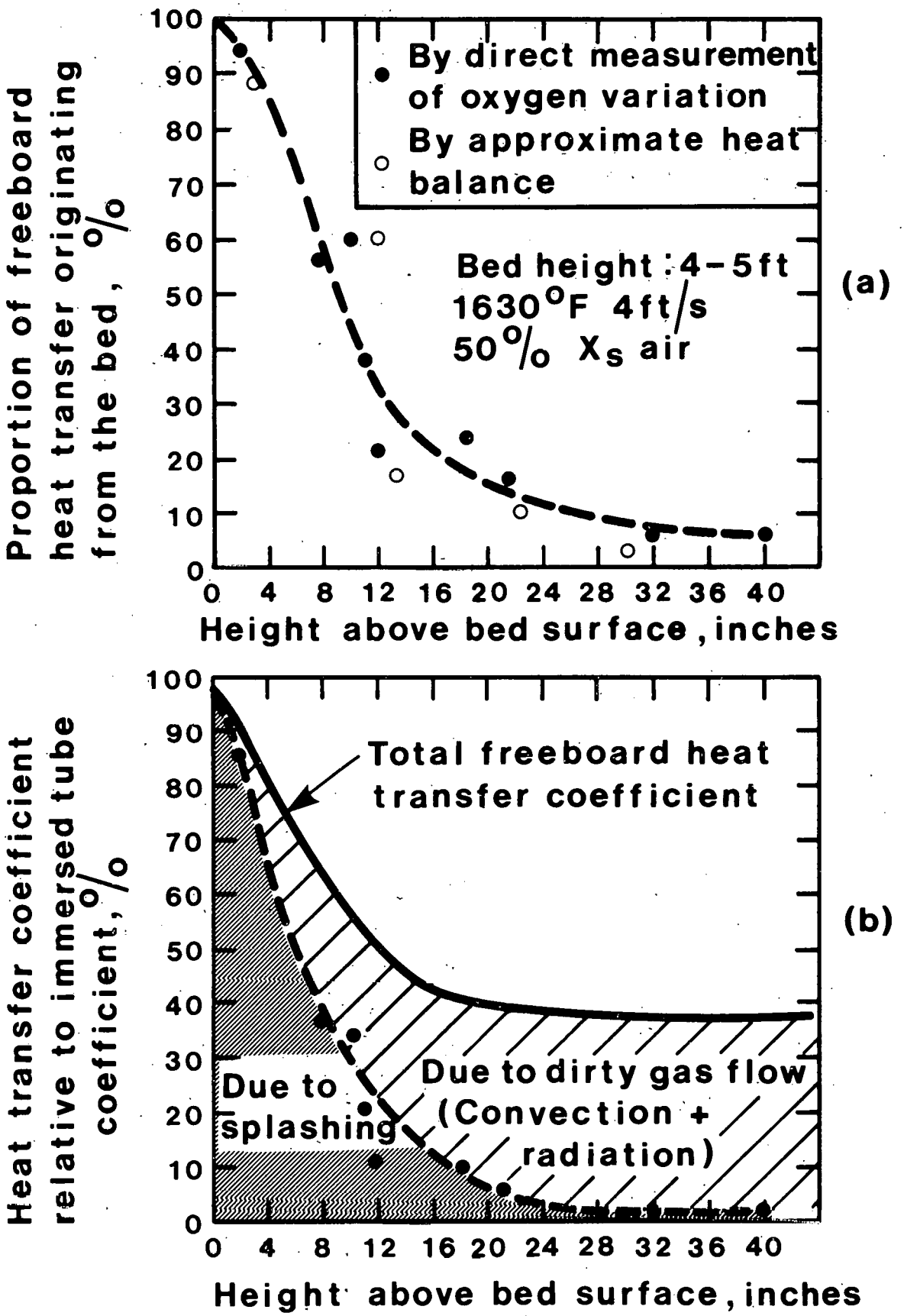

Fig. 45 Heat transfer in the freeboard due to "splashing"

D592

6.6 BED TEMPERATURE RESPONSE MEASUREMENT BY FREQUENCY RESPONSE ANALYSIS

An understanding of the dynamic behaviour of a process is essential to the correct design of systems for the automatic control of the process. In addition the measurement of dynamic response leads to a greater understanding of the mechanism by which the process works both in the steady and transient states.

Frequence response analysis is a method of dynamic testing which, in the absence of a mathematical model, leads directly to the design of the correct control system. In addition the measured frequency response may be compared with that predicted by a particular mathematical model in order to verify the model.

Frequency response analysis was used to determine the response of bed temperature to changes in coal feed rate during all three tests of the series and data were obtained for a number of operating conditions.

6.6.1 Experimental technique. The characterisation of the dynamic relationship of a system output to an input (in this case bed temperature and coal feed, respectively) by a frequency response analysis involves varying the input sinusoidally, at a number of frequencies and measuring the response of the output in terms of an Amplitude Ratio (AR) and a Phase Shift (ϕ). Results are presented in the form of a Bode plot.

This was carried out using the coal feed/bed temperature control system shown schematically in Fig. 46. During normal operation the system was in automatic control and the temperature controller received a temperature signal from a bed thermocouple and by comparing this with the temperature set point as specified by the control panel operator, sent a signal to the set point input of the rotary valve speed controller. The system thereby attempted to correct for any change in conditions which resulted in a change in bed temperature, by increasing or decreasing the coal feed rate.

In order to vary the coal feed rate sinusoidally the bed temperature controller was switched to manual control to provide a constant base signal to the rotary valve speed control. The bed temperature was then allowed to stabilise after any change resulting from the switch from automatic to manual control and a check made that any such change did not take the plant too far from the reference operating conditions. It was felt that a deviation of steady state temperature of less than

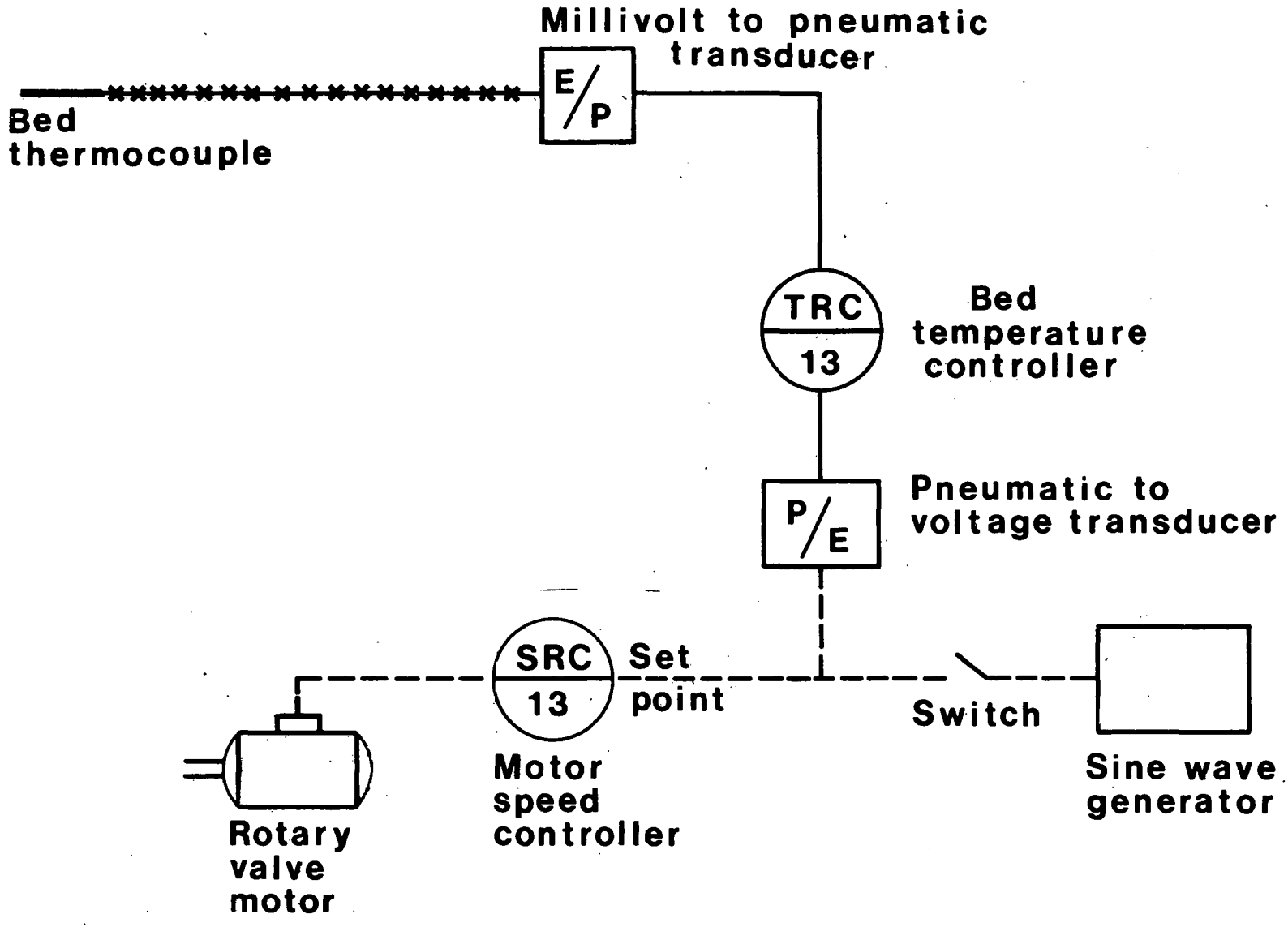

Fig.46 Bed temperature control system with sine wave generator for frequency response analysis

±40°F from the reference temperature would result in little error due to non-linearity, although the sinusoidal variation was normally maintained well within this limit. A feedback PFG 605 function generator was then connected to the circuit as shown in Fig. 46, so that its output could be added to the base signal. At some point close to the start of the test the charts were simultaneously marked to provide a point of synchronisation. The duration of a run depended on the frequency at which the plant response was being determined. At least one cycle of a run was allowed for the dying out of transients so that at the low frequencies (0.0006 Hz) the run lasted for 1 to 2 hours to obtain two cycles of usable response data. At the high frequency end of a series of runs (≤0.015 Hz) a 15 minute duration gave approximately 15 cycles. Each frequency response test was started at a 'guessed at' mid-frequency and the amplitude ratio part of the Bode Plot was fitted to this point assuming a single first order response. The aim at the low and mid frequencies was to obtain a bed temperature variation of ±8 to 15°F and the preliminary AR plot was used to predict the amplitude ratio at the next test frequency enabling approximate calculation of the required rotary valve speed amplitude. At high frequencies and small amplitude ratio a smaller bed temperature variation had to be tolerated in order to prevent excessive variations of rotary valve speed, the amplitude limits being those that would either stop the valve or cause near sub-stoichiometric conditions within the combustor.

In addition to the process control instrumentation of Fig. 46 a number of bed temperatures, the two rotary valve speeds and all gas analysis measurements were recorded on flat-bed recorders with 25 cm wide charts and a range of chart speeds. Temperatures were measured using type 'K' thermocouples on a 400°F scale adjustable between 1380-1780°F and 1250-1650°F according to the bed temperature. This scale allowed the resolution of temperature fluctuations at least as small as 4°F.

Rotary valve speeds were measured using an incremental shaft encoder coupled to a frequence-to-current converter.

6.6.2 Analysis of Results. Fig. 47 shows a section of chart from a single frequency test. The bed temperature, as represented by one thermocouple, and the rotary valve speeds are indicated. The average amplitude of each was determined by measuring each half wave amplitude and the amplitude ratio calculated as:-

$$AR = \left[\frac{\Delta\theta}{\Delta Y}\right]\left[\frac{m_g c_{g\theta} + h_w A_w}{m_g c_{g(\theta-\theta_0)} + h_w A_w}\right]^{-1}\left[\frac{Y_{\theta-\theta_0}}{\theta-\theta_0}\right]$$

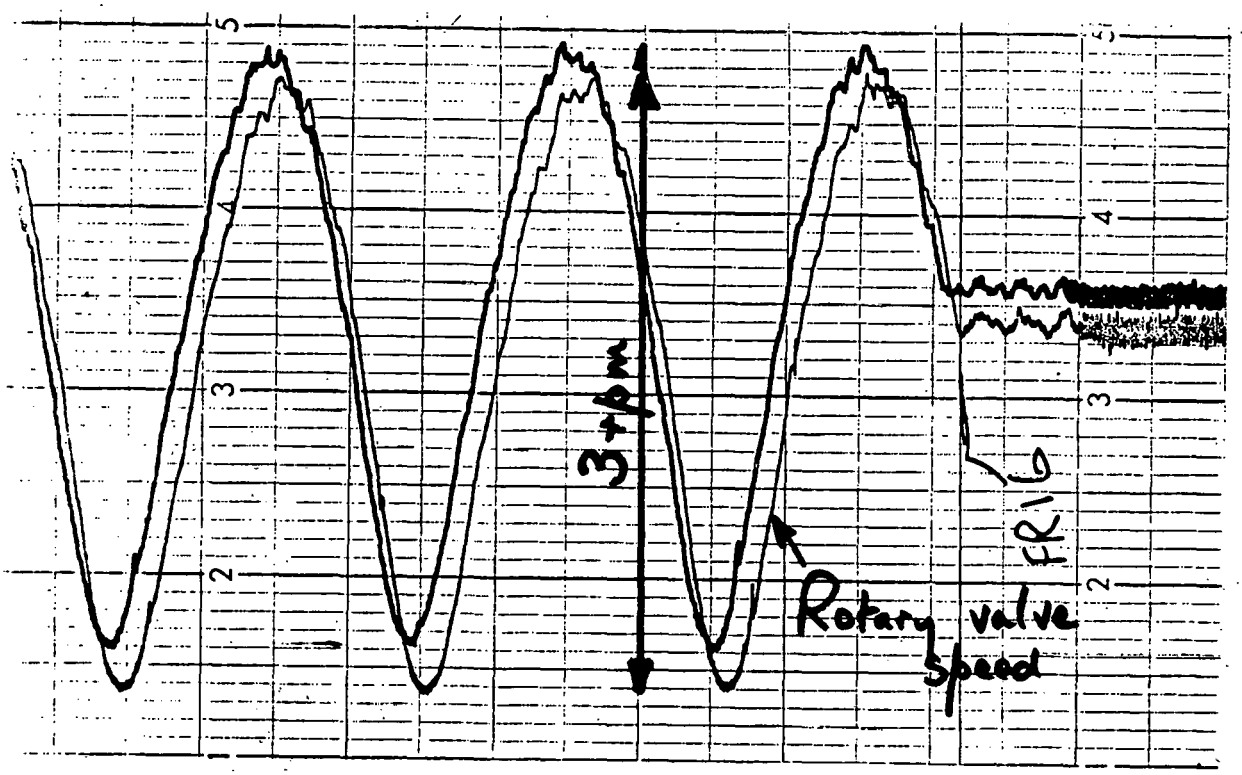

Chart speed 2cm/min

Fig. 47. Typical frequency response data at .05 radians/s

Where Θ and Y are respectively the steady state bed temperature and rotary valve speed as measured before a test and $\Delta\Theta$ and ΔY are the corresponding sine wave amplitude. Θ_o represents the inlet air temperature and the average cooling water temperature which in the case of the Leatherhead rig were approximately equal. The denominator of this expression represents the temperature rise which would occur were the change ΔY in rotary valve speed made as a step and the system allowed to go to steady state. It assumes a proportionality between rotary valve speed and coal feed rate.

The relationship between coal feed rate and temperature is given by

$$\frac{\Delta M_{c\Theta}}{M_{c(\Theta-\Theta_o)}} = \left[\frac{m_g C_{g\Theta} + h_w A_w}{m_g C_{g(\Theta-\Theta_o)} + h_w A_w}\right] \frac{\Delta\Theta}{(\Theta-\Theta_o)}$$

where $\Delta M_{c\Theta}$ = variation in coal feed rate at temperature Θ

$M_{c(\Theta-\Theta_o)}$ = steady state coal feed rate at temperature Θ

m_g = flue gas flow

$C_{g\Theta}$ = gas specific heat at temperature Θ

$C_{g(\Theta-\Theta_o)}$ = gas specific heat integrated between Θ and Θ_o

h_w = overall heat transfer coefficient to bed tubes

A_w = total submerged heat transfer surface

$\Delta\Theta$ = small temperature variation associated with $\Delta M_{c\Theta}$

Θ = steady state temperature

Θ_o = reference temperature

Phase shift (ϕ) was obtained by measurement of chart length from peak of input signal (rotary valve speed) to corresponding peak of output signal (bed temperature) and by comparison with the chart length equivalent to one wave of input signal.

$$\text{hence} \quad -\phi = \frac{\Delta L}{L_{360}} \times 360^o$$

where ΔL = average length from peak of input signal to peak of output signal

L_{360} = chart length equivalent to one wave of input signal.

The analysis assumes that the temperature response involves one or more first order mechanisms in series, each of which responds to an input of the type

$$y = A \sin \omega t$$

with an output

$$x = \frac{A}{\sqrt{\omega^2 T^2 + 1}} \sin (\omega t + \phi)$$

where ϕ = -arctan (ωt)

ω = frequency

T = time constant

A = amplitude

t = time

The expression relating amplitude ratio to frequency is then

$$AR = \frac{1}{\sqrt{\omega^2 T^2 + 1}}$$

or, more generally, for a number of system in series

$$AR = \prod_{n=1}^{n} \frac{1}{\sqrt{\omega^2 T_n^2 + 1}}$$

where T_n is the time constant of the nth mechanism.

The general expression for phase shifts is

$$-\phi = \omega T_D + \sum_{n=1}^{n} \arctan (\omega T_n)$$

where T_D is the dead time.

A micro computer was programmed to produce a visual display of the Bode plot of first, second and third order systems with dead time together with the experimentally determined AR and ϕ data. By adjusting the value of time constants of the theoretical plot a fit to the data was obtained. Typical visual displays are reproduced in Figs. 48 and 49.

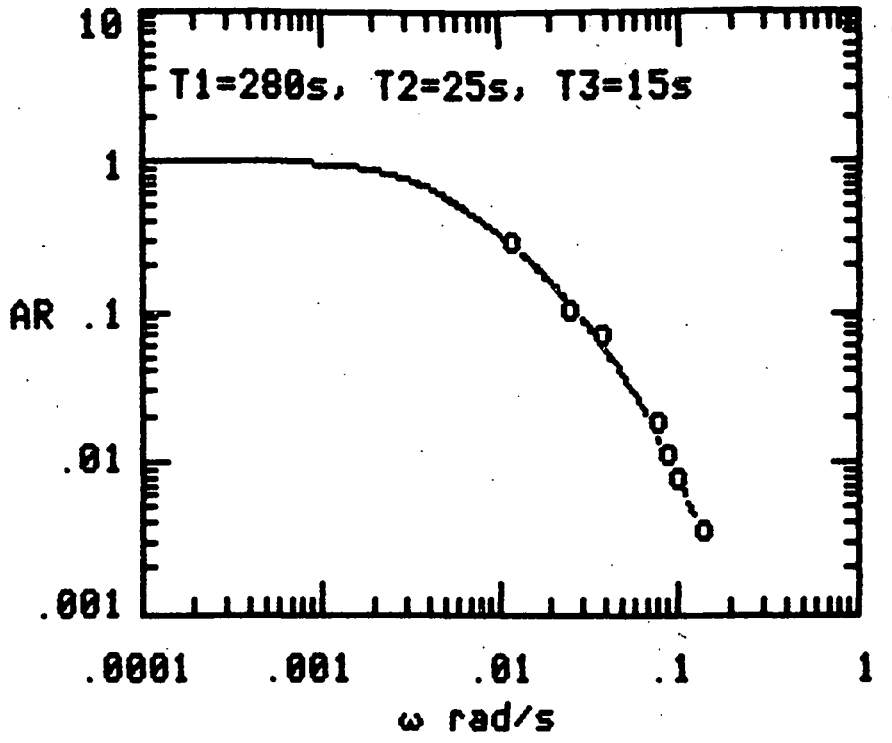

AR = amplitude ratio

ω = frequency

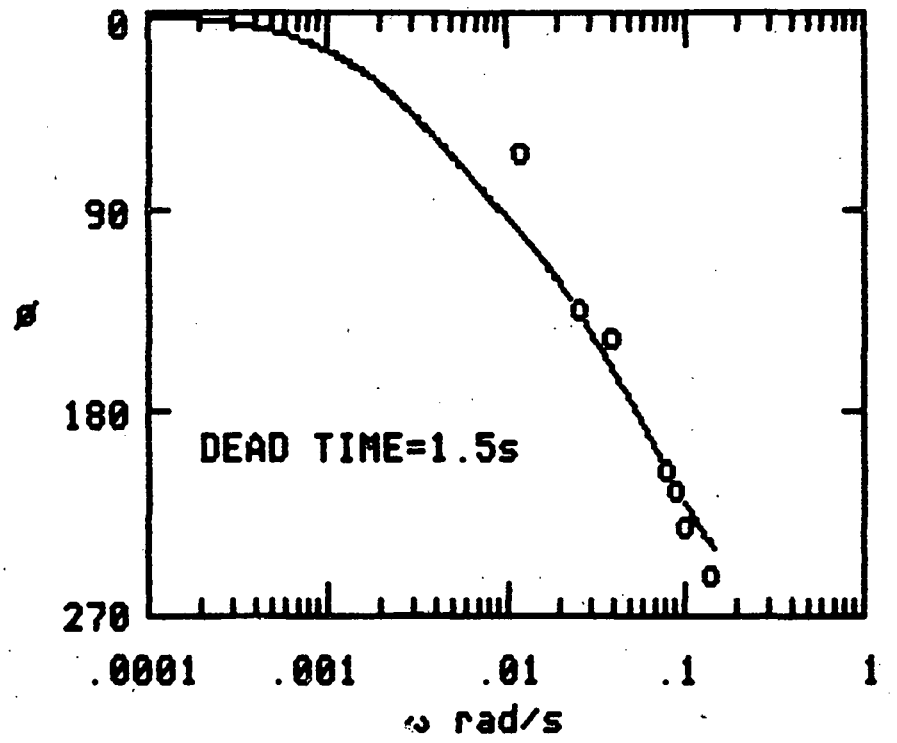

ϕ = phase shift

TEST NO. FR/DOE/3A

Fig.48 Bode diagrams. Test 3/1 conditions

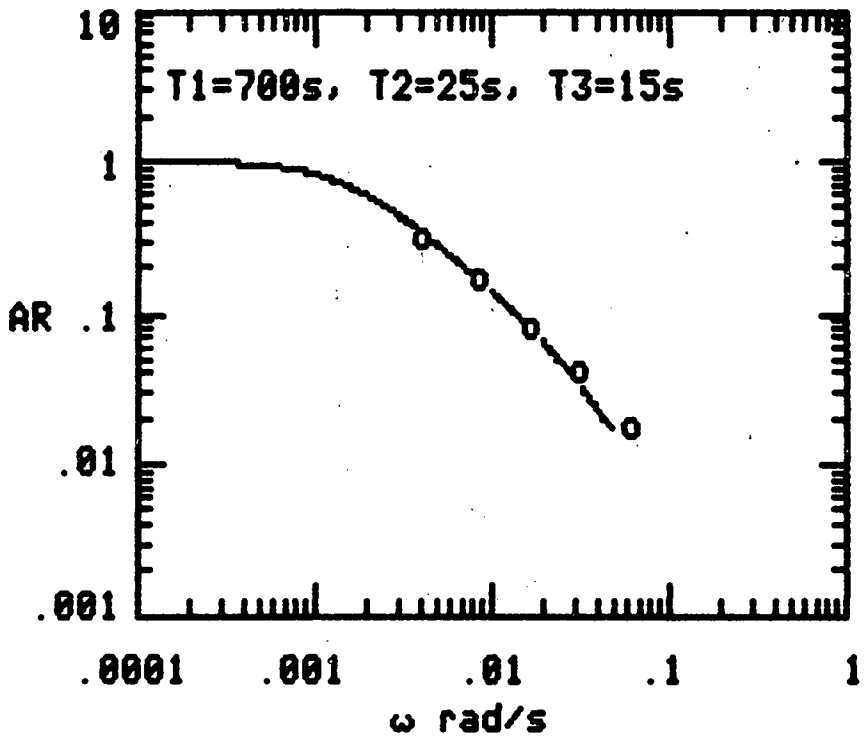

AR = amplitude ratio

ω = frequency

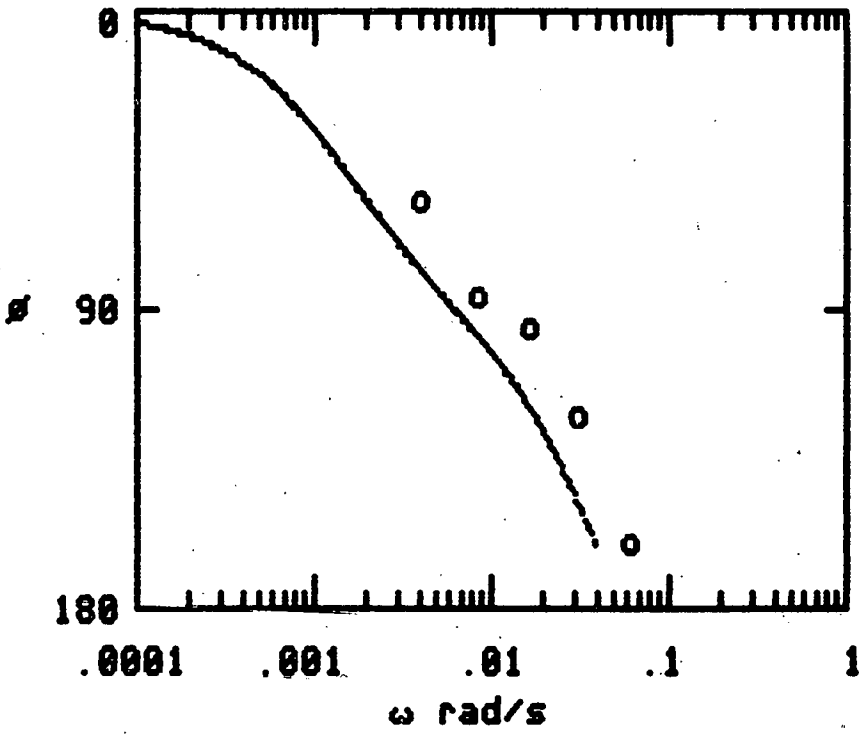

ϕ = phase shift

TEST NO. FR/DOE/3C

Fig.49 Bode diagrams. Test 3/3 conditions

6.6.3 Comparison of results with a simple combustor model. Consideration of an unsteady state heat balance for the combustor, assuming that the incoming air temperature and water temperature are identical and that the coal burns and liberates its heat to the bed instantaneously, leads to the following first order differential equation

$$M_b C_b \frac{d\theta}{dt} = c_v m_c(t) - (m_g c_g + h_w A_w)\,\theta$$

where θ = bed temperature (referred to inlet air temperature)

M_b = mass of bed

c_b = specific heat of bed

c_v = net calorific value of coal

$m_c(t)$ = coal feed rate as a function of time

m_g = mass flow rate of gas leaving the bed surface

c_g = specific heat of flue gas

h_w = overall heat transfer coefficient for water cooled tubes

A_w = total surface area of water cooled tubes

The time constant of such a system is

$$T = \frac{M_b c_b}{m_g c_g + h_w A_w}$$

Uncooled tubing submerged in the bed is assumed, because of its small cross section, to behave as if it were part of the bed and its thermal capacity is added to that of the bed so that the time constant becomes

$$T = \frac{M_b c_b + M_m c_m}{M_g C_g + h_w A_w}$$

Where M_m = mass of uncooled tubing

c_m = specific heat of tubing

The experimental values of time constant obtained during the programme are compared with the theoretical values, derived from the above expression in Table 12. In this comparison it is assumed that the longer of the two time constants indicated by the Bode analysis corresponds to the heat balance mechanism.

Table 12. Response rate investigations - Comparison of Measured and Calculated Time Constants

		Test 1	Test 2	Test 3/1	Test 3/2	Test 3/3
Mass of bed	lb	2054	1328	889	1109	1842
Specific heat of bed	Btu/lb ^{o}R	0.305	0.301	0.304	0.301	0.309
Mass of uncooled tubes	lb	687	301	189	155	668
Specific heat of tube material	Btu/lb^{o}R	0.2	0.2	0.2	0.2	0.2
Flue gas flow rate	lb/sec	2.76	3.11	2.88	1.95	2.78
Specific heat of flue gas	Btu/lb^{o}R	0.286	0.281	0.286	0.281	0.286
Area of cooling surface -	ft^2	34.67	57.6	38.52	41.09	38.52
Average overall heat transfer coefficient -	Btu/sec ft^2 ^{o}R	0.015	0.014	0.014	0.013	0.015
Calculated time constant (T_c) -sec		582	274	223	331	510
Measured time constant (T_m) - sec		700	380	280	450	700
T_m/T_c		1.2	1.39	1.26	1.36	1.37

APPENDIX 1

Derivation of combustion efficiency correlation

The combustion efficiency attainable within a fluidised bed combustor is determined by the rate at which unburnt or partially burnt fuel is lost from the system. The loss of potentially combustible fuel can occur by three mechanisms:-

(1) elutriation of unburnt solids
(2) removal of unburnt solids along with bed material
and (3) as combustible gaseous effluent.

Of these, elutriation is by far the most important and generally accounts for over 95% of the losses in PFBC systems. The losses through removal of bed material become significant only when the carbon concentration in the bed becomes significant (i.e. with non-reactive fuels or with fuels of large particle size). The losses due to unburnt gaseous effluent are generally very low within the range of temperatures envisaged for fluidised bed combustors (1400-1700°F).

The physics of the processes within a fluidised bed combustor are not yet sufficiently understood to predict combustion efficiency from first principles. The mechanisms by which coal burns within the bed, by which unburnt material burns in the freeboard and by which elutriation occurs have yet to be established.

In empirical terms however the general principles governing losses and therefore combustion efficiency are well known:-

(1) Factors increasing elutriation increase the losses (i.e. increasing velocity, decreasing coal feed size).

(2) Increasing reactivity reduces losses (i.e. increasing coal reactivity, bed temperature, pressure)

(3) Increasing the extent of reaction while in the bed reduces losses (i.e. increasing particle residence time, gas residence time, resistance to attrition, excess air).

(4) Increasing the extent of freeboard combustion reduces losses (i.e. increasing freeboard temperature, freeboard residence time, excess air).

An empirical correlation of all the data generated in pressurised combustors at NCB, CURL has been obtained as:-

$$1-\eta = \frac{A^{0.5}}{R\, t_b\, t_f^{0.33}(1+X)} \exp\left[\frac{2535}{T_B}\right] \exp\left[\frac{-3.67(T_f - T_B)}{T_B}\right]$$

where
- η = fractional combustion efficiency
- A = bed area per coal feed nozzle (ft^2)
- t = gas phase residence time in the bed (s)
- t_f = gas phase residence time in the freeboard (s)
- X = fractional excess air
- T_B = bed temperature (^oR)
- T_f = mean freeboard temperature (^oR)
- R = coal reactivity factor

It should be emphasised that this correlation has been generated only from pressurised data (5-6 atmospheres) and does not include any pressure effects. Equally coal feed size is not explicitly included although it is partly implicit in t_b through the influence of fluidising velocity on t_b and because coal feed size is usually chosen to suit the velocity.

Based on some 65 data sets obtained using very similar US coals (Illinois No. 6, Illinois No. 5 and Glen Brook) the above form of the correlation was established and a suitable value of R was derived. Analysis of variance indicated that the form of the correlation was significant to greater than the 99.9% level. The form was then used with a further 10 data sets to obtain values of R for seven different coals.

The correlation is illutration in Fig. 24 where those data originating from work sponsored by the US DOE (or by their predecessors, ERDA and the Office of Coal Research) are identified separately. All the data are given in Table 1.

One of the measures of coal reactivity is the oxygen content of the coal (on a dry ash-free basis). Fig. 26 illustrates the relationship between derived values of the coal reactivity factor R and the oxygen content. It is apparent that a strong relationship exists and this provides further confidence in the form assumed for the correlation.

Fig. A1 illustrates the effect of temperature as a family of efficiency curves, as given by the correlation, for the following conditions:-

Coal type:-	U.S. Bituminous (Illinois or similar)		
bed residence time,	t_b	=	2.5s
freeboard residence time	t_f	=	3s
area per coal feed nozzle,	A	=	6 ft^2
excess air	x	=	0.5 (i.e. 50% excess air)

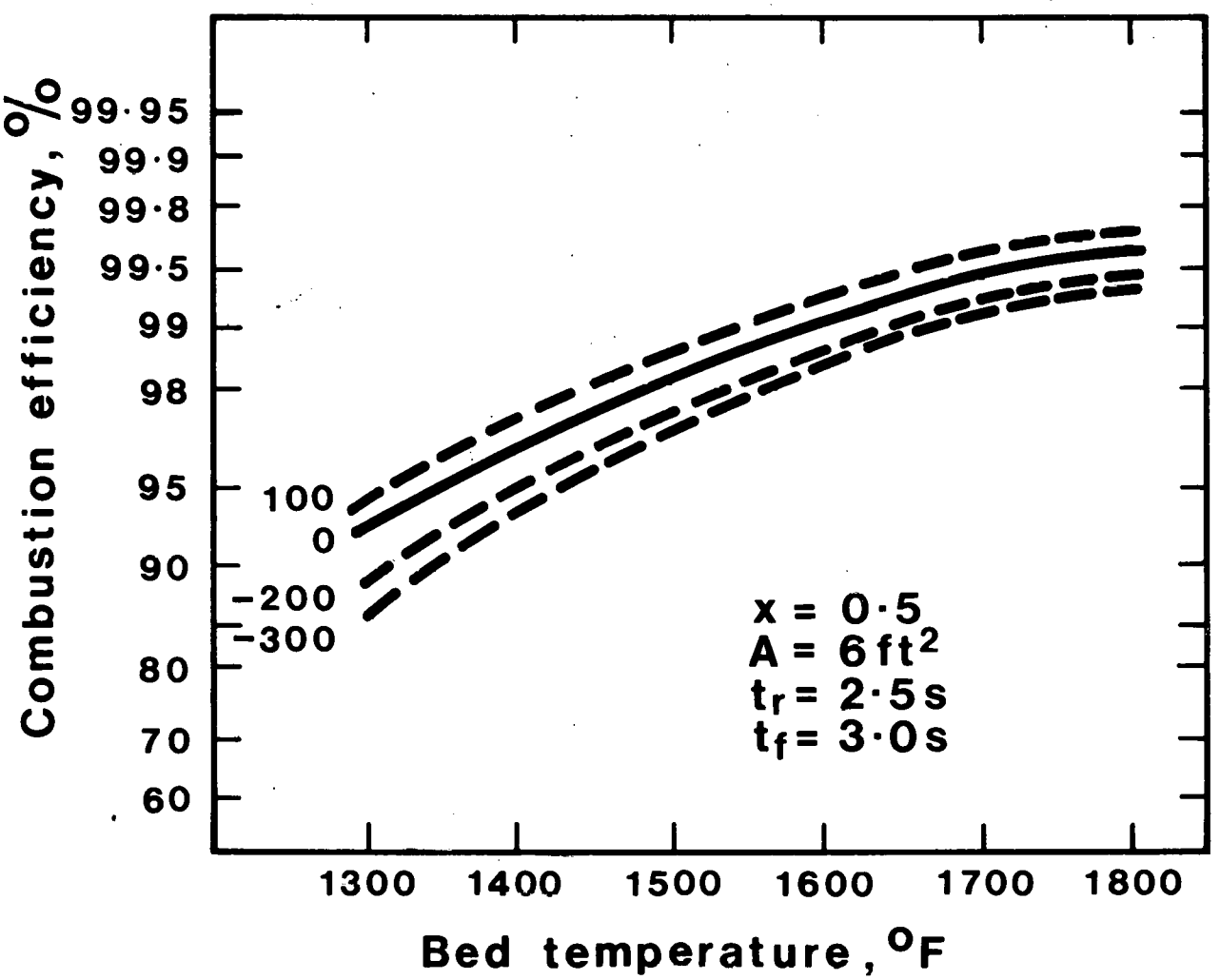

Fig.A1 Effect of temperatures on combustion efficiency

Table A1 Combustion Efficiency Data

CODE		Coal	A ft^2	t_b s	t_f s	T_B °R	T_F °R	X %	R x 10^6	η_{obs}	η_{cale}
Main combustor:-											
ERDA	Test 1	Illinois	1.5	1.91	5.0	2090	2070	18	10.7	99.3	99.4
	2	"	1.5	2.0	4.6	2210	2150	23	10.7	99.6	99.7
	3	"	1.5	2.04	5.0	2115	2080	17	10.7	99.4	99.5
	4	"	1.5	1.78	5.2	2195	2060	17	10.7	99.7	99.6
	5	"	3.0	1.92	5.0	2050	2035	90	10.7	99.4	99.4
	6/1A	"	2.0	3.0	3.0	2060	2010	25	10.7	99.0	99.4
	6/1B	"	2.0	3.0	3.0	2060	2015	30	10.7	99.3	99.4
	6/2A	"	3.0	3.2	3.2	2060	1990	100	10.7	99.7	99.6
	6/2B	"	3.0	3.2	3.2	2060	2000	120	10.7	99.7	99.6
	7A	"	3.0	1.17	1.1	2115	2050	95	10.7	98.5	98.8
	7B	"	3.0	1.26	1.2	2115	2050	63	10.7	98.2	98.7
GE	8	"	3.0	2.0	1.6	2080	2035	30	10.7	98.5	98.9
	9	"	3.0	1.85	1.6	2170	2125	30	10.7	99.0	99.3
Sponsor A	2A	UK bituminous	6.0	0.65	1.8	2020	1586	40	11.6	92.0	88.1
	2B	"	6.0	0.96	1.5	2010	1775	35	11.6	93.1	93.4
	2C	"	6.0	1.29	1.2	2040	1975	35	11.6	96.1	96.7
Sponsor B	6/1	Glen Brook	6.0	1.17	3.7	1955	1890	260	10.7	97.7	98.3
	6/1A	" "	6.0	1.17	3.7	1970	1900	230	10.7	97.7	98.3
	6/4	" "	6.0	2.33	7.4	1880	1825	300	10.7	98.9	99.0
	6/5	" "	6.0	1.25	3.0	1970	1925	250	10.7	97.7	98.5
DOE 1000 h	1/1	" "	9.0	2.19	2.7	2000	1935	97	10.7	98.7	98.3
	1/2	" "	9.0	2.22	2.4	2005	1940	114	10.7	98.5	98.5
	2/1	" "	9.0	2.10	2.6	2030	1985	100	10.7	98.4	98.6
	2/2	" "	9.0	2.23	2.4	2035	1990	96	10.7	98.2	98.6
	2/3	" "	9.0	2.40	2.3	2045	2000	96	10.7	98.5	98.8
	2/4	" "	9.0	2.24	2.6	2035	1990	99	10.7	98.7	98.7

Table A1 Combustion Efficiency Data (Contd.2)

CODE	Coal	A ft^2	t_b s	t_f s	T_B °R	T_F °R	X %	R x 10^6	η_{obs}	η_{cale}
DOE 1000 h Test 3	Glen Brook	9.0	2.37	2.3	2035	1985	108	10.7	99.1	98.8
" 4	" "	9.0	2.33	2.3	2040	1990	100	10.7	99.3	98.8
" 5	" "	9.0	2.47	2.2	2035	1980	104	10.7	99.2	98.8
" 6	" "	9.0	2.47	2.2	2035	1980	104	10.7	99.2	98.8
DOE 1980 " 1/1	" "	3.0	1.11	3.2	1920	1970	55	10.7	97.8	96.8
" 1/2	" "	3.0	2.26	1.8	2090	1990	65	10.7	99.0	99.2
" 1/3	" "	3.0	2.29	1.9	1875	1835	60	10.7	96.7	97.0
" 1/4	" "	3.0	2.33	1.8	2060	1920	25	10.7	97.8	98.6
" 2/1	" "	3.0	1.45	2.6	1860	2015	60	10.7	97.1	96.9
" 2/2	" "	3.0	1.46	2.4	1860	1790	65	10.7	95.8	95.2
" 3/1	" "	3.0	1.05	2.9	2090	1600	62	10.7	96.0	97.1
" 3/2	" "	3.0	1.68	4.7	1855	1615	50	10.7	95.3	94.6
" 3/3	" "	6.0	2.15	1.8	2040	1975	58	10.7	99.0	98.9
Sponsor C " 1/1	Illinois	3.0	3.6	3.4	2055	1990	28	10.7	98.5	99.4
" 1/2	"	3.0	3.19	3.0	2065	1990	36	10.7	99.0	99.4
" 1/4	"	3.0	3.2	3.2	1915	1865	41	10.7	99.0	98.5
" 1/5	"	3.0	2.03	2.3	1960	1925	43	10.7	97.5	98.1
Sponsor D " 1	High ash sub-bituminous	3.0	1.64	3.0	2020	1980	178	22.0	98.8	99.6
" 2	"	3.0	3.22	6.4	2005	1935	162	22.0	99.9	99.8
12 inch Combustor										
Sponsor B Test 1	Glen Brook	.785	0.78	2.8	2025	1980	140	10.7	99.2	99.1
" 2	" "	.785	0.81	2.9	2025	1980	140	10.7	99.3	99.1
" 3	" "	.785	1.05	2.7	2025	1980	115	10.7	99.3	99.2
" 4	" "	.785	0.99	2.6	2015	1980	135	10.7	99.0	99.2
" 5/1	" "	.785	0.97	2.7	2025	1980	110	10.7	99.1	99.1

Table A1 Combustion Efficiency Data (Contd. 3)

CODE	Coal	A ft^2	t_b s	t_f s	T_b ^oR	T_F ^oR	X %	R x 10^6	η_{obs}	η_{cale}
Sponsor B Test 5/2	Glen Brook	.785	1.03	2.9	1765	1730	160	10.7	95.7	95.9
" 5/3	" "	.785	1.03	2.9	1765	1730	150	10.7	96.0	95.7
" 5/4	" "	.785	1.05	2.7	1835	1800	140	10.7	97.5	97.5
" 5/5	" "	.785	0.85	1.8	2035	2000	135	10.7	98.5	99.1
Sponsor A " 1	FRG Bituminous	.785	0.92	2.6	2115	2090	160	7.4	98.9	98.9
" 2	Anthracite	.785	1.06	2.7	2117	2090	170	2.1	96.4	96.4
" 3	US Lignite	.785	1.14	2.7	2110	2080	170	72	99.9	99.9
" 4	Glen Brook	.785	0.99	2.7	2100	2070	170	10.7	99.3	99.2
" 5	FRG Bituminous	.785	1.00	2.7	2100	2070	170	4.5	98.0	98.0
" 6	UK Bituminous	.785	1.03	2.7	2115	2090	170	11.6	99.3	99.3
Sponsor C " 4	Illinois	.785	0.87	2.1	2115	1970	136	10.7	99.7	99.5
" 6	"	.785	0.56	1.4	2115	2090	156	10.7	99.2	99.1
" 7	"	.785	0.41	0.9	2115	2090	156	10.7	98.9	98.6
" 8	"	.785	0.31	0.7	2095	2090	166	10.7	98.4	97.9
" 9	"	.785	0.21	0.6	2140	2140	162	10.7	97.3	97.5
" 10/2A	"	.785	0.29	1.0	2135	2115	133	10.7	98.4	98.2
" 10/1	"	.785	0.21	0.7	2135	2090	162	10.7	98.1	97.3
" 10/2B	"	.785	0.14	0.6	2095	2205	122	10.7	95.9	95.3
" 11	"	.785	0.24	1.0	2115	2090	116	10.7	97.8	97.3
" 12/1	"	.785	0.38	1.5	2105	2050	157	10.7	98.8	98.6
" 12/2	"	.785	0.27	1.1	2105	2105	140	10.7	98.2	97.9

APPENDIX 2

Elutriation of sorbent and coal ash

The bed consists of coal ash and partly-calcined, partly-sulphated SO_2 sorbent (dolomite or limestone). The material elutriated from such a bed consists mainly of particles smaller than that size for which the gas velocity - at the prevailing temperature and pressure - is the terminal or free-fall velocity. This critical size is termed the "elutriated" size and "fines" are defined as that material smaller than the elutriable size. The elutriable size - based on the velocity, temperature and pressure at the combustor exit - is calculated from an expression based on Pettyjohn and Christiansen's data for particles of sphericity = 0.8 (Ref. 6), which when rearranged to be explicit in particle size, gives

$$d_t = \frac{\rho U_t^2}{2ag\sigma} + \left[\left(\frac{\rho U_t^2}{2ag\sigma}\right)^2 + \frac{b U_t \mu}{ag\sigma}\right]^{0.5}$$

where d_t = elutriable size

ρ = gas density

μ = gas viscosity

g = gravitational acceleration

σ = particle density (specific gravity = 2.7 for coal ash or dolomite ash)

U_t = gas velocity at combustor exit

a = 1.285

b = 26.20

all in self-consistent units.

Material smaller than the elutriable size in the solid feed streams is rapidly elutriated. The remaining material is retained in the bed until its size is reduced to smaller than the elutriable size, after which it is also rapidly elutriated.

Processes causing size reduction are:-

(1) attrition and abrasion of particles in the bed

and (2) decrepitation of the incoming particles due to the sudden evolution of CO_2 and to shock heating of the particle.

Ref. 6. Battcock, W.V. and Pillai, K.K. Proc. 5th International Conference on Fluidised Bed Combustion, Washington, Dec. 1977.

Sorbent elutriation

To avoid ambiguity, dolomite is expressed on an inert basis, i.e. (100 - % H_2O - % Cl - elemental carbon - % CO_2 - % SO_3) %

Consider a sorbent ash feed rate w_d, having a fines fraction f_{dt} (i.e. material smaller than d_t). If the sorbent ash actually elutriated, expressed as a fraction of the sorbent ash input, is f_{de}, then the rate of production of fines in the bed is

$$\dot{f} = (f_{de} - f_{dt}) w_d$$

The rate of fines production due to attrition and abrasion can be expected to be proportional to the bed weight, W_b, the dolomite content of the bed, Σ_d, and some function of the velocity in the bed such as $(U - U_{mf})^n$

The rate of fines production due to decrepitation is complex, but is likely to be related to the feed rate and to the rate of evolution of CO_2 For the moment the extent of calcination of the bed particles α, is taken as a likely indication of the rate of evolution.

It is suggested that the total rate of fines production is given by an expression of the type

$$\dot{f} = (f_{de} - f_{dt}) w_d \propto k_1 W_b \Sigma_d (U - U_{mf})^n + k_2 \alpha w_d$$

Data generated by some 24 tests on the Leatherhead PFBC are given in Table A2 and a correlation has been developed along the lines indicated above to give the expression

$$(f_{de} - f_{dt}) = 0.218 \times 10^{-3} \frac{W_b \Sigma_d}{w_d} + 86.1 \times 10^{-3} \alpha w_d - 0.0329$$

A comparison of observed and predicted values $(f_{de} - f_{dt})$, based on the above expression, is given in Fig. A2 and shows a reasonable correlation. However, examination of this expression shows that the contribution of the 2nd and 3rd terms (i.e. $86.1 \times 10^{-3} \alpha w_d$ -0.0329) is small and suggests that decrepitation due to CO_2 evolution is negligible in PFBC situations. The same is not true at atmospheric pressure, of course, where the evolution of CO_2 from limestone can be extremely rapid.

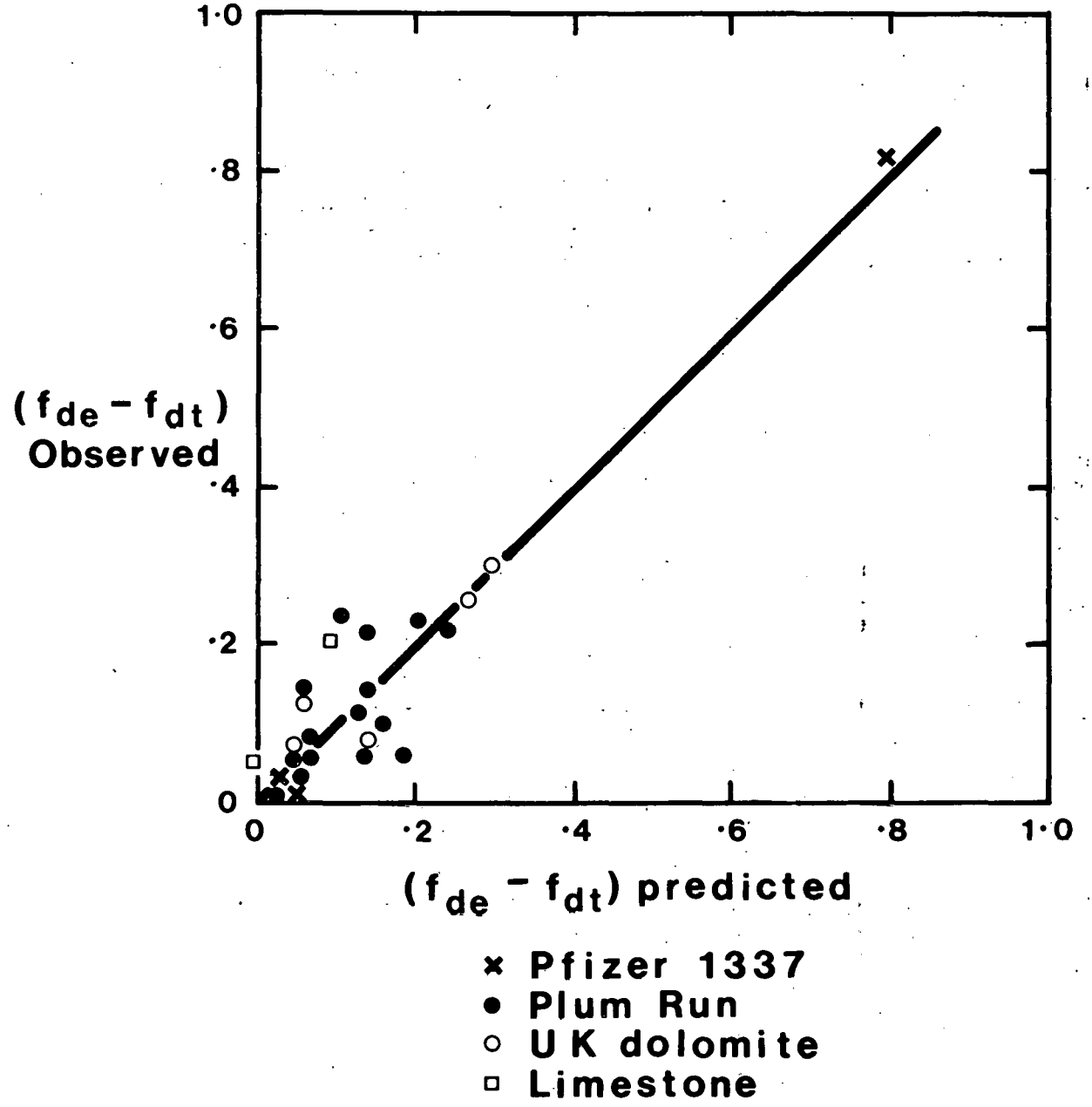

Fig. A2 Correlation of fines (sorbent) production in the bed

The amount of dolomite fines produced in the bed is generally extremely small, so that almost any method of estimating this quantity is likely to be effective. In section 6.4.1 and Fig. 35 it was shown that the simpler expression

$$\dot{f}/W_b \xi_d \propto (U - U_{inf})$$

gives an equally good correlation.

Coal ash elutriation

Although a similar correlation might be expected to apply to the attrition of coal ash, it has not been possible to devise one. Amongst the reasons for this are the facts that (1) the hardness of coal ash varies considerably from coal seam to coal seam and can also vary with the mining technique (2) the size distribution of the ash produced by burning the coal differs from the size distribution of the original coal and (3) the proportion of coal ash in the bed is usually small so that the amount of coal ash in the bed cannot be estimated as accurately as the amount of dolomite.

For reference, data relating to the elutriation of coal ash from 24 tests are reproduced in Table A3.

Table A2. Elutriation data (dolomite)

Code		Velocity			Temperature									Sorbent
		U ft/s	U_{mf} ft/s	U_t ft/s	T_B °R	T_F °R	d_t µm	W_b lb	ε_d	W_d lb/h	f_{dt}	f_{de}	α	
EFDA	Test 6/1	2.7	0.9	2.5	2060	2010	180	2600	0.20	63	0.34	0.35	0.77	Pfizer 1337
	" 6/2	2.5	0.9	2.4	2060	1990	170	2400	0.28	38	0.20	0.23	0.51	"
	" 7A	7.0	1.2	6.8	2115	2050	415	2100	0.68	116	0.01	0.83	0.97	"
GE	" 8	4.5	0.6	4.4	2080	2035	270	1550	0.84	103	0.06	0.32	0.98	UK dolomite
	" 9	4.6	0.6	4.5	2170	2125	275	1600	0.91	112	0.07	0.37	0.99	"
DOE 1000 h	" 1/1	4.0	1.4	2.8	2000	1935	185	2200	0.59	98	0	0.03	0.37	Plum Run
	" 1/2	4.0	1.3	2.8	2005	1940	190	2400	0.74	134	0	0.06	0.42	" "
	2/2	4.0	0.8	2.8	2035	1990	190	2100	0.90	123	0.02	0.12	0.60	" "
	2/3	4.0	0.6	2.9	2045	2000	190	2100	0.86	122	0.10	0.33	0.91	" "
	3	4.0	0.7	2.8	2035	1985	190	1900	0.89	119	0.17	0.23	0.79	" "
	4	4.0	0.9	2.8	2040	1990	190	1900	0.84	119	0.15	0.29	0.68	" "
	5	4.0	0.8	2.8	2035	1980	190	1850	0.87	136	0.06	0.28	0.75	" "
	6	4.0	1.1	2.8	2035	1980	190	1900	0.89	117	0.14	0.20	0.90	" "
DOE 1980	1/1	37	1.1	3.8	1920	1970	235	1100	0.85	115	0.01	0.07	0.56	" "
	1/2	3.9	1.1	3.7	2090	1990	230	2000	0.85	123	0.01	0.13	0.97	" "
	2/1	4.0	1.1	4.1	1860	1835	255	1350	0.59	118	0.35	0.49	0.51	" "
	2/2	4.1	1.1	3.9	1860	1920	245	1400	0.67	119	0.38	0.46	0.50	" "
	3/1	4.1	0.8	3.1	2090	2015	200	1200	0.51	106	0.40	0.64	0.97	" "
	3/2	2.5	0.7	2.2	1855	1790	155	1400	0.78	104	0.33	0.34	0.53	" "
Sponsor A	2A	6.5	2.3	5.0	2020	1585	310	750	0.41	125	0.20	0.26	0.41	UK dolomite
	2B	6.5	2.6	5.7	2010	1775	345	1100	0.40	126	0.15	0.28	0.40	"
	2C	6.5	2.6	6.2	2040	1975	375	1500	0.63	128	0.27	0.35	0.63	"
Sponsor D	1	4.4	1.1	2.9	2020	1980	200	1300	0.25	14	0.14	0.35	0.25	(Limestone)
	2	2.1	0.7	1.4	2005	1935	120	1300	0.29	35	0.09	0.14	0.29	(")

U = fluidising velocity
U_{mf} = minimum fludising velocity
U_t = terminal velocity at combustor exit
T_B = bed temperature
T_F = freeboard temperature

d_t = particle size corresponding to U_t
W_b = weight of bed material
ε_d = fraction of dolomite 'inerts' in the bed
W_d = feed rate of dolomite 'inert'
f_{dt} = fraction of dolomite 'inert' feed which was finer than d_t
f_{de} = fraction of dolomite 'inert' feed which was elutriated
α = calcination of dolomite in bed

Table A3 Elutriation data (coal ash)

		Velocity			Temperature								
		U ft/s	U_{mf} ft/s	U_t ft/s	T_B °R	T_f °R	d_t μm	w_b lb	ε_c	W_c lb/h	f_{ct}	f_{ce}	Coal
ERDA	Test 6/1	2.7	0.9	2.6	2060	2010	180	2600	.08	52	0.25	0.63	Illinois
	" 6/2	2.5	0.9	2.4	2060	1990	170	2400	.10	33	0.29	0.53	"
	" 7A	7.0	1.2	6.8	2115	2050	415	2100	.12	80	0.36	0.95	"
GE	" 8	4.5	0.6	4.4	2080	2035	270	1550	.09	62	0.44	0.83	"
	" 9	4.6	0.6	4.5	2170	2125	275	1600	.09	62	0.29	0.86	"
	" 1/1	4.0	1.4	2.8	2000	1935	185	2200	.11	101	0.14	0.73	Glen Brook
	" 1/2	4.0	1.3	2.8	2005	1940	190	2400	.19	113	0.26	0.68	"
	" 2/2	4.0	0.8	2.8	2035	1990	190	2100	.10	75	0.16	0.76	"
	" 2/3	4.0	0.6	2.9	2045	2000	190	2100	.14	73	0.16	0.76	"
	" 3	4.0	0.7	2.8	2035	1985	190	1900	.10	76	0.23	0.85	"
	" 4	4.0	0.9	2.8	2040	1990	190	1900	.14	78	0.31	0.85	"
	" 5	4.0	0.8	2.8	2035	1980	190	1850	.13	76	0.21	0.81	"
	" 6	4.0	1.1	2.8	2035	1980	190	1900	.11	75	0.25	0.78	"
DOE 1980	" 1/1	3.7	1.1	3.8	1920	1970	235	1100	.06	83	0.27	0.80	"
	" 1/2	3.9	1.1	3.7	2090	1990	230	2000	.14	95	0.31	0.75	"
	" 2/1	4.0	1.1	4.1	1860	1835	255	1350	.06	107	0.31	0.83	"
	" 2/2	4.1	1.1	3.9	1860	1920	245	1400	.12	101	0.31	0.87	"
	" 3/1	4.1	0.8	3.1	2090	2015	200	1200	.23	84	0.25	0.85	"
	" 3/2	2.5	0.7	2.2	1855	1790	155	1400	.10	53	0.17	0.83	"
Sponsor A	" 2A	6.5	2.3	5.0	2020	1585	310	750	.56	319	0.23	0.52	UK Bituminous
	" 2B	6.5	2.6	5.7	2010	1775	345	1100	.58	328	0.28	0.52	"
	" 2C	6.5	2.6	6.2	2040	1975	375	1500	.38	192	0.27	0.69	High ash sub-bituminous
Sponsor D	" 1	4.4	1.1	2.9	2020	1980	200	1300	.56	306	0.16	0.85	
	" 2	2.1	0.7	1.4	2005	1935	120	1300	.60	165	0.10	0.48	

ε_c = concentration of coal ash in the bed

W_c = feed rate of coal ash

f_{ct} = fraction of coal feed which was finer than d_t

f_{ce} = fraction of coal feed ash which was elutriated

*U.S. GOVERNMENT PRINTING OFFICE: 1981-740-145/2929